Mojtaba Bandarabadi

Low-Complexity Measures for Epileptic Seizure Prediction and Early Detection Based on Classification

Doctoral Thesis Submitted to the Doctoral Program in Information Science and Technology
Supervised by Professor António Dourado Pereira Correia and Co-supervised by Professor César Alexandre Domingues Teixeira
Presented to the Department of Informatics Engineering of the Faculty of Sciences and Technology of the University of Coimbra

February 2015

· U C ·

Universidade de Coimbra

I would like to dedicate this thesis to my parents …

Acknowledgements

Now that I'm preparing the final lines of this dissertation, the names of many individuals are crossing my mind, all of which I owe special thanks and respect. During almost past five years of my doctoral program which started in March 2010, I have been feeling quite gifted to be allowed to carry out research in the Center of Informatics and Systems at the University of Coimbra (CISUC).

Foremost, I should thank my dear supervisor Professor António Dourado Pereira Correia, who has been much kind and understanding, and for being an excellent supervisor not only with my academic career and thesis, but also for his warm support on personal issues. His availability and fast responses to all of my requests for meetings to discuss new ideas, verifying of the new results obtained, reviewing of the manuscripts, supporting in bureaucratic procedures, and so on, made it possible to carry out a productive research. In my belief, the best part of this thesis is based on his suggestions, contributions, and scientific discussions. Moreover, success of the European project EPILEPSIAE would not become possible without his key role and strong commitment.

I also wish to acknowledge Professor César Alexandre Domingues Teixeira who was my co-supervisor during my PhD years. I've been motivated and learned a lot from him, through our discussions and by his enthusiasm in troubleshooting of difficult problems and crossing new barriers. My gratitude also goes to Mr. Jalil Rasekhi with whom I shared both successes and failures throughout the past five years. His relation to my research and thesis is far beyond simple scientific discussions, or just sharing of new results and methods.

For five months, there was an opportunity to visit US and take part in the professor Netoff's epilepsy lab and the Professor Parhi's Lab at the University of Minnesota, where I came up with some new ideas for seizure detection and prediction. I would like to thank my honorable US Professors Keshab K. Parhi and Theoden I. Netoff for making it possible to

earn such an invaluable experience. In this short visit, we had daily meetings for discussing new approaches, and during which they wholeheartedly shared their ideas and comments.

I would like to thank the members of CISUC, specially Bruno Direito and Pedro Martins, my colleagues at Adaptive Computing Group (ACG). I also would like to acknowledge the Department of Informatics Engineering for the conditions and resources that allowed me to accomplish this research. I'm also grateful to the staff of the epilepsy unit of the Hospital of the University of Coimbra (HUC) and especially Dr. Francisco Sales for their support. I would particularly like to acknowledge the Portuguese Foundation for Science and Technology (Fundação para a Ciência e Tecnologia - FCT) for its financial support of this thesis based on the 4-years fellowship SFRH/BD/71497/2010, as well as the EU EPILEPSIAE FP7 211713 Grant.

Although being several thousand kilometers away from my family, yet I have always felt their love and mental supports during these years, especially from my father and mother who I owe so much to. Last but not least, I wish to thank my beloved wife Padideh, for her unceasing understanding and perpetual love, from the beginning. I could not finish this work without your unconditional support, patience, encouraging words, and the warm beautiful smile.

Abstract

This thesis concerns the problems of epileptic seizure prediction and detection. We analyzed multichannel intracranial electroencephalogram (iEEG) and surface electroencephalogram (sEEG) recordings of patients suffering from refractory epilepsy, to access the brain state in real time by using relevant EEG features and computational intelligence techniques, and aiming for detection of pre-seizure state (in the case of prediction) or seizure onset times (in the case of detection). Our main original contribution is the development of a novel relative bivariate spectral power feature to track gradual transient changes prior to ictal events for real-time seizure prediction. Furthermore a novel robust and generalized measure for early seizure detection is developed, aimed to be used in closed-loop neurostimulation systems.

The development of a general platform embeddable on a transportable low-power-budget device is of utmost importance, for real time warning to patients and their relatives about the impending seizure or beginning of an occurring seizure. The portable device can also be integrated to work in conjunction with a closed-loop neurostimulation or fast-acting drug injection mechanism to eventually disarm the impending seizure or to suppress the just-occurring seizure. Therefore, in this thesis we try to meet the dual-objective of developing algorithms for seizure prediction and early seizure detection that provide high sensitivity and low number of false alarms, fulfilling the requirements of clinical applications, while being low computational cost.

To seek the first objective, a patient-specific seizure prediction was developed based on the extraction of novel relative bivariate spectral power features, which were then preprocessed, dimensionally reduced, and classified using a machine-learning algorithm. The introduced feature bears low complexity, and was classified using the powerful support vector machine (SVM) classifier. We analyzed the preictal EEG dynamics across different brain regions and throughout several frequency bands, using relative bivariate features to

reveal the transient preictal changes ending in epileptic seizures. The suggested prediction system was evaluated on long-term continuous sEEG and iEEG recordings of 24 patients, and produced statistically significant results with average sensitivity of 75.8% and false prediction rate of 0.1 per hour.

Furthermore a novel statistical method was developed for proper selection of preictal period, and also for the evaluation of predictive capability of features, as well as for the predictability of seizures. The method uses amplitude distribution histograms (ADHs) of the features extracted from the preictal and interictal iEEG and sEEG recordings, and then calculates a criterion of discriminability among two classes. The method was evaluated on spectral power features extracted from monopolar and bipolar iEEG and sEEG recordings of 18 patients, in overall consisting of 94 epileptic seizures.

To approach the objective of early seizure detection, we have formulated power spectral density (PSD) of bipolar EEG signal in the form of a measure of neuronal potential similarity (NPS) between two EEG signals. This measure encompasses the phase and amplitude similarities of two EEG channels in a simultaneous fashion. The NPS measure was then studied in several narrow frequency bands to find out the most relevant sub-bands involved in seizure initiations, and the best performing ratio of two NPS measures for seizure onset detection was determined. Evaluating on long-term continuous iEEG recordings of 11 patients with refractory partial epilepsy (overall of 1785 h and 183 seizures) the results showed high performance, while requiring a very low computational cost. On average, we could achieve a sensitivity of 86.9%, a low false detection rate (FDR) of 0.06/h, and a mean detection latency of 13.1s from electrographic seizure onsets, while in average preceding clinical onsets by 6.3s.

Apart from the above mentioned primary objectives, we introduced two new and robust methods for offline or real-time labelling of epileptic seizures in long-term continuous EEG recordings for further studies. Methods include mean phase coherence estimated from bandpass filtered iEEG signals in specific frequency bands, and singular value decomposition (SVD) of bipolar iEEG signals. Both methods were evaluated on the same dataset employed in the previous study and demonstrated sensitivity of 84.2% and FDR of 0.09/h for sub-band mean phase coherence, and sensitivity of 84.2% and FDR of 0.05/h for bipolar SVD, on average.

Most of this work was established in collaboration with the EPILEPSIAE project, aimed to predict of pharmacoresistant epileptic seizures. The developed methods in this thesis were evaluated by the accessibility of long-term continuous multichannel EEG recordings of more than 275 patients with refractory epilepsy, referred to as The European Epilepsy Database. This database was collected by the three clinical centers involved in EPILEPSIAE, and contains well-documented metadata.

The results of this thesis are backing the hypothesis of the predictability of most of epileptic seizures using linear bivariate spectral-temporal brain dynamics. Moreover, the promising results of early seizure detection sustain the feasibility of integrating the proposed method with closed-loop neurostimulation systems. We hope the developed methods could be a step forward towards the clinical applications of seizure prediction and onset detection algorithms.

Keywords

Epilepsy; epileptic seizure prediction, early seizure detection; electroencephalogram; preictal period; univariate features; bivariate features; linear analysis; nonlinear analysis; power spectral density; mean phase coherence; singular value decomposition; neuronal potential similarity; support vector machines; feature selection.

Resumo

Esta tese versa os problemas de predição e de deteção de crises epiléticas. Analisa-se o eletroencefalograma multicanal intracraniano (iEEG) e de superfície (sEEG) de pacientes que sofrem de epilepsia refratária, para a estimação em tempo real do estado cerebral, usando características relevantes do EEG e técnicas de inteligência computacional, ambicionando a deteção do estado pré-ictal (no caso de previsão) ou dos instantes de início de uma crise (no caso de deteção). A principal contribuição original é o desenvolvimento de uma característica de potência espectral bivariada relativa para captar as mudanças transitórias graduais que levam a crises e que poderão ser usadas para previsão em tempo real. Além disso, é desenvolvida uma nova medida, robusta e generalizada para a deteção precoce, destinada a ser utilizada em sistemas de neuro estimulação em malha fechada.

O desenvolvimento de uma plataforma geral possível de ser integrada num dispositivo transportável, energeticamente económico, é de grande relevância para o aviso em tempo real do doente e dos seus próximos sobre a eminência da ocorrência de uma crise. O dispositivo transportável também pode ser usado em malha fechada com um neuro estimulador ou com um dispositivo de injeção rápida de um fármaco que desarme eventualmente a crise em curso. Por isso nesta tese persegue-se o objectivo de desenvolver algoritmos para previsão mas também para deteção de crises. Em ambos os casos, pretende-se que os algoritmos tenham uma elevada sensibilidade e uma baixa taxa de falsos positivos, tornando viável a sua utilização clínica.

Para o objectivo de previsão, desenvolveu-se um método de previsão personalizado baseado na extração de uma característica nova, denominada de potência relativa espectral bivariada, que foi submetida a pre-processamento, redução de dimensão e classificação com Máquinas de Vetores de Suporte (SVM). Esta nova característica, de baixa complexidade, é computacionalmente simples, mas permite a análise da dinâmica do EEG preictal em diferentes regiões do cérebro e ao longo de várias bandas de frequência, de modo a descobrir

os mecanismos subjacentes às crises epiléticas. O sistema de previsão obtido foi avaliado em registos contínuos de sEEG e iEEG de 24 pacientes, e produziu resultados estatisticamente significativos com sensibilidade média de 75.8% e taxa de predição falsa de 0.1 por hora.

Além disso, foi desenvolvido um novo método estatístico para a seleção apropriada do período preictal, e também para a avaliação da capacidade preditiva das características, assim como para a própria previsibilidade das crises. O método utiliza os histogramas de distribuição de amplitude (ADHS) das características extraídas nos períodos pré-ictal e ictal dos registos de iEEG e sEEG e, em seguida, calcula um critério de discriminabilidade entre as duas classes. O método foi avaliado nas características de potencia espectral extraídas de registos iEEG e sEEG, monopolares e bipolares de 18 pacientes, consistindo num número total de crises epilépticas de 94.

O segundo objetivo, a deteção precoce de crises, foi abordado através da formulação da densidade de potência espectral (PSD) de canais de EEG bipolares na forma de uma medida da similaridade do potencial neuronal (NPS) entre dois sinais de EEG. Esta medida usa as similaridades entre as fases e as amplitudes de dois canais de EEG de um modo simultâneo. A medida NPS foi estudada em várias bandas estreitas de frequência de modo a descobrir-se quais as sub-bandas mais envolvidas na inicialização das crises; buscou-se assim a melhor razão entre duas NPS do ponto de vista da deteção precoce. Avaliadas em iEEG contínuos de longa duração de 11 doentes com epilepsia refratária parcial (num total de 1785 h e 183 crises), os resultados apresentam um desempenho com sensibilidade de 86.9% e taxa de deteção falsa (FDR) de 0.06/h, uma latência de 13.1 s em relação ao início eletrográfico, sendo uma crise detetada em média 6.3 s antes da sua manifestação clínica.

Para além dos objetivos principais referidos acima, introduziram-se dois novos métodos, robustos, para etiquetagem em diferido e em tempo real das crises em registos contínuos de EEG de longa duração para estudos posteriores. Esses métodos incluem a coerência de fase média (mean phase coherence) estimada a partir de registos iEEG em bandas de frequência específicas (usando filtros passa-banda), e a decomposição em valores singulares (SVD) de sinais iEEG bipolares. Ambos os métodos foram avaliados no mesmo conjunto de dados do estudo anterior e apresentaram, em média, uma sensibilidade de 84.2% e um FDR de 0.09/h para a coerência de fase média calculada para as sub-bandas, e sensibilidade de 84.2% e FDR de 0.05/h para a metodologia que usa a decomposição SVD bipolar.

Grande parte deste trabalho foi feito no âmbito do projeto EPILEPSIAE, visando a previsão de crises em doentes epiléticos fármaco-resistentes. Os métodos desenvolvidos nesta tese aproveitaram a acessibilidade aos dados bem documentados de mais de 275 pacientes que constituem a Base de Dados Europeia de Epilepsia (European Epilepsy Database), provenientes dos três centros hospitalares participantes no projeto.

Os resultados desta tese apoiam a hipótese da previsibilidade da maioria das crises epiléticas usando dinâmicas cerebrais bivariadas lineares espetrais e temporais. Além disso os resultados são promissores relativamente à deteção precoce de crises e sustentam a fazibilidade da integração desses métodos com técnicas de neuroestimulação em malha fechada. Esperamos que os métodos desenvolvidos resultem num avanço no que respeita à aplicação clínica de algoritmos de previsão e deteção de crises.

Palavras-chave

Epilepsia; previsão de crises epiléticas; deteção precoce de crises; eletroencefalograma; período preictal; características univariadas; características bivariadas; análise linear; análise não-linear; densidade de potência espectral; coerência média de fase; decomposição em valores singulares; similaridade potencial neuronal; máquinas de vetores de suporte; seleção de características.

Contents

Contents xiii
List of Figures xvii
List of Tables xxi
Nomenclature 1
Notation 3
Chapter 1 Introduction 5
1.1 Neurophysiology of epilepsy 8
1.1.1 Seizure types 9
1.1.2 Predictability of seizures 10
1.2 Summary of contributions 11
1.2.1 Seizure prediction 11
1.2.2 Seizure detection 13
1.2.3 List of publications related to this thesis 15
1.3 Thesis outline 17
Chapter 2 Background and problem statement 19
2.1 Electroencephalography 19
2.1.1 Intracranial and surface EEG 20
2.1.2 Bipolar electroencephalogram 23
2.1.3 Moving window analysis 23
2.2 Prerequisite definitions 24
2.2.1 Clinical discussions 26
2.3 Technical background 27
2.3.1 Spectral analysis of electroencephalogram signals 27
2.3.2 Mean phase coherence 28
2.3.3 Minimum redundancy maximum relevance feature selection 30
2.3.4 Support vector machine classifier 30
2.3.5 Alarm generation using firing power method 31
2.4 Performance evaluation 32
2.4.1 Performance metrics in seizure prediction 32

2.4.2 Performance metrics in seizure onset/event detection 33
2.4.3 Statistical validation of performance 33
Chapter 3 The last 40 years of seizure prediction and detection 35
3.1 Past efforts in seizure prediction 35
3.1.1 Linear univariate analysis 36
3.1.2 Nonlinear univariate analysis 41
3.1.3 Linear bivariate measures 46
3.1.4 Nonlinear bivariate measures 47
3.1.5 Combination of features 49
3.1.6 Self-prediction of epileptic seizures 51
3.2 Past efforts in seizure detection 52
3.2.1 Early seizure detection 53
3.2.2 Seizure event detection 55
3.3 Summary 56
Chapter 4 Novel seizure prediction approaches 59
4.1 Seizure prediction using ratio of spectral powers 60
4.1.1 Dataset description 60
4.1.2 Methods 62
4.1.3 Results 69
4.1.4 Discussion 75
4.2 On the proper selection of preictal period 79
4.2.1 Dataset description 80
4.2.2 Optimal preictal criterion 82
4.2.3 Results 85
4.2.4 Discussion 88
4.3 Conclusion 96
Chapter 5 New seizure detection algorithms 97
5.1 Dataset description 98
5.2 Methods 100
5.2.1 Early seizure detection using neuronal potential similarity 101
5.2.2 Phase synchronization in frequency sub-bands 106
5.2.3 Singular value decomposition of bipolar EEG 108
5.2.4 Preprocessing of features 111
5.2.5 Threshold based classifier 112
5.2.6 Improved performance metrics for early seizure detection 113
5.3 Results 113
5.3.1 Results of early seizure detection 114

5.3.2 Results of seizure event detection 116
5.4 Discussion 117
5.4.1 Early seizure detection 117
5.4.2 Seizure event detection 121
5.4.3 Channel selection 123
5.4.4 Robustness of algorithms 125
5.5 Conclusion 126
Chapter 6 Conclusions and perspectives 127
6.1 Conclusions on seizure prediction approaches 127
6.2 Conclusions on seizure detection approaches 129
References 131

List of Figures

Figure 1.1 – Some of the current commercialized neurostimulation systems for epilepsy disease 8

Figure 1.2 – Invasive EEG recordings (30 sec) covering the initial and developed states of an epileptic seizure. 9

Figure 2.1 – Surface and intracranial EEG electrodes 20

Figure 2.2 – EEG recordings are mixed of electrical activities of different brain parts (Sanei et al. , 2008) 21

Figure 2.3 – Multichannel sEEG and iEEG signals of a sample seizure recorded simultaneously. The vertical red lines indicate seizure onset and offset times. 22

Figure 2.4 – Epileptic brain states; interictal, preictal, ictal, and postictal 25

Figure 4.1 – Overall diagram of the proposed method for seizure prediction 62

Figure 4.2 – Time-frequency representation of 10 min of raw hippocampal iEEG signal. The sampling rate for this patient was 1024 Hz. Most of the spectral energy is limited to <100 Hz frequencies, showing that the power within the frequencies higher than 128 Hz is negligible in comparison to the frequency range of 30-128 Hz. 63

Figure 4.3 – Raw feature and its preprocessed version (α_{ORFRG6} / δ_{AMYGG1} for patient 18). The feature was extracted from 100 minutes of iEEG signals of patient 18. Each smoothed sample was obtained by averaging on current and past 11 raw feature samples. Non-preprocessed features are highly vibrant around the smoothed feature values, indicating that preprocessing has reduced the effects of artifacts. 65

Figure 4.4 – The normalized ADHs of relative spectral features for patient 19; (a) highest rank: D_{ADHs} =0.70, (b) lowest rank: D_{ADHs} =0.06. The dotted black histogram represents the ADH of non-preictal samples, while the blue histogram represents the ADH of preictal samples. For maximum discrepancy of the features (maximum D_{ADHs}), the common area under two histograms (highlighted area) should be minimized. 67

Figure 4.5 – Decision making on the outputs of the SVM classifier for alarm generation using FP method. Highlighted area depicts a 30 min preictal period, and the black, blue and red lines represent the SVM outputs, regularization output and the generated alarm respectively. By upward passing of regularization output across the threshold value (0.5), and fulfilling

two constraints of the FP method, an alarm is generated. Alarms outside this preictal window are considered as false alarms. Seizure onset is marked by the longer vertical black line. 69

Figure 4.6 – Sensitivity and FPR results achieved by the proposed seizure prediction method for 24 studied patients using both MDAD and mRMR feature selection methods. 72

Figure 4.7 – The output of the FP method for 42 h continuous recordings of test data for one of the studied patients. The highlighted areas show 30 min preictal periods, and the vertical red lines are the alarms raised by the firing power method. The five vertical black lines indicate the seizure onsets. 73

Figure 4.8 – Finding the proper preictal period for a feature/seizure. (a) Spectral power of 102-125 Hz extracted from 5.5 hours of iEEG recordings, including a seizure onset at 5h (seizure 4, patient 1). (b, c, d, e) The normalized ADHs of preictal and interictal samples using four preictal periods of 10, 30, 50, and 70min, respectively. Among these four preictal periods, the 30min preictal period provided less C_{ADHs}. 83

Figure 4.9 – The graph presents the C_{ADHs} of preictal and interictal classes with respect to different preictal periods for the same feature and seizure as in Figure 4.8. The OPP is located at 32min. 84

Figure 4.10 – The C_{ADHs} of interictal and preictal classes with respect to different preictal periods, and for the 14 features of two studied seizures. (a) A seizure with an identifiable OPP using monopolar spectral power features (seizure 22, patient 5): the OPP is located around 22min, with spectral powers of 352-512, 252-348, and 202-248 Hz providing lower C_{ADHs} in OPP. (b) A seizure with no distinguishable preictal period using the monopolar spectral power features (seizure 12, patient 3). 88

Figure 4.11 – Histogram of OPPs for 63 epileptic seizures with distinguishable preictal period 89

Figure 4.12 – Distribution of training feature samples in a two-dimensional feature space (patient 5, seizure No. 22, spectral powers of 252-348 Hz and 352-512 Hz) using (a) 5 min preictal period, (b) 10 min preictal period, (c) 15 min preictal period, (d) optimal preictal period of 22 min, (e) 30 min preictal period, and (f) 40 min preictal period. The overlap between the preictal and interictal feature samples increases when using preictal periods smaller or larger than the OPP (a, b, c, e, f). As a result, separability of the features is maximal when preictal period is selected equal to the OPP (d). The performance of a trained model would be decreased significantly, if the preictal samples are mislabeled as the interictal samples, or vice versa. 90

Figure 4.13 – Determining of the seizure prediction horizon (SPH) and the seizure occurrence period (SOP) according to the obtained OPPs from the training set. The SPH can be defined using the minimum OPP, whereas the SOP can be specified using the maximum OPP and this SPH. 91

Figure 4.14 – The C_{ADHs} with respect to different preictal periods obtained from (a) monopolar and (b) bipolar iEEG recordings, and for the four highest ranked features of a studied seizure (seizure 13, patient 3). As seen from the graphs, the monopolar montage provided significantly lower C_{ADHs} than bipolar montage using iEEG recordings. 94

Figure 4.15 – The C_{ADHs} with respect to different preictal periods obtained from (a) monopolar and (b) bipolar sEEG recordings, and for the four highest ranked features of a studied seizure (seizure 71, patient 13). As seen from the curves, there is no significant difference between C_{ADHs} of monopolar and bipolar montages. 95

Figure 5.1 – Two states of an epileptic seizure. An early seizure detection method would be suitable for closed-loop neurostimulation systems, if it could detect the seizure during its electrographic phase 97

Figure 5.2 – Four minutes multichannel iEEG recordings of a seizure from patient 1. The vertical red lines indicate electrographic onset and offset times. HAR1 and HAR2 electrodes were selected for this patient 100

Figure 5.3 – General block diagram of the proposed methods for seizure onset/event detection 100

Figure 5.4 – Bandpass filtered bipolar iEEG signals into 0.5-3 Hz and 12-26 Hz (patient 3). (a) four minutes of bandpass filtered signals including a seizure onset at 120s. (b, c) bandpass filtered signals from highlighted non-ictal and ictal periods of figure (a) respectively. As seen from the figures, the average power of 0.5-3 Hz is higher than 12-26 Hz during non-preictal periods, while is less during seizure initiation. 104

Figure 5.5 – The proposed measure for early seizure detection for one seizure from patient 5. The left and right vertical dotted red lines indicate the electrographic seizure onset and offset times, respectively 105

Figure 5.6 – Smoothed MPC measures extracted from bandpass filtered iEEG signals including a studied epileptic seizure (patient 5, seizure 1). The vertical dotted red lines indicate the electrographic onset and offset times. The MPC measure reaches its maximum prior to seizure termination in almost all studied frequency bands. Desynchronization is also observable with seizure initiation. 107

Figure 5.7 – Singular values (65-128) extracted from 10 minutes of bipolar iEEG signal contains one seizure. Vertical red lines indicate electrographic onset and offset times. The SVs first start to increase by seizure development, and then suddenly decrease approaching the seizure termination. 110

Figure 5.8 – The normalized SVs (1-128) extracted from seizure 7 of patient 2. After normalization by information of first hour of iEEG recording, the range of all SVs is almost equalized. 111

Figure 5.9 – The proposed measure (*RNPS*) for early seizure detection for whole recordings of patient 5. The vertical dotted red lines indicate the seizures. 115

Figure 5.10 – Boxplot representation of seizure durations for 11 studied patients 120

Figure 5.11 – Sub-band and wideband MPC measures extracted from 2 hours of iEEG recordings of patient 5, containing two epileptic seizures. The vertical dotted red lines indicate onset times. The sub-band MPC measures extracted from 12-18 Hz and 18-28 Hz were more robust than wideband MPC measure, and generated lower number of false alarms. 122

Figure 5.12 – Proposed measure using singular values extracted from bipolar iEEG signals (patient 5). Black line is the measure, and the vertical dotted red lines are seizure onsets. The horizontal dotted blue line is the threshold value. 122

Figure 5.13 – Seizure propagation information for patient 1, available in dataset. (a) Channels placed over the foci, where the seizures originated, (b) channels involved during early states of seizure propagation. HAR1 and HAR2 electrodes were selected for this patient. 124

Figure 5.14 – Histogram of seizure occurrence times across circadian cycle, with almost a uniform distribution 125

List of Tables

Table 4.1 – Information of the 24 studied patients 61

Table 4.2 – Results for the 24 studied patients 71

Table 4.3 – Results obtained using the three highest ranked features 74

Table 4.4 – The five highest ranked features for each of the 24 patients 76

Table 4.5 – Characteristics of 18 studied patients and their EEG recordings 81

Table 4.6 – OPPs of 59 seizures recorded using iEEG signals and the three high ranked features for each seizure 86

Table 4.7 – OPPs of 35 seizures recorded using sEEG signals and the three high ranked features for each seizure 87

Table 4.8 – The five most relevant spectral power features for seizure prediction 92

Table 4.9 – The average of OPP and C_{ADHs} results of the 94 studied seizures 93

Table 5.1 – Characteristics of studied patients and iEEG recordings 99

Table 5.2 – Results of proposed early seizure detection for 11 studied patients 115

Table 5.3 – Results of proposed seizure event detection methods for 11 studied patients 116

Table 5.4 – Reported results for early seizure detection by other researches 119

Nomenclature

ADH: Amplitude Distribution Histogram

AED: Anti-epileptic drug

AR: Autoregressive

CPS: Complex Partial Seizure

CT: Computed Tomography

DBS: Deep Brain Stimulation

DSI: Dynamical Similarity Index

ECG: Electrocardiography

ECoG: Electrocorticography

EEG: Electroencephalography

EMG: Electromyogram

FDA: USA Food and Drug Administration

FDR: False Detection Rate

FFT: Fast Fourier Transform

FLE: Frontal Lobe Epilepsy

fMRI: functional Magnetic Resonance Imaging

FP: Firing Power

FPR: False Prediction Rate

FPR_{max}: maximum False Prediction Rate

FSPEEG: Freiburg Seizure Prediction EEG database

iEEG: Intracranial Electroencephalography

IIR: Infinite Impulse Response

LLE: Largest Lyapunov Exponent

LTLE: Lateral Temporal Lobe Epilepsy

MDAD: Maximum Difference between Amplitude Distributions

MDLC: Mean Detection Latency from Clinical Onset

MDLE: Mean Detection Latency from Electrographic Onset

MEG: Magnetoencephalography

MPC: Mean Phase Coherence

mRMR: minimum Redundancy Maximum Relevance

MTLE: Mesial Temporal Lobe Epilepsy

NPS: Neuronal Potential Similarity

OPP: Optimal Preictal Period

PS: Prodromal Symptoms

PSD: Power Spectral Density

RBF: Radial Basis Function

RNS: Responsive Neurostimulator

RP: Random Predictor

sEEG: surface Electroencephalography

SOP: Seizure Occurrence Period

SPS: Simple Partial Seizure

SS: Sensitivity

STL_{max}: Short-Term Maximum Lyapunov Exponent

SVD: Singular Value Decomposition

SVM: Support Vector Machine

TLE: Temporal Lobe Epilepsy

VNS: Vagus Nerve Stimulator

Notation

α_{RP}	-	*Significance level for random predictor*
σ	-	*Singular value*
σ^2	-	*Variance*
τ	-	*Number of feature samples in a preictal interval*
α	-	*Alpha frequency band (8-15 Hz)*
β	-	*Beta frequency band (15-30 Hz)*
θ	-	*Theta frequency band (4-8 Hz)*
δ	-	*Delta frequency band (<4 Hz)*
γ	-	*Gamma frequency band (>30 Hz)*
a	-	*Feature vector*
$\overline{a}$	-	*Pre-processed feature vector*
ADH	-	*Amplitude distribution histogram*
ADH_{norm}	-	*Normalized amplitude distribution histogram*
C_{ADHs}	-	*Common area under normalized amplitude distribution histograms*
D_{ADHs}	-	*Difference between normalized amplitude distribution histograms*
Ed	-	*Euclidean distance*
FP	-	*Output of firing power regularization method*
FPR_{norm}	-	*Normalized false prediction rate*
H_X	-	*Hankel matrix of x*
K	-	*Kernel function*
M	-	*Mean phase coherence*
$MDLE$	-	*Mean detection latency from electrographic seizure onsets*

ns	-	*Number of feature samples of each class*
NPS	-	*Neuronal potential similarity*
$RNPS$	-	*Relative neuronal potential similarity*
NP_i	-	*Normalized spectral power*
O	-	*Classifier output*
P	-	*Probability of random predictor to raise at least one true alarm*
P_{Binom}	-	*Probability of predicting n out of N events by a random predictor*
$P_{Binom,d}$	-	*Probability of predicting n out of N events by a random predictor, considering d optimizations*
P_i	-	*Sub-band spectral power*
P_{tot}	-	*Total spectral power*
ϕ_x^H	-	*Hilbert phase*
SS	-	*Sensitivity of raised alarms by predictor*
SS_{RP}	-	*Sensitivity of the random predictor*
Σ	-	*Singular value matrix*
U	-	*Left singular vector matrix*
V	-	*Right singular vector matrix*
w	-	*Bin-width*
x	-	*A segment of signal*
$\tilde{x}$	-	*Hilbert transform of* x
x_d	-	*Difference between two time series*
Z_x	-	*Analytic form of signal* x

Chapter 1 Introduction

Epilepsy is known and has attracted interests since ancient times, during which epileptic events were believed as originated from supernatural causes. In fact, the first records about epileptic events date back to around 3000 years ago in Babel and were known as *miqtu*. Ancient Greeks considered epilepsy as an extraordinary phenomena and a holy disease. In their belief, only god could throw the man on the floor, take his every sense, cause him seizure and finally return him back to the life with his normal appearances. Hippocrates was the first to find out that seizure was a disease and then had tried on its medication. Religious beliefs had by 1800s prohibited the scientific and routine study of the seizures (Magiorkinis et al. , 2010). Today seizures are considered as a window to the anatomy and complex function of the brain, and thus have been transformed into a multi-disciplinary field of study, and overwhelming research is directed towards them worldwide.

Second to stroke, epilepsy is the most common brain disorder, from which nearly 0.9% of the world's population is suffering. According to recent statistics, this happens with 63 million men and women worldwide, of all conditions and ages. Epilepsy related direct and indirect costs in Europe were estimated as €15.5 billion (10^9) per year, equivalent to an amount of €33 per capita (Pugliatti et al. , 2007). Also in the United States, the cost of covering just the direct medical expenditure related to epilepsy is estimated around $9.5 billion per year (Yoon et al. , 2009). Epilepsy is caused either by brain injuries or by out of balance chemicals in the brain. In fact, anything that injures the normal brain tissue can lead to seizures. However, in more than 50% of the epileptic cases, no certain cause can be identified (Sun et al. , 2001). Furthermore, the type of injury that can lead in a seizure is age-dependent. Children for example, during the very first years are quite easily affected by epilepsy, through birth-related issues, by inheritance, usual infections such as meningitis and

even uncontrolled fevers. In the middle age however, epilepsy is mainly kicked off by accidents which damage brain tissue. Such accidents include but are not limited to infections, alcohol, and side effects of medications. Finally, strokes and traumas are main triggers of the epileptic seizures throughout the last years of one's lifetime.

Epilepsy is usually controlled by medication, but not cured. Most treatments provided for epilepsy are in the form of anticonvulsant drugs. However their critical side effects should be taken into account and for about 30%-35% of the patients, the antiepileptic drugs (AEDs) are not effective (Carney et al. , 2011). In such cases, brain surgery is the alternative solution, which tries to remove the region in the brain where seizures are generated. However surgery is not always possible, and many patients are not eligible for that, because of the involved high risks (Spencer et al. , 2008). As a consequence about 30% of patients with epilepsy can be treated neither by medication nor by surgery, and must live with the seizures that can happen anytime, anywhere. Despite medical costs associated with the treatment of epilepsy, the injuries resulting from uncontrolled seizures represent an even higher cost to the society (Strzelczyk et al. , 2013).

Success in prediction of epileptic seizures would improve the living conditions of patients suffering from ictal events. Patients would have the possibility to ask for emergency help and early medications, therefore various interventions such as responsive neurostimulation (RNS) (Morrell, 2011, Sun et al. , 2014a), vagus nerve stimulation (VNS) using electrical impulses (Shoeb et al. , 2011b), deep brain stimulation (DBS) (Wu et al. , 2013), trigeminal nerve stimulation (TNS) (DeGiorgio et al. , 2006), or delivering fast-acting AEDs could be applied to overcome the seizures. Moreover, patients are enabled to take precautionary actions to preserve safety and privacy, keeping them away from potentially dangerous situations. In (Schulze-Bonhage et al. , 2010) some advantages such as avoidance of injuries, increasing the feeling of security, improved working hours, more fruitful leisure times, avoiding embarrassing situations, driving without fear, and reduction of anxiety are mentioned.

Neurostimulation therapies could provide reduction in seizure frequency and intensity, and produce more effective results after several years of implantation (Fisher et al. , 2014).

The immediate reduction in seizure frequency using neurostimulation is approximately 40%, increasing to 50-69% after several years (Fisher et al. , 2014). The performance of neurostimulation systems would be increased significantly if they could be implanted using a closed-loop approach, sending the electrical stimulation pulses in proper times, e.g. prior to seizure onset or within few second after seizure initiation.

During the last decade, there has been a growing progress in commercialization of the seizure intervention systems using neurostimulation techniques. Different USA-based companies have registered patents and produced devices for open-loop and closed-loop neurostimulation of the refractory epilepsy. At the time of writing this thesis, open-loop VNS (by Cyberonics, Inc.) and closed-loop RNS (by NeuroPace, Inc.) have been approved by the USA Food and Drug Administration (FDA), while the DBS (by Medtronic, Inc.) is awaiting the FDA approval. However in Europe the VNS and DBS of the anterior nucleus of thalamus have been already approved, and the RNS system, which is just approved in USA, will probably be approved in near future in Europe. Currently, the RNS system is the solo operational closed-loop neurostimulator for epilepsy therapy. RNS continuously monitors the intracranial EEG signals using four strip electrodes, and releases the electrical stimulation pulses upon detecting abnormal brain activities. Figure 1.1 shows the above mentioned commercialized products.

In a standardized study by Schulze-Bonhage et al. (Schulze-Bonhage et al. , 2010) on 141 epileptic outpatients, including one hundred outpatients from the tertiary epilepsy center at University Hospital Freiburg (Germany) and 41 outpatients from the department of neurology at Coimbra University Hospital, to learn the patients' views on the importance of seizure prediction devices, patients expressed their interest in the development of methods for seizure prediction, both for warning as well as closed-loop interventions. In average, 66.6% of all patients feel that the unpredictability of seizures plays an important (or very important) role in their everyday life. According to this study, in average more than 90% of the patients believed that the development of special tools to predict seizures is important or very important (Schulze-Bonhage et al. , 2010), regardless of the severity of seizures. It is interesting to know that patients going through aura considered, more than other patients, EEG-based seizure prediction efforts to be helpful (Schulze-Bonhage et al. , 2010).

Deep brain stimulator (DBS)
Medtronic, Inc.

Responsive neurostimulator (RNS)
NeuroPace, Inc.

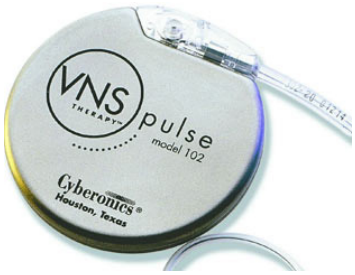

vagus nerve stimulator (VNS)
Cyberonics, Inc.

Figure 1.1 – Some of the current commercialized neurostimulation systems for epilepsy disease

The first step to control epilepsy is the prediction or early detection of seizures, in a way that can be done anytime and anywhere. Prediction and control of seizures can be very difficult due to unknown exact causes, and chaotic nature of the brain. Regarding the current technologies, electroencephalography (EEG) is one way to measure and record brain signals, using some electrodes implanted inside the brain or placed on the scalp skin. Despite emerging technologies such as Magnetic Resonance Imaging (MRI), functional MRI, Magnetoencephalography (MEG), and X-ray Computed Tomography (X-ray CT), EEG remains yet as the most-economic and less-harmful technology for the diagnosis of this widespread disease, and detailed analysis of continuous EEG records can provide us with valuable information regarding such disorders. EEG provides a good temporal resolution for the measurement of instant electrical changes in the brain. Therefore, EEG is widely used as the most important tool in the study of epilepsy.

1.1 Neurophysiology of epilepsy

Epileptic seizure is the abrupt occurrence of highly coherent activity throughout large numbers of neurons inside the brain, which can distort normal brain activity, and which usually lasts from seconds to minutes. Such an activity may be just as simple as to only cause a partial distortion in the consciousness level, or in its severe forms can cause complex abnormal motor and sensory disorders. The most frequent disorders caused by seizures are those with repeating transient changes in the electrical functions of the brain, eventually causing hyperactive and highly synchronous neurons in parts of the brain cortex. These

highly coherent neural activities play the central role in the development of epileptic seizures, usually lasting from seconds to minutes. Among the earliest indications of epilepsy is the presence of transient waveforms (spikes and sharp waves) in the EEG signal. As the seizure develops, the waveforms gradually change into semi-periodic and quite orderly signals having high amplitudes (Figure 1.2). Appearance and magnitude of these waves vary in different patients, but all follow certain patterns.

1.1.1 Seizure types

An epileptic seizure is usually classified according to its origin or seizure onset zone within the brain as well as how it develops and spreads. This can be done using multichannel EEG recordings. Over 40 varieties of epileptic seizures are identified and categorized under two main groups of partial and generalized seizures.

Partial (focal) epilepsy affects around 65% of the epileptic patients and is characterized by seizures which originate from a limited numbers of neuronal clusters in the brain. These patients will exhibit meaningless behaviors such as random walking, mumbling, head turning, or pulling at clothing, none of which can be remembered by the patient after the seizure. The most widespread form of partial epilepsy is the temporal lobe epilepsy (TLE), with mesial temporal lobe (MTLE) and lateral temporal lobe (LTLE) as its two main sub-categories. While MTLE originates from interior parts of the temporal lobe (hippocampus, the parahippocampal gyrus or the amygdala), LTLE originates from exterior surface of the temporal lobe (neocortex) and is less common (Engel, 2001). Frontal lobe epilepsy (FLE) is the second most common type of partial epilepsy after TLE, often occurring during sleep.

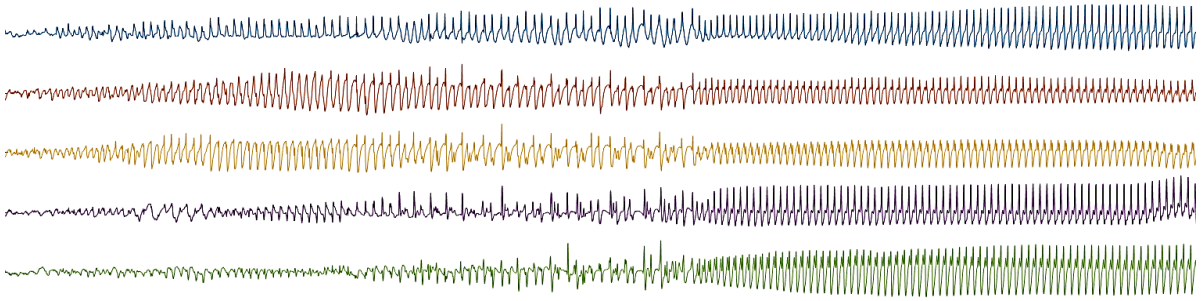

Figure 1.2 – Invasive EEG recordings (30 sec) covering the initial and developed states of an epileptic seizure.

Partial seizures are also sub-classified into simple partial and complex partial seizures. Simple partial seizures (SPS) involving small temporal lobe areas are not that strong to cause a loss of consciousness. Contrarily, complex partial seizures (CPS), which are usually the result of simple partial seizures spreading to larger areas of temporal lobe, are so much strong that throw the patient unconscious, impairing him/her from normally interacting with the surrounding environment. Partial seizures can occur alone, or can be followed by a generalized seizure.

In the generalized epilepsy, the seizure strikes both left/right hemispheres of the brain simultaneously and causes a lack of awareness. The generalized seizure is in a form that, from the very beginning, causes a wide range of sensing/movement changes. These changes can vary from simple local muscle movements in one part, to the more widespread paralyzing activities in the whole body. The tonic-clonic seizure (grand mal) is the most well-known seizure among generalized seizures, during which the patient usually falls to the floor.

From the medical point of view, epilepsy and epileptic seizures can also be studied according to a larger variety of aspects such as from their order of occurrence and frequency to the physiological effects on patient's body. In general, seizures can extend from hundreds per one day in some patients, to just a few in a whole year in some others.

1.1.2 Predictability of seizures

In nature every phenomenon has at least one cause, and epileptic seizure is not an exception. Considering the complexity of the brain, two scenarios are imaginable as the cause of an epileptic seizure (da Silva et al. , 2003). According to the first scenario, some instantaneous factors trigger the epileptic seizure. Although this scenario seems logical due to the sudden nature of seizures, it implicitly implies that we are accepting the unpredictability of the seizures, since it will not be possible to link the seizure with any long term dynamical changes in the brain, and consequently predict the seizure by analyzing the EEG records.

In the second scenario, the pattern distinguishing the seizure is known to be the gradual change in the brain from normal state to the abnormal state, which is evident in the recorded EEG signals (da Silva et al. , 2003). Thus it should be possible to predict seizures before by

using EEG signals. Here, the studies on seizure prediction are developed based on the second scenario, and the results of proposed approaches are supporting the hypothesis of the predictability of most of epileptic seizures. The summary of our contributions in seizure prediction and detection are presented in the next subsection.

1.2 Summary of contributions

This thesis aims to contribute to the development of methodologies with appropriate sensitivity and specificity to be integrated in a transportable device, to alarm in real time the impending seizures or just occurring seizures in refractory epileptic patients. This purpose is approached through two solutions: seizure prediction and early seizure detection. Seizure prediction refers to the reliable prediction of epileptic seizures by minutes or hours in advance. Early seizure detection refers to the electrographic onset detection of a seizure within a few seconds, and preceding the clinical onset, which is the actual cause of disabling clinical symptoms. Several new techniques are introduced for prediction of epileptic seizures. Moreover a very cost-effective yet robust method is proposed for real-time early seizure detection. Furthermore, two novel measures are investigated for the problem of automated seizure event detection. All of the algorithms of this thesis were simulated using MATLAB software package from MathWorks Inc. The summary of our contribution to these epileptic seizure problems is detailed below.

1.2.1 Seizure prediction

Our contributions for seizure prediction can be categorized as two approaches: a relative bivariate prediction method and a novel statistical method for finding optimal preictal period. Our main contribution in seizure prediction is a novel bivariate relative measure based on spectral power features extracted from six EEG recordings. We aimed to improve sensitivity and specificity of prediction methods, and to reduce the number of false alarms. For this purpose, relative combinations of sub-band spectral powers of EEG recordings across all possible channel pairs were utilized for tracking gradual changes preceding seizures. Furthermore, by using a specifically developed feature selection method, a set of

best candidate features were selected and fed to SVM classifier with Gaussian kernel in order to discriminate cerebral state as preictal or non-preictal. The proposed algorithm was evaluated on continuous long-term multichannel surface and invasive recordings of more than 5 months (183 seizures, 3565 hours, for all patients). On average, the best results demonstrated a sensitivity of 75.8% (66 out of 87 seizures) and a false prediction rate of 0.1 h^{-1} on 1537 hours of test data. Performance was validated statistically, and was superior to that of analytical random predictor. We have concluded that applying machine learning methods on a reduced subset of proposed features could predict seizure onsets with high performance. The number of selected features was 9.9 in average showing the efficiency of the introduced relative bivariate features. One of the significances of the study was evaluating on long-term continuous recordings of overall about 5 months, contrarily to the majority of previous studies using short-term fragmented and prepared data. It is of very low computational cost, while providing acceptable levels of alarm sensitivity and specificity.

The second approach specifically deals with preictal period. Supervised machine learning based seizure prediction methods consider preictal period as an important prerequisite parameter during training. However the exact length of preictal state is seizure-specific and ambiguous. The improper selection of this parameter can extensively affect the prediction efficiency, and thus plays a significant role. Therefore, a novel statistical method for finding the optimal preictal period (OPP) to be used in epileptic seizure prediction algorithms was developed. The proposed method uses amplitude distribution histograms of a candidate feature extracted from EEG signals. Additionally, the optimal preictal method can be helpful in two ways. First it can provide a means of measuring the efficiency of a feature, and second it can say whether a specific seizure has distinguishing preictal changes or not. To evaluate this method, spectral power features in different frequency bands were extracted from monopolar and space-differential EEG signals of 18 patients (94 seizures) suffering from pharmacoresistant epilepsy. Results indicated that OPP vary from seizure to seizure even for the same patient. Furthermore comparisons among monopolar with space-differential channels, as well as intracranial EEG (iEEG) and surface EEG (sEEG) signals, indicated that while monopolar signals perform better in iEEG recordings, no significant difference is noticeable in sEEG recordings.

1.2.2 Seizure detection

Nevertheless the long track of efforts on seizure prediction, the findings are still far beyond from being exploitable by clinical applications. Due to low sensitivities and high number of false alarms of the existing prediction methods, they cannot fully satisfy the technical requirements of closed-loop neurostimulation systems. However, thanks to the recent progresses of the neurostimulation systems for epilepsy, which are capable of quickly acting to effectively suppress a good portion of the seizures (Fisher, 2012, Fisher et al. , 2014), one of the objectives of seizure prediction methods may eventually be fulfilled by more realistic approaches of early seizure detection (Jouny et al. , 2011, Kharbouch et al. , 2011, Zheng et al. , 2014a). Therefore, several researchers are working on the early detection of the epileptic seizures as an alternate option, deployable in the closed-loop neurostimulation systems.

In line with that evolution, we have also developed a very low complex yet robust method for early seizure detection using a proposed neuronal potential similarity measure. The power of a bipolar signal is formulated as a neuronal potential similarity criterion between two channels. The method then uses ratio of spectral power features in specific frequency bands, obtained from the bipolar iEEG signal recorded from seizure foci. A threshold based classifier is subsequently applied on the proposed measure to generate the alarms. Our proposed measure could provide high sensitivities, very low number of false alarms, and very short detection latencies in a group of 11 studied patients.

The first requirement for our study was collecting adequately long-term continuous multichannel EEG recordings from epileptic patients, which became possible in the framework of the EPILEPSIAE project. The cumbersome task of visual inspection of these bulky recordings by epileptologists collaborating in the EPILEPSIAE project motivated us for developing new robust and automated seizure event detection methods for the accurate labelling of seizures. The state-of-the-art seizure detection methods suffer from high number of false detections, even when designed to be patient-specific. We have proposed two generalized methods for seizure event detection using a set of two iEEG channels.

The first approach is based on phase synchronization of neuronal activity in different frequency sub-bands. Mean phase coherence (MPC) as a measure of phase synchronization is extracted from the two immediately adjacent iEEG recordings, which were previously bandpass filtered within the desired frequency bands. A threshold-based classifier is applied to generate the alarms. The proposed method was applied on 11 invasive recordings selected from the European Epilepsy Database. The results are compared with the MPC measures extracted from wideband iEEG signals, and show significant improvement for automated epileptic seizure detection. On average the sub-band MPC results attains a sensitivity of 84.2% (154 of 183 seizures in 1785 h recordings) and a false detection rate of 0.09 per hour. Results can be useful in two ways: for automated seizure detection, and for gaining better understanding of the synchronization behavior of epileptic seizures in different frequency bands.

The second proposed method for seizure detection is based on the singular value decomposition (SVD) of bipolar iEEG recordings. The novel idea of our method is applying the SVD on bipolar recordings, which incredibly reduced the number of false alarms, while providing a high sensitivity. Two channels were selected on the foci, as a pairs of very close electrodes. Signals from the electrodes were then subtracted from each other to make a bipolar iEEG signal. The average of specific singular values achieved from SVD of this signal was used as measure. A threshold was subsequently applied on the measures. Results indicate that by using bipolar iEEG channel, one can build more robust algorithms than using a single channel. The method was applied on invasive recordings of 11 patients, containing 183 seizures in 1785 h. On average, the results revealed 84.2% sensitivity and a very low false detection rate of 0.05 per hour in long-term continuous iEEG recordings.

1.2.3 List of publications related to this thesis

1.2.3.1 Journals

1. M. Bandarabadi, C. A. Teixeira, J. Rasekhi, and A. Dourado, "Epileptic seizure prediction using relative spectral power features," *Clinical Neurophysiology,* 2015;126:237-48
2. M. Bandarabadi, J. Rasekhi, C. A. Teixeira, M. R. Karami, and A. Dourado, "On the proper selection of preictal period for seizure prediction," *Epilepsy & Behavior,* 2015.
3. C. A. Teixeira, B. Direito, M. Bandarabadi, M. Le Van Quyen, M. Valderrama, B. Schelter, A. Schulze-Bonhage, V. Navarro, F. Sales, and A. Dourado, "Epileptic seizure predictors based on computational intelligence techniques: A comparative study with 278 patients," *Computer Methods and Programs in Biomedicine,* 2014.
4. J. Rasekhi, M. R. Karami, M. Bandarabadi, C. A. Teixeira, and A. Dourado, "Preprocessing effects of 22 linear univariate features on the performance of seizure prediction methods," *Journal of Neuroscience Methods,* 2013.
5. J. Rasekhi, M. R. Karami, M. Bandarabadi, C. A. Teixeira, and A. Dourado, "Epileptic seizure prediction based on ratio and differential linear univariate features," *Journal of Medical Signals and Sensors*, 2015.
6. M. Bandarabadi, J. Rasekhi, C. A. Teixeira, T. I. Netoff, K. K. Parhi, and A. Dourado, "Early seizure detection using neuronal potential similarity: a generalized low-complexity and robust measure," *International Journal of Neural Systems,* revised and resubmitted, 2015.

1.2.3.2 Book Chapter

1. C. A. Teixeira, G. Favaro, B. Direito, M. Bandarabadi, H. Feldwisch-Drentrup, M. Ihle, C. Alvarado, M. Le Van Quyen, B. Schelter, A. Schulze-Bonhage, F. Sales, V. Navarro, and A. Dourado, "Brainatic: A System for Real-Time Epileptic Seizure Prediction," in *Brain-Computer Interface Research.* vol. 6, ed: Springer, 2014, pp. 7-18.

1.2.3.3 Conference proceedings

1. M. Bandarabadi, J. Rasekhi, C. A. Teixeira, and A. Dourado, "Epileptic Seizure Detection Using Bipolar Singular Value Decomposition," in *8th international conference on bio-inspired systems and signal processing, Biosignals 2015*, Lisbon, Portugal.
2. M. Bandarabadi, C. A. Teixeira, T. I. Netoff, K. K. Parhi, and A. Dourado, "Robust and Low Complexity Algorithms for Seizure Detection," in *Engineering in Medicine and Biology Society, EMBC, 2014 36th Annual International Conference of the IEEE*, 2014, Chicago, USA.
3. M. Bandarabadi, J. Rasekhi, C. A. Teixeira, and A. Dourado, "Sub-band Mean Phase Coherence for Automated Epileptic Seizure Detection," in *The International Conference on Health Informatics*. vol. 42, Y.-T. Zhang, Ed., ed: Springer International Publishing, 2014, pp. 319-322.

4. M. Bandarabadi, J. Rasekhi, C. A. Teixeira, and A. Dourado, "Optimal preictal period in seizure prediction," in *Bioinformatics and Biomedical Engineering, 2014, IWBBIO 2014, 2nd International Work-Conference on*, 2014, Granada, Spain.
5. B. Direito, C. A. Teixeira, M. Bandarabadi, F. Sales, and A. Dourado, "Automatic warning of epileptic seizures by SVM: the long road ahead to success," in *Automatic Control, 2014. IFAC '14, 19th World Congress of the International Federation of*, 2014, Cape Town, South Africa.
6. M. Bandarabadi, A. Dourado, C. A. Teixeira, T. I. Netoff, and K. K. Parhi, "Seizure prediction with bipolar spectral power features using Adaboost and SVM classifiers," in *Engineering in Medicine and Biology Society, EMBC, 2013 35th Annual International Conference of the IEEE*, 2013, pp. 6305-6308, Osaka, Japan.
7. C. A. Teixeira, B. Direito, M. Bandarabadi, H. P. Grebe, F. Sa, F. Sales, A. Dourado, "Real-time epileptic seizure prediction at Centro Hospitalar e Universitario de Coimbra," in *Experiment@ International Conference (exp.at'13), 2013 2nd*, 2013, pp. 196-198, Coimbra, Portugal.
8. M. Bandarabadi, C. A. Teixeira, B. Direito, A. Dourado, "Epileptic seizure prediction based on a bivariate spectral power methodology," in *Engineering in Medicine and Biology Society, EMBC, 2012 34th Annual International Conference of the IEEE*, 2012, pp. 5943-5946, San Diago, USA.
9. C. A. Teixeira, B. Direito, M. Bandarabadi, and A. Dourado, "Output regularization of SVM seizure predictors: Kalman Filter versus the "Firing Power" method," in *Engineering in Medicine and Biology Society, EMBC, 2012 Annual International Conference of the IEEE*, 2012, pp. 6530-6533, San Diago, USA.
10. M. Bandarabadi, C. A. Teixeira, F. Sales, and A. Dourado, "Wepilet, optimal orthogonal wavelets for epileptic seizure prediction with one single surface channel," in *Engineering in Medicine and Biology Society, EMBC, 2011 Annual International Conference of the IEEE*, 2011, pp. 7059-7062, Boston, USA.

1.2.3.4 Abstracts in conference proceedings

1. M. Bandarabadi, and A. Dourado, "A Robust Low Complexity Algorithm for Real-Time Epileptic Seizure Detection," in *11th European Congress on Epileptology*, 2014, Stockholm, Sweden.
2. A. Dourado, C. A. Teixeira, B. Direito, M. Bandarabadi, and F. Ventura, "Data Mining in Electroencephalogram with the Aim of Epileptic Seizure Prediction," in *11th Annual European Network for Business and Industrial Statistics (ENBIS) Conference,* 2011, Coimbra, Portugal.

1.3 Thesis outline

This thesis is organized in six chapters. In chapter 2, the theoretical and technical aspects of seizure prediction and detection are presented. Different types of electroencephalography are explained with some examples. It provides a brief description of the prerequisite definitions and clinical issues concerning seizure prediction and detection. Major techniques used in the thesis, including spectral power analysis, support vector machine classifier, regularization using firing power method, and random predictor will be reviewed. Furthermore the performance metrics in seizure prediction and detection will be addressed.

Chapter 3 is devoted to the reviews of the prior studies and achievements in seizure prediction and detection during the last four decades. This Chapter is organized by features, and according to linear/nonlinear and univariate/bivariate analysis. Moreover the recent studies using combination of various features and employing computational intelligence methods are summarized. Furthermore some studies on self-prediction of seizures using prodromal symptoms are pointed out.

Our contributions to seizure prediction are demonstrated in chapter 4. The first section of this chapter covers our main contribution. The proposed method uses the ratio of spectral power features across six EEG channels, which are then pre-processed by normalization and smoothing. A feature selection scheme is developed, and applied to the resulting high dimensional feature space. A reduced set of these features is then fed to nonlinear SVM classifier, followed by a moving average window regularization stage along with some constraints to generate alarms. In the second section of this chapter a novel statistical approach for proper selection of the preictal period is presented, which can also be considered either as a measure of predictability of a seizure or as the prediction capability of an understudy feature. The method is applied on spectral power features estimated from monopolar/bipolar iEEG/sEEG signals of 18 patients, providing comparison between monopolar and bipolar EEG analysis in seizure prediction, as well as surface versus invasive recordings.

In chapter 5, three different approaches are presented for seizure onset and event detection. The seizure onset detection method, also referred to as early seizure detection, is aimed to provide high performance detection and low detection latency for closed-loop neurostimulation systems. The early detection method employs power spectral density of a single bipolar iEEG channel, and is very cost effective for implantable low-power-budget hardware devices. Furthermore to facilitate long-term continuous monitoring of EEG recordings by experts in the clinical studies, two novel approaches are introduced for automated labelling of seizure events. All of these three methods are applied on the same intracranial EEG recordings of 11 patients.

Chapter 6 concludes the thesis with a discussion of the findings, and suggesting potential road plans for future researches on seizure prediction and detection.

Chapter 2 Background and problem statement

This chapter is dedicated to the theoretical and technical aspects of seizure prediction and detection using EEG signals. First an overview of electroencephalography and its types is presented, followed by the concept of moving window analysis of EEG signals. Afterwards some prerequisite definitions and clinical issues of seizure prediction and detection are summarized. Subsequently some technical methods used in this thesis are briefly described. Also, the final section of this chapter presents the performance evaluation metrics in seizure prediction and detection.

2.1 Electroencephalography

Human brain comprises a complex network of neurons highly interconnected through axons. As these interconnections are electrochemical, both electrical and magnetic fields are produced in the vicinity of the induced electrical currents. The electrical field can be recorded using electroencephalography, while the magnetic field can be recorded using Magnetoencephalography (MEG).

EEG measures the electrical potentials generated by neurons of the brain over the time, and contains important information about its physiological and pathological state. In electroencephalography, the signal recorded from each individual electrode represents the electrical activity of bunch of neurons located in the vicinity of that electrode. By this, the microscopic electrical activity of neurons is translated into macroscopic recordings of electrodes. EEG patterns involve generic ordinary states, and any deviation from those states, would indicate abnormal condition in the brain. The EEG signal contains special waveforms with different amplitudes and frequencies, which are capable of describing various patterns like resting, consciousness and some neurological diseases.

2.1.1 Intracranial and surface EEG

Recording electrical brain signals can be done both in an invasive or a non-invasive way. Electrocorticography (ECoG) is an example of invasive recording also known as intracranial EEG (iEEG), in which electrodes are inserted into the brain and remain in direct contact with the brain tissue. On the other hand, surface EEG (sEEG) recording is the non-invasive way of electrical recording, where the electrodes are placed over the scalp. For surface recording there exist several standard electrode placement configurations among which the international 10-20 system is the most well-known. However for invasive electrode placement there is no unique standard and the positions of implanted electrodes depend upon the particular study requirements. Figure 2.1 shows the invasive and surface electrodes.

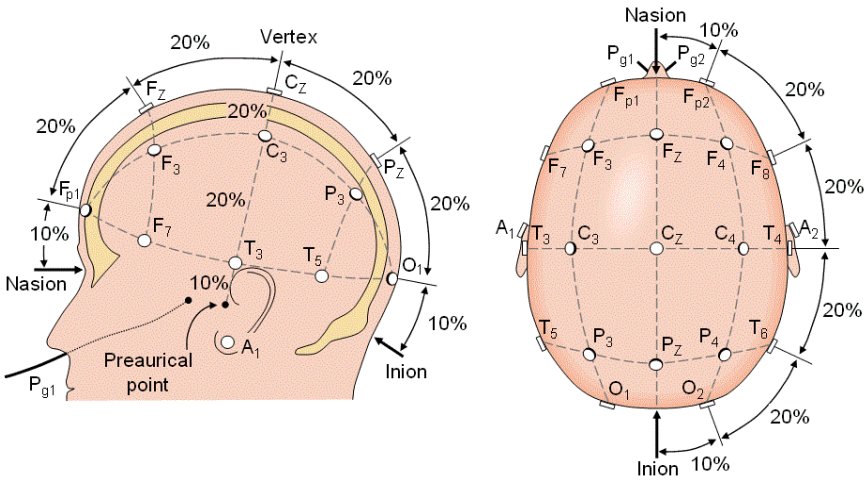

(a) International 10-20 system electrode placement (Malmivuo et al. , 2002)

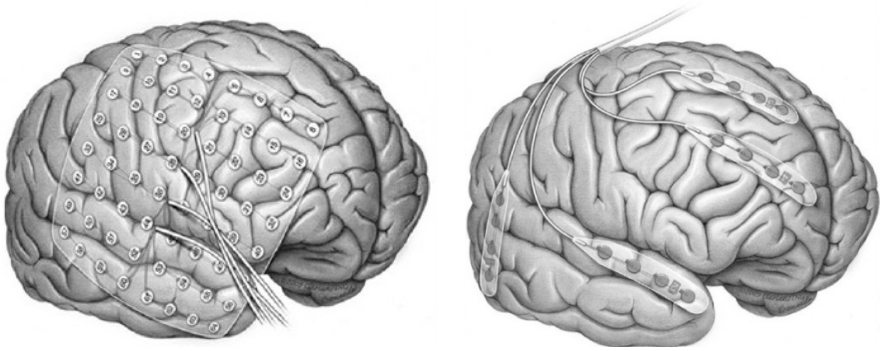

(b) Grid (left) and strip (right) electrodes for invasive EEG recording (Voorhies et al. , 2013)

Figure 2.1 – Surface and intracranial EEG electrodes

Time-frequency analysis of the signals recorded from different electrode sites would indicate that although the signals of distinct electrodes at any instant of time contain similar frequencies, the amplitudes of these frequencies vary among the different electrodes. The reason is that the recorded signals include the attenuated effects of the electrical activities from different parts of the brain (Figure 2.2). This issue is more severe in sEEG, as the electrodes are placed a little far away from the desired electrical source locations, and recorded through the skull. This is the major drawback of the non-invasive brain signal recording methods such as 10-20 system. As an example, electrode X_1 in Figure 2.2 is used to measure the electrical activities of region S_1. However, since electrical fields are present across the whole space surrounding their source, this electrode will also capture the electrical activities from S_2, S_3 and S_4 regions with a weaker intensity, and will thereby contain the information from those parts of the brain.

Although the sEEG recording cannot provide localized neuronal potential activities, it can present a more generalized spatiotemporal view of brain's dynamical system. Among the advantages of the invasive methods are the high signal to noise ratio (SNR) and the localized recording of the brain activity by minimizing the unwanted interferences from other brain sites on the signals recorded from the region of interest. Figure 2.3 depicts the simultaneously recorded multichannel sEEG and iEEG signals of a sample seizure.

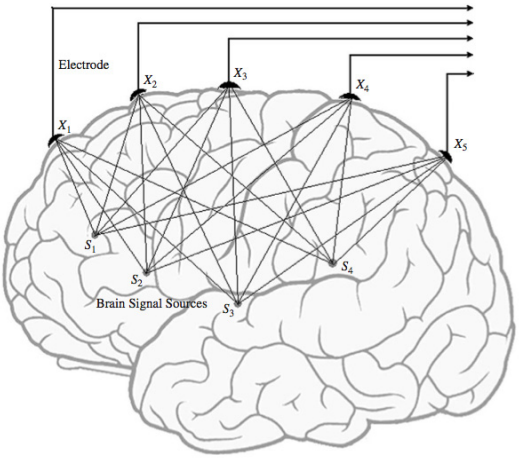

Figure 2.2 – EEG recordings are mixed of electrical activities of different brain parts (Sanei et al. , 2008)

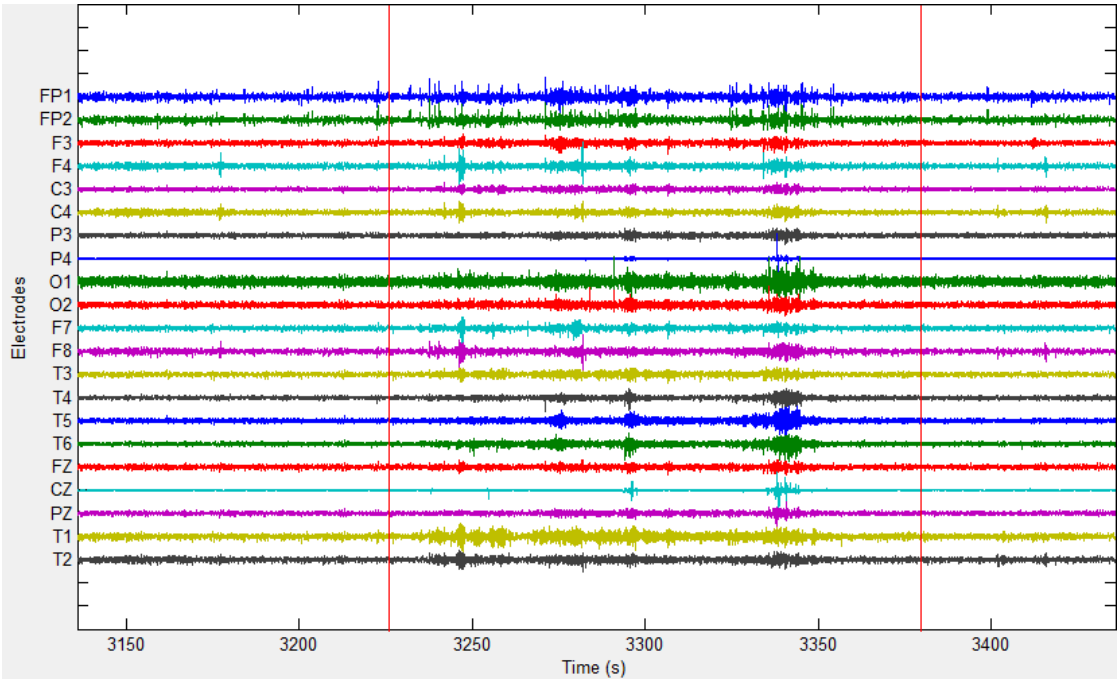

(a) Surface EEG recordings

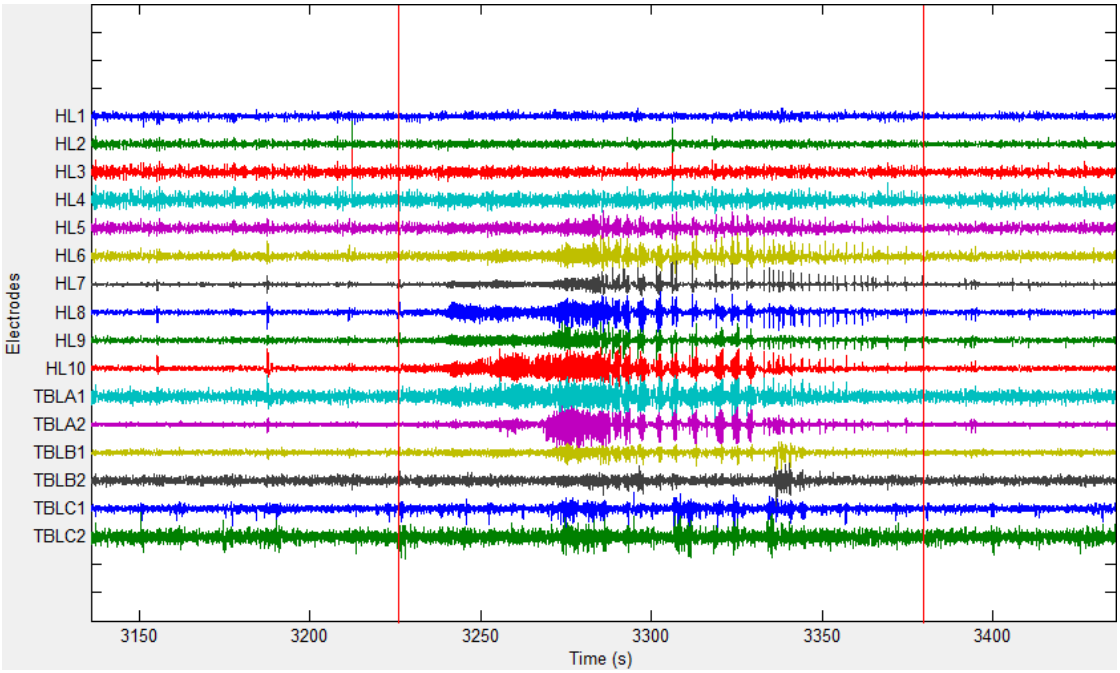

(b) Invasive EEG recordings

Figure 2.3 – Multichannel sEEG and iEEG signals of a sample seizure recorded simultaneously. The vertical red lines indicate seizure onset and offset times.

2.1.2 Bipolar electroencephalogram

EEG is an electrical potential difference measured between an electrode over the region of interest and a fixed reference electrode, and is therefore bipolar by nature. The positioning of electrodes and reference channels can both affect the nature of the recorded signal (Nunez et al. , 1997). By tradition however, these voltages between an electrode and the fixed reference are called monopolar signals or channels, and the difference of two monopolar signals, selected physically in close proximity, is known as bipolar signal or channel. The bipolar montage can also be directly derived by considering just two adjacent electrodes during recording, where the signals of two electrodes are being passed in to the inputs of an amplifier. For sufficiently close-by configurations, the bipolar signal may be considered as an approximation of the tangential component of brain's electrical field (Wendel et al. , 2009).

Contrary to the monopolar iEEG, the bipolar montage is less susceptible to artifacts (Aarabi et al. , 2007) and provides better spatial resolution (Srinivasan et al. , 1996, Nunez et al. , 1997, Tang et al. , 2007). Bipolar processing can remove common mode interferences mounted evenly on the two adjacent electrodes. These common mode interferences may include physiological artifacts, e.g. electromyogram (EMG) and eye movement artifacts, or non-physiological artifacts, e.g. power line noise (50 or 60 Hz and their harmonics). Bipolar recordings can better reduce the volume conduction effects compared to the monopolar recordings, by acting as a high-pass spatial filter (Nunez et al. , 1997). Moreover, topographical variations invisible to monopolar recordings can be identified using bipolar schemes (Baranov-Krylov et al. , 2005). In this thesis, bipolar iEEG channel was derived by subtracting the signals from two immediately adjacent iEEG electrodes, selected from a candidate probe array on foci. Array can be in the form of grid, strip, or depth probes.

2.1.3 Moving window analysis

It is common practice in detection and prediction studies, to first segment the continuous EEG recordings into windows of short lengths prior to feature extraction. This process is referred to as the moving window analysis of EEG signals, with consecutive windows which may or may not overlap with each other depending upon the step size. In the

case of overlapping, a portion of signal is shared among the two consecutive windows. Moreover the moving window analysis will allow performing simulations close to real-time, where there is no access to the future data, and the designed algorithm first has to buffer a sufficient amount of sampled data, e.g. 5 seconds, and then apply the desired methodology on this data to make decisions about the brain's state. Then the algorithm should wait again for the next portion of data to be recorded and analyzed.

In this thesis, we consider different window lengths for seizure prediction and detection. For prediction, since the preictal period is assumed to be of gradual changes prior to seizure onsets, within a time duration in a range of tens of minutes, therefore longer windows of either non-overlapping 5-sec (for the first study) or half-overlapped 8-sec (for the second study) are considered. However, for detection studies, since the ictal period is relatively short, and we are interested to detect seizures in their early initiation states, therefore a window length of 2 seconds with 50% overlap is employed, providing alarm generation every second.

2.2 Prerequisite definitions

Before starting the state of the art chapter on seizure detection and prediction methods, it is necessary to become familiar with the general concepts used by researchers of this field. Studies by neurologists, categorize brain activity in epileptic patients into four states (Figure 2.4): interictal (normal), preictal (before seizure), ictal (across seizure) and postictal (after seizure). Preictal is the state just before the seizure, which is to be detected in order to predict the proceeding seizure; depending on the starting time of seizure symptoms, the preictal can cover from several seconds up to several hours before the seizure (Litt et al. , 2002, Ebersole, 2005, Mormann et al. , 2007). Ictal state is the time period in which seizure happens. Postictal state encompasses the moments after seizure onset. Interictal state, during which the patient enjoys a normal brain activity, is the interval beginning right after the postictal state of a seizure and ending before the preictal state of the next seizure. The prime goal in seizure prediction is to distinguish the preictal period against the rest of these states, whereas in seizure detection the adequate identification of the ictal state among these four states is the objective.

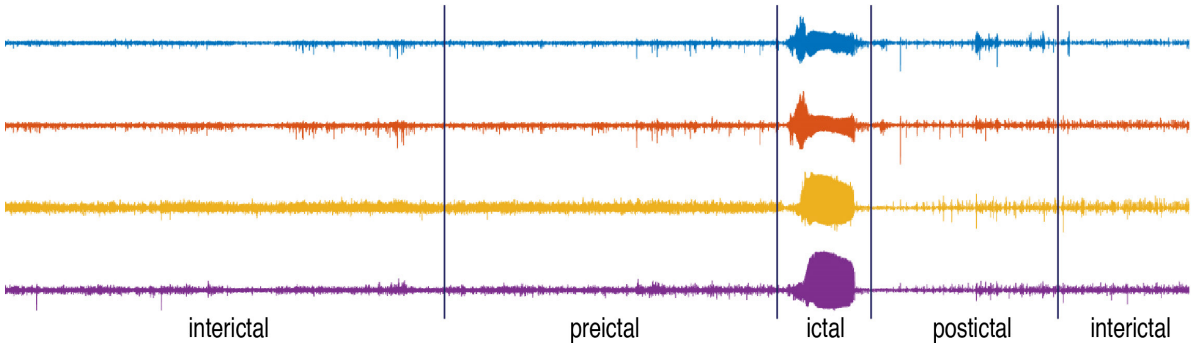

Figure 2.4 – Epileptic brain states; interictal, preictal, ictal, and postictal

The ictal period can be identified precisely by epileptologists through the visual inspection of EEG recordings, as well as the video monitoring of patients during their stay in the hospital. A postictal state can also be estimated either by looking at EEG patterns following a seizure event, or by applying complex EEG based techniques. However, the correct identification of the preictal period is a matter of controversy, for which there is no clinical agreement among experts. The choice of preictal length is a major issue with seizure prediction algorithms, and may differ from patient to patient, and even among the seizures of a patient. To tackle this issue, researchers have therefore defined some common definitions.

Also EEG patterns can change significantly according to the daily living conditions, such as the level of activity, awareness, sleep stage, and tiredness, further complicating seizure prediction and detection. Additionally demanding brain functions such as study and thinking would alter different levels of neuronal activities, which add up to the electrical fields of the brain. In presence of such interfering parameters, extraction of preictal and ictal patterns sometimes becomes very difficult, and can be easily mistaken by other brain activities.

An epileptic seizure prediction system should ideally pinpoint the exact moment of seizure onsets, a goal that has not yet been practically possible. Instead, algorithms are developed which try to distinguish specific time periods having highest seizure occurrence chances. This time period is simply known as seizure occurrence period (SOP), and is a major prerequisite in developing prediction algorithms. Since preictal period cannot be defined precisely and varies among seizures and patients, it is usually a rule of thumb to use

the SOP time as preictal period. In this respect, a prediction is marked as true, if the alarm is raised inside an SOP window preceding the seizure onset.

2.2.1 Clinical discussions

Adequate selection of preictal interval is very important for seizure prediction methods, and proper choices on one hand should increase the efficiency of the prediction algorithm, and on the other hand should improve the physical/emotional living conditions of the patient. A prediction algorithm is essentially favored by the refractory epileptic patients, if it can satisfactorily provide them with both physical and emotional relief. An excessively long preictal period may expose the patients to high emotional stresses, and is psychologically unpleasant. Therefore it is necessary to define an upper bound value for the preictal time. In the study by Schulze-Bonhage et al. (Schulze-Bonhage et al. , 2010) on 141 epileptic patients, more than 89.9% of the patients preferred SOPs of less than 1 hour long. 47.4% of patients considered 10 minutes as optimal, whereas only 9.2% of patients regarded ≥3 hours a good prediction window. Based on two separate studies by Mormann et al. (Mormann et al. , 2006) and Schelter et al. (Schelter et al. , 2007), most patients preferred a relatively short seizure prediction window. However, the suggestion of longer but seizure-prone periods was also considered worthwhile (Schulze-Bonhage et al. , 2010).

A prediction system capable of generating alarms even tens of seconds in advance of a seizure will be quite satisfactory to keep patients safe from dangerous situations. Apart from what the patients expect, the choice of preictal time is also dependent on and constrained by the particular prevention algorithm of interest. Although prediction is always an important issue for patients' safety, however with the recent progresses in neurostimulation systems, early seizure detection methods have found practical applications for closed-loop fast acting neurostimulation systems, which require only few seconds to affect and suppress oncoming seizures.

In every detection/prediction algorithm, a percent of false alarms is inevitable. Such errors could have various origins, both intrinsic and induced. For every false prediction, patient has to be prepared for the seizure, which will never occur. For the cases where closed-

loop neurostimulation or AED injection systems are employed to prevent seizures, higher false alarm rates will increase the side-effects of unnecessary neurostimulation or drugs. Also, accumulated side-effects of the neurostimulation or drugs can themselves cause other neural disorders. Moreover, for such excessive false prediction rates, patients may either not consider generated alarms seriously even those of true predictions, or would go through intensive psychological stresses. Depending upon preventing methods, the acceptable range for false detection/prediction rates could be different and has to be determined and validated clinically.

2.3 Technical background

2.3.1 Spectral analysis of electroencephalogram signals

Power spectral density (PSD) indicates the distribution of power of a signal or time series within frequencies (Dressler et al. , 2004). The PSD is calculated based on the assumption that the EEG signal is statistically stationary, thus the raw EEG signal is first segmented into short windows to minimize nonstationarity effects. The length of window was selected by a tradeoff between two extremes: it should be long enough to cover the trends related to brain's current state, and short enough to be considered as quasistationary. Normally the PSD has a dimension of watts per hertz ($W.Hz^{-1}$). It is also common to use units of $V^2.Hz^{-1}$ for the PSD of voltage (V) signals (Norton et al. , 2003). To compute the spectral power of desired sub-bands, an integration/summation over PSD values is the only required operation. Spectral power of sub-bands can be expressed in the form of absolute or normalized values. The absolute values are calculated by (2.1),

$$P_i = \sum_i PSD(x) \tag{2.1}$$

where p_i is the spectral power of *i*-th sub-band, *x* is the windowed raw EEG signal, *i* indexes the *i*-th frequency sub-band, and $PSD(x)$ is the PSD of the signal. The normalized spectral power feature for a given sub-band was computed by dividing the spectral power of the sub-band by the total power as in (2.2).

$$NP_i = \frac{P_i}{P_{tot}} = \sum_i PSD(x) \Big/ \sum_{tot} PSD(x) \tag{2.2}$$

Compared with using absolute values, normalized values decrease the effect of total power changes on spectral power of sub-bands (Van Laar et al. , 2011). Absolute values are completely dependent upon the overall power of the signal. Since the power of the signal changes with different daily life parameters of the patient, such as sleep state, consciousness level, physical or mental activities, absolute values can easily change. In contrast, normalized values are more robust (with respect to the fluctuations in the patient's daily life) for revealing the preictal state.

Furthermore the computational cost for PSD estimation is very low. For instance, Parhi et al. (Parhi et al. , 2014) proposed a low-complexity Welch's PSD computation mechanism using 65nm technology and 1-Volt supplying power. The power consumption and hardware area of their method was around 210 *nJ* and 176 um^2 respectively, for PSD calculation of 8 overlapping segments of length 1024 samples each.

2.3.2 Mean phase coherence

Neuronal signal synchrony is an indication of phase synchrony between the two signals recorded from two brain regions. During epileptic seizure development, neurons in the focus start firing up in a synchronous fashion. Therefore quantization, measurement and detection of the phase synchrony provide a mechanism of detecting seizures. Mean Phase Coherence (MPC) has been considered as the most prominent statistical tool for measuring phase synchrony (Mormann et al. , 2000).

The MPC measure is explained here. Suppose two real time series $x_1(t)$ and $x_2(t)$, having amplitude and phase differences. In every instant of time, the instantaneous phases of $x_1(t)$ and $x_2(t)$ are determined as $\phi_{x_1}(t)$ and $\phi_{x_2}(t)$ respectively. Based on the analytic signal processing approach, one can first start from the analytic form of $x(t)$ as (2.3),

$$Z_x(t) = x(t) + i\tilde{x}(t) = A_x^H e^{i\phi_x^H(t)} \tag{2.3}$$

where $\tilde{x}(t)$ is the Hilbert transform of $x(t)$,

$$\tilde{x}(t) = \frac{1}{\pi} p.v. \int_{-\infty}^{+\infty} \frac{x(t')}{(t-t')} dt' \tag{2.4}$$

where *p.v.* stands for the Cauchy principal value. Now it is possible to obtain the Hilbert phase $\phi_x^H(t)$ using the analytic signal (2.5),

$$\phi_x^H(t) = \tan^{-1}\left(\frac{\tilde{x}(t)}{x(t)}\right) \tag{2.5}$$

Hence, if $x_1(t)$ and $x_2(t)$ are two real signals with instantaneous phases of $\phi_{x_1}^H(t)$ and $\phi_{x_2}^H(t)$, they are said to be phase locked in case the following restriction holds (2.6),

$$m.\phi_{x_1}^H(t) - n.\phi_{x_2}^H(t) = cte \tag{2.6}$$

where *m* and *n* are integers, and *cte* is a constant value. For real life signals however, this is hard to hold and is usually replaced by much loose criterions such as in phase entrainment measure (2.7).

$$\left| m.\phi_{x_1}^H(t) - n.\phi_{x_2}^H(t) \right| < cte \tag{2.7}$$

MPC is an special case of phase entrainment where $m = n$, and is obtained mathematically by averaging on absolute instantaneous phase differences of two signals (Mormann et al. , 2000) as (2.8),

$$M = \left| \frac{1}{N} \sum_{j=1}^{N} e^{j[\phi_{x_1}^H(t_j) - \phi_{x_2}^H(t_j)]} \right| \tag{2.8}$$

where *N* is length of the signals. Also, *M* is a value falling in the interval [0 1], where *M*=1 and *M*=0 indicate complete synchrony and complete asynchrony respectively.

2.3.3 Minimum redundancy maximum relevance feature selection

Feature selection refers to finding a subset of features which can retain enough discriminative information for clustering or classification methods, while improving the overall performance. Most of the feature selection approaches attempt to find those features with highest relevance to the target classes, and possessing the maximum discriminative capability (Saeys et al. , 2007). However, there may exist many features which have duplicate information within the selected subset. To further reduce from the dimension of the selected features, one approach may try to remove from those redundant features in the selected subset. Minimum redundancy maximum relevance (mRMR) feature selection method was developed to approach this dual objective optimization problem (Peng et al. , 2005). The first objective is to find a subset of features, among which the mutual information is minimized. This leads to minimum redundancy between the features of the subset. The second objective is the maximum relevancy of the selected features to the target classes.

2.3.4 Support vector machine classifier

Support vector machines (SVM) are commonly used supervised classifiers (Schölkopf et al. , 2002, Lopes et al. , 2015), and were adopted for our classification problems because they have good generalization capabilities. They exploit the statistical learning theory (Vapnik, 1998). SVM classifiers in their simplest form use linear boundaries to classify two-class data. To classify more complex datasets with nonlinear boundaries (i.e. datasets that are not linearly separable, as is the case in this thesis), SVM use a special transformation of the features space into a higher order space where linear boundaries may eventually separate the data into two classes. We can say that the transformation linearizes the space. This transformation may be done implicitly by using special functions (the so-called kernel functions) and vector operations. The Gaussian radial basis function (RBF) kernel is one of the most used kernels for nonlinear classification problems, and is defined by (2.9),

$$K(x_i, x_j) = \exp\left(\frac{-\left\|x_i - x_j\right\|^2}{2\sigma^2}\right) \tag{2.9}$$

where σ is the scale parameter (openness of the Gaussian), and x_i is feature vector in the original input space; it replaces each point in the feature space by the Gaussian of its squared Euclidean distance from support vectors. With the Gaussian kernel, there are two parameters to control the classification performance: the scale parameter σ and the soft margin parameter of C. The parameter C controls the tradeoff between maximization of the margin width (with respect to the classification boundary) and the minimization of the number of misclassified samples in the training set (Schölkopf et al. , 2002); the larger the margin, the higher misclassified samples. In turn, the scale parameter σ controls the width of the Gaussian surface of the RBF kernel.

2.3.5 Alarm generation using firing power method

Classifiers are essentially defined to generate independent outputs for the input test samples, and not all samples are usually correctly classified. This issue becomes severe with EEG prediction where sample feature lengths are in the range of few seconds. As a result, pure hard classification schemes may eventually lead to a significant number of false alarms. The regularization methods are therefore designed to reduce the number of false alarms by taking the most recent classifications into account by making some corrective manipulations on the classifier outputs.

Kalman filter and moving average window methods are two common approaches for regularization of classifier outputs. In this thesis we investigated a modified version of moving average window with some conditions for the regularization of the SVM outputs, called the firing power (FP) method and proposed in (Teixeira et al. , 2011). In a comparative study, we observed the superiority of FP method over Kalman filter (Teixeira et al. , 2012). Using a sliding window with a size equal to the preictal period, the FP measure is computed by (2.10),

$$FP[n] = \frac{\sum_{k=n-\tau}^{n} O[k]}{\tau} \tag{2.10}$$

where $FP[n]$ is the FP at the discrete time n, τ is the number of samples during one preictal period, and $O[k]$ is the output of the two-class SVM classifier for the k-th test sample. If $O[k]=1$, the k-th sample is classified as preictal and if $O[k]=0$ as non-preictal. Non-preictal state covers the three states of ictal, postictal, and interictal. The FP measure quantifies the relative number of samples classified as preictal class inside a moving window with a length equal to the preictal period. Suppose a preictal period of 30 minutes covering 360 feature samples, each extracted from a 5-sec window. The FP is calculated at every moment based on the past 360 samples (τ =360). A firing power of one indicates that all of the samples from the past preictal period have been classified as preictal.

Furthermore, the regularized output of $FP[n]$ is normalized between zero and one, and some decision-making is necessary as the final step to generate alarm. The threshold 0.5 is selected here: if the regularized output is equal or greater than 0.5 then 50% or more of the samples are classified as preictal and the methodology decides that we are in face of a preictal situation, raising an alarm. After an alarm is raised, there are two limitations on raising other alarms, which should hold together: (i) generation of more alarms is inhibited during a time interval equal to the preictal period. This constraint guarantees the generation of only one single true alarm per seizure; (ii) after a preictal period is passed the $FP[n]$ must first fall below the threshold level, resetting the normal alarm generation, before another alarm is raised by another threshold overpassing. This prevents false alarms.

2.4 Performance evaluation

2.4.1 Performance metrics in seizure prediction

Two parameters of sensitivity (SS) and false prediction rate (FPR) are more commonly used in comparing prediction methods. Sensitivity is the measure of the system's ability for correct prediction of seizures and is defined as the fraction of correctly predicted seizures within the total number of seizures (2.11).

$$SS = \frac{Correctly\ predicted\ seizures}{Total\ number\ of\ seizures} \times 100 \tag{2.11}$$

In practice, false predictions are inevitable and represented by the false prediction rate (FPR) parameter. The FPR is the number of false predictions per time interval, here per hour. Unfortunately, both parameters cannot be optimally set simultaneously, as improving one means worsening the other. Therefore a tradeoff has to be made in their selection. As an example, during preictal period where amplitude of the signals increases significantly, one can make predictions choosing a threshold level. For a relatively low threshold level, all 100% of seizures will be correctly predicted while FPR will increase. In contrast higher thresholds will decrease FPR while decreasing sensitivity.

2.4.2 Performance metrics in seizure onset/event detection

The performance of the proposed methods for seizure event detection usually is evaluated in terms of sensitivity (SS) and false detection rate (FDR), whereas for early seizure detection (onset detection) is evaluated using SS, FDR, and mean detection latency from electrographic onset (MDLE). Sensitivity is the fraction of correctly detected seizures within the total seizures. A seizure is detected correctly if the alarm is raised inside the ictal period, as marked by epileptologists. FDR is the number of false detections per time unit (here per hour). A false detection is a raised alarm outside the ictal period. MDLE refers to the average of time gaps between the actual electrographic seizure onset occurrence times and the times of raising the corresponding true alarms. Unfortunately, the three parameters of SS, FDR, and MDLE cannot be simultaneously set optimally. Again, as improving one leads to worsening of others, a tradeoff has to be made in their selection.

2.4.3 Statistical validation of performance

The performance of a proposed seizure prediction methods should naturally exceed that of a random predictor, which is not aware of any information contained in the studied EEG signals (Winterhalder et al. , 2003). To verify the superiority of the proposed methods for seizure prediction, we have compared our results with those achieved from the analytical random predictor (RP) introduced by (Schelter et al. , 2006). The probability of a random

seizure predictor to raise at least one alarm during a preictal period (SOP), for a maximum false prediction rate (FPR_{max}), is given by (2.12).

$$P = 1 - e^{-FPR_{\max} \times SOP} \tag{2.12}$$

Moreover, it is usually necessary to study more than one seizure to ensure sensitivity reliability. Therefore, assuming that all seizures occur independently from each other, the probability of predicting by chance the *n* out of *N* seizures will follow a binomial distribution and can be written as (2.13) (Schelter et al. , 2006, Feldwisch-Drentrup et al. , 2011b).

$$P_{Binom}\{n; N; P\} = \sum_{j \geq n} \binom{N}{j} P^j (1-P)^{N-j} \tag{2.13}$$

Some parameters of prediction algorithms such as preictal period, localization and number of selected channels can be optimized to improve the prediction performance (Schelter et al. , 2006, Feldwisch-Drentrup et al. , 2011b). Accordingly, the random predictor (RP) should be updated to incorporate the optimization effect, and improvement of performance. If d independent optimizations are applied on the method, the probability to randomly predict at least *n* out of *N* seizures by at least one of the d optimizations is obtained as (2.14).

$$P_{Binom,d}\{n; N; P\} = 1 - \left[1 - \sum_{j \geq n} \binom{N}{j} P^j (1-P)^{N-j}\right]^d \tag{2.14}$$

In this study we examined four different preictal periods to find the optimized one, thus we considered *d=4*. The critical sensitivity of the corresponding analytical random predictor is (2.15),

$$SS_{RP} = \frac{\arg\max_n \left\{P_{Binom,d}\{n; N; P\} > \alpha_{RP}\right\}}{N} \times 100\% \tag{2.15}$$

where α_{RP} is a significance level. Any sensitivity above this SS_{RP} value could be regarded as statistically significant. A significant cutoff of $\alpha_{RP} = 0.05$ was selected in this thesis.

Chapter 3 The last 40 years of seizure prediction and detection

In this chapter we review the past efforts on seizure prediction and detection. We start from the first studies on seizure prediction reported around 40 years ago, and then move on to the current findings. Recently there is a growing research interest on these problems, especially considering the last 10 years. We attempted to cover as many important studies as possible, reported by different groups and using different methods. Furthermore a literature review of seizure detection methods will be presented.

3.1 Past efforts in seizure prediction

The objective of seizure predicting algorithms is to find patterns appearing during preictal state, i.e. a transition state between interictal and ictal states. Prediction methods are possible if one can find features that will change in the preictal state, and if one can find a set of features that change throughout all preictal states, then the epileptic seizure prediction problem may be solved. Up to now, many researches have been made on epileptic seizure prediction, most of which believe and show results indicating that seizure is predictable (Le Van Quyen et al. , 2001, D'Alessandro et al. , 2003, Iasemidis, 2003, Le Van Quyen et al. , 2005, Lehnertz et al. , 2005, Mormann et al. , 2005, Mormann et al. , 2007, Park et al. , 2011, Stacey et al. , 2011, Rasekhi et al. , 2013, Howbert et al. , 2014).

In spite of the recent progresses and the state of the art knowledge on epilepsy, the prediction and control of epileptic seizures is still a hard problem to tackle. In fact, although around 40 years have passed from the first published study on physiology of seizures (Viglione et al. , 1975), and after the development of numerous prediction methods,

researchers are still far from a complete and reliable approach which can practically be used in real medical applications. The main drawback with most of these studies is that they were not properly evaluated, i.e., they were not applied for long-term continuous situations close to the real conditions, making impossible to evaluate the clinical validity of the proposed approaches (Mormann et al. , 2007, Andrzejak et al. , 2009, Stacey et al. , 2011).

Epileptic seizure prediction was exercised traditionally either by simply applying threshold to a given measure extracted from the EEG (Schelter et al. , 2006), or by nonlinear analysis (Le Van Quyen et al. , 2001, Lehnertz et al. , 2003). More recently, classification methods based on high-dimensional feature spaces were used to detect the preictal state (Chisci et al. , 2010, Park et al. , 2011, Cabrerizo et al. , 2012, Rasekhi et al. , 2013, Teixeira et al. , 2014b).

A univariate measure refers to the quantization of single-channel electrical activities. In univariate seizure prediction, preictal activities are identified based on this quantization, and can be obtained using linear or nonlinear approaches. Similar to univariate measures, the bivariate measures can also be divided to linear and nonlinear measures. Linear bivariate measures represent linear relations between different parts of the brain, while the main goal of a nonlinear bivariate measure is to extract the nonlinear spatiotemporal synchronization patterns existing in different parts of the brain. In the next sub-sections, a vast range of linear/nonlinear univariate/bivariate features investigated for seizure prediction are reported.

3.1.1 Linear univariate analysis

Linear measures are the mathematical techniques using phase/frequency and amplitude information of signal. Under assumption of quasistationarity of EEG signal for short periods of time, linear measures can be estimated. By segmentation of EEG into time-windows, as one of the preliminary processing stages, this estimation is possible and reliable.

3.1.1.1 Statistical moments

The four statistical moments of mean, variance, skewness and kurtosis, also known as first, second, third and fourth moments respectively, provide information about the amplitude

distribution of the time series. Skewness and kurtosis reveal information on the shape of the distribution, whereas mean and variance provide information on the location and variability (spread, dispersion). Ideally, skewness is zero for symmetric amplitude distributions, and kurtosis measures the relative peakedness or flatness. Studies have been made in (Mormann et al. , 2005) employing these statistical measures to verify their ability to distinguish between the inter-ictal and preictal periods using iEEG data. Also variance and kurtosis have shown significant changes in preictal period in comparison to the inter-ictal period (a decrease for variance and an increase for kurtosis).

3.1.1.2 Spectral power analysis

The EEG signal is traditionally expressed in terms of particular frequency bands: Delta 'δ' (less than 4 Hz), Theta 'θ' [4-8 Hz), Alpha 'α' [8-13 Hz), Beta 'β' [13-30 Hz), and Gamma 'γ' (equal or greater than 30 Hz). Mormann et al. (Mormann et al. , 2005) have indicated the relative decrease in the power of the Delta band in preictal period in comparison with the interictal period, which was accompanied by a relative increase of the power in other bands. The spectral power of raw EEG signal has been investigated by several studies, and proved the ability to track the transient changes from interictal to ictal states (Cerf et al. , 2000, Mormann et al. , 2005, Park et al. , 2011, Direito et al. , 2012, Bandarabadi et al. , 2013, Rasekhi et al. , 2013).

Park et al. (Park et al. , 2011) proposed a patient-specific seizure prediction algorithm using four different methods to compute spectral power of the iEEG. They had extracted spectral power features from raw, bipolar, time-differential, bipolar/time-differential iEEG signals. Also, to achieve better resolution in high frequencies and improve results, they had considered gamma band as four narrower sub-bands of (30-50 Hz], (50-70 Hz], (70-90 Hz], (90 Hz-Nyquist frequency]. The proposed algorithm was applied on 80 seizures, and a total of 433.2-hour of interictal data from FSPEEG dataset. The best results obtained from bipolar approach were 97.5% sensitivity and 0.27 false positives per hour in out-of-sample data. They also argued that the spectral power in certain sub-bands of the iEEG, specifically in high gamma bands, may play a key role in seizure prediction. In a recent study by Rasekhi et

al. (Rasekhi et al. , 2013), the spectral power of gamma band also has shown significant changes prior to seizure onsets.

3.1.1.3 Accumulated energy

The accumulated energy (AE) is computed by applying a moving average window on the squared values of a time series. Applied on the focus channels, this measure has been reported in (Litt et al. , 2001) to show promising results for seizure prediction for all the patients analyzed, however in that report asleep and awake records were solely utilized for predictions in their relevant states. Esteller et al. (Esteller et al. , 2005) investigated a long-term AE reference to eliminate the constraints such as the requirement of asleep and awake staging in the study by (Litt et al. , 2001). They compared short-term and long-term AEs for window lengths of 1 and 20 min, and using an adaptive decision threshold. However they argued that AE alone is not sufficient for predicting seizures. Accumulated energy calculated from wavelet coefficients in a multiresolution approach were also reported to predict 12 out of 13 epileptic seizures for different types of epilepsy (Gigola et al. , 2004). However, the results of these reports were questioned by other studies (Maiwald et al. , 2004, Harrison et al. , 2005a).

3.1.1.4 Hjorth parameters

The three time domain measures of activity, mobility and complexity are defined by Hjorth (Hjorth, 1970) to quantitatively describe EEG signals, and have been used in seizure prediction. Activity is defined as the variance of the signal. Mobility is the root of variance of the slopes of the signal divided by variance of the amplitude, and provides an estimation of the mean frequency. Complexity measures the variance of the rate of slope changes with reference to an ideal possible curve, and is an estimation of the signal bandwidth. In a comparative study on seizure prediction by Mormann et al. (Mormann et al. , 2005), the Hjorth mobility and complexity parameters showed significant increase during preictal, and performed best among a vast range of competing univariate features. The predicting ability of mobility and complexity features were also reported in (Rasekhi et al. , 2013).

3.1.1.5 Decorrelation time

Autocorrelation, a measure usually used to detect the whiteness or stationarity of time series, is defined as the temporal correlation between values of the same signal at different points. The first zero-crossing of the autocorrelation function is an important feature known as decorrelation time (Box et al. , 2008). Mormann et al. (Mormann et al. , 2005) examined epileptic EEG signals and distinguished preictal from interictal periods by looking for a decrease in the decorrelation time. However in (Rasekhi et al. , 2013), this measure showed poor changes prior to seizure onsets compared to a vast range of univariate linear features.

3.1.1.6 Autoregressive modeling

In autoregressive (AR) modeling the current value of a given time series is determined only according to the weighted sum of previous values of the same time series as well as noise. The method assumes the signal to be stationary or at least to be quasistationary, something that is implicitly achieved by the moving window analysis of EEG signals. Autoregressive modeling has been reported to locate the preictal changes (Rogowski et al. , 1981, Salant et al. , 1998, Chisci et al. , 2010).

Chisci et al. (Chisci et al. , 2010) proposed a seizure prediction methodology based on order-6 AR coefficients of 6 iEEG channels as features classified by SVM, and a Kalman regularization on the SVM outputs to attenuate the chattering noise, and produce lower FPRs. They reported 100% sensitivity, 60 minutes anticipation time, and with no false alarm on 21 patients from the Freiburg Seizure Prediction EEG (FSPEEG) database (Aschenbrenner-Scheibe et al. , 2003). They also found that applying Kalman filter on the SVM outputs significantly improves the results. More recently Rasekhi et al. (Rasekhi et al. , 2013) investigated mean square error (MSE) between the original EEG signal and the synthesized output from the related order-10 AR model as a feature. Statistical comparison of this measure between preictal and interictal samples has not proved a significant capability for this feature in seizure prediction.

3.1.1.7 Wavelet coefficients

Considering multiresolution nature of the wavelet transform, it has found a significant role in processing of EEG signals. Applied recurrent neural networks in combination with wavelet coefficients, demonstrated the feasible prediction of seizures some minutes in advance of clinical onsets (Petrosian et al. , 2000). In a comparative study (Direito et al. , 2011) on 22 univariate features, and using feature selection methods, the selected features highlighted the significance of wavelet coefficients energy especially within low frequency bands, which also was confirmed by a recent study of Rasekhi et al. (Rasekhi et al. , 2013). We have also developed patient-specific orthogonal mother wavelets for seizure prediction, called Wepilet (Bandarabadi et al. , 2011), using parameterization of mother wavelets and optimizing them by Genetic algorithm.

3.1.1.8 Spectral edge frequency and spectral edge power

The spectral power of EEG signal distributes across a range of frequencies. However, a good part of this power is contained under 40 Hz. A useful quantization of how the power is actually scattered within these frequencies is to calculate the features known as spectral edge frequency and spectral edge power. Spectral edge frequency stands for the frequency below which x percent of the overall power of the signal is located. x can hold any percentage values ranging from zero to 100. In the context of seizure prediction however, a x value of 50% has been successfully employed, describing the minimum frequency up to which 50% of the overall power of the 0-40 Hz band is contained. Also the power covered under spectral edge frequency is called spectral edge power (Stanski et al. , 1984). These features were investigated in (Rasekhi et al. , 2013) and proved predictive capability for spectral edge power.

3.1.1.9 Spike rate

Spike wave discharges are the main characteristics of ictal period. Yet isolated spike waves can also be observed as well throughout interictal periods of epileptic patients. Several studies have examined the spike rate as a measure for seizure prediction, which would

quantify distribution of the spikes during interictal/preictal periods. A decreased focal spike rate coinciding with an increased bilateral spike rate was reported preceding the seizures (Lange et al. , 1983). However, some studies using more sophisticated EEG recordings, have questioned the predictive capability of spike rates (Gotman et al. , 1985, Gotman et al. , 1989, Katz et al. , 1991). More recently, Li et al. (Li et al. , 2013) extracted spikes from the low-pass filtered iEEG signals using a morphology filter, and used the smoothed spike rate as a measure. Predictions with this method were reported to achieve a sensitivity of 75.8% and a FDR of 0.09 h^{-1} on 21 patients from FSPEEG dataset.

3.1.2 Nonlinear univariate analysis

Throughout the years, and in search for better prediction methods, researchers have moved from linear to nonlinear signal processing methods, which are capable of describing the more complex dynamics such as EEG signals. According to the nonlinear modeling, any system or signal can be described using two key terms namely state and dynamic, state defining the system at a given time, and dynamics describing the rules for evolving of system over the time (Sprott et al. , 2003). The system state is generally described by a point in an m-dimensional space known as state (phase) space, where m is called embedding dimension.

3.1.2.1 Largest Lyapunov exponent

One of the first and most famous measures extracted from the EEG signal in epilepsy is Lyapunov exponent, a measure of system's chaotic behavior, which was noticed to reduce several minutes prior to the seizures, and was a sign of reduction in signal's chaosness (Iasemidis et al. , 1990). Lyapunov exponents are the measure of predictability of a dynamical system, and mathematically quantify the exponential divergence of two state-space trajectories starting close to each other. The separation rate of these trajectories can be different for different orientations of the initial separation. The largest Lyapunov exponent is usually used to detect existence of chaos in dynamical systems, usually yielding a negative value in the case of converging trajectories (e.g. stability), and positive vice versa.

In (Iasemidis et al. , 1990) premonitory events were reported several minutes before the seizure onsets in several datasets using this measure. Corsini et al. (Corsini et al. , 2006) investigated largest Lyapunov exponent measure extracted from preprocessed sEEG and iEEG data. They initially applied blind source separation on the raw EEG data to separate underlying sources in the brain. Evaluating on simultaneous iEEG and sEEG recordings of 20 patients, they concluded that similar results could be achieved for sEEG and iEEG recordings. Mammone et al. (Mammone et al. , 2010) investigated the brain topography based on the short-term maximum Lyapunov exponents (STLmax) extracted from EEG recordings, and pointed out a relationship between changes in spatial distribution of STLmax and dynamical changes leading to the seizure. For 3 out of 4 studied patients, they reported reduction in STLmax extracted from focal electrodes long before seizures. Nevertheless of the high hopes raised by the above mentioned studies, there also exist several studies claiming that Lyapunov exponents may lack the sufficient prediction capability (Lai et al. , 2003, 2004, Mormann et al. , 2006).

3.1.2.2 Correlation dimension and integral

Correlation dimension of a signal measures the space dimension occupied by signal samples (Grassberger et al. , 1983), and is one of various methods of calculating fractal dimension. From the mathematical point of view, this measure estimates the complexity of the attractors related to non-linear systems. The correlation integral is defined as the probability by which any two randomly selected points on the state space are located within a given distance from each other. It can be used to verify if a time series is random deterministic(Grassberger et al. , 1983). The suitability of the correlation dimension for seizure prediction had been proved by (Elger et al. , 1998, Lehnertz et al. , 1998). They showed significant decreases in correlation dimension 5–25 min before seizure onset, for features extracted from selected focal channels. Later in (Aschenbrenner-Scheibe et al. , 2003) and (Maiwald et al. , 2004) it was indicated that the correlation dimension cannot satisfactorily be used in clinical applications. But Mormann et al. (Mormann et al. , 2005) found a discrepancy with previous reports, by observing an increase in the correlation dimension during preictal by analyzing 46 seizures in 311 h of iEEG recordings of five

patients. However a subsequent report (Harrison et al. , 2005b) strongly rejected the ability of correlation dimension and correlation integral to predict seizures in a comprehensive work, using over 2000 hours of iEEG recording from twenty patients with intractable epilepsy. They argued that the earlier results obtained from correlation dimension and integral were not reproducible since they had failed to validate on long-term interictal recordings, and on sufficient number of patients.

3.1.2.3 Correlation density

Correlation density is a statistical spatiotemporal complexity measure that can detect both linear and nonlinear correlations, which can be computed by counting the fraction of pairs of points having distances less than a certain value of r (McSharry et al. , 2003). Lerner (Lerner, 1996) compared correlation density and correlation dimension for tracking preictal changes, and found that correlation density was more robust with respect to the changes in embedding dimension, time delay, and more specifically to the value of r. In (Martinerie et al. , 1998) it was demonstrated that seizures could be anticipated well in advance in most cases by a preictal decrease in the correlation density. Later however, McSharry et al. (McSharry et al. , 2003) questioned the ability of correlation density to predict seizures, by re-evaluating the data from (Martinerie et al. , 1998). They found that this measure just reflected the variance of the EEG signal.

3.1.2.4 Entropy

Entropy measures the uncertainty of the samples in a time series, and quantifies the expected value of the information within that time series. Entropy can detect preictal changes developing towards synchronous or coherent brain state by quantizing EEG signal's complexity. A feasibility study by (Drongelen et al. , 2003) in five patients on Kolmogorov entropy demonstrated prediction capability in 3 out of 5 patients for iEEG and 2 out of 5 patients using sEEG recording 2~40 minutes in advance. In a study by (Li et al. , 2007) sample entropy and permutation entropy were investigated for predicting the absence seizures in rats, and permutation entropy could better distinguish preictal dynamical changes. Blanco et al. (Blanco et al. , 2013) extracted spectral entropies extracted from low, median, and high

frequency bands in iEEG recordings, to find the optimum frequency range for seizure prediction. Spectral entropy is calculated by applying Shannon entropy to the spectral density of EEG signal, followed by a proper normalization. The results indicated that the entropy obtained from high frequency band is a better criterion. Zhang et al. (Zhang et al. , 2014) utilized approximate entropy, and reported improved prediction accuracy by combining statistically relevant theory and nonlinear dynamics, using an optimized set of five electrodes.

3.1.2.5 Marginal predictability

Marginal predictability (MP) is a measure based on the correlation integral (Savit et al. , 1991), that measures the probability of two length-d time series being similar to each other, within a certain distance. In (Drury et al. , 2003) and (Li et al. , 2003) the difference of marginal predictabilities extracted from remote and adjacent electrodes to the seizure focus, have shown robust prediction ability by decreasing several tens of minutes before seizures, in patients with TLE. Furthermore, distinguishable difference in MPs between epileptic and healthy subjects throughout interictal was reported in (Drury et al. , 2003). A later study (Li et al. , 2006a) on 33 preictal periods of 14 patients revealed that the differences between marginal predictabilities were apparently consciousness state independent, but dependent on the time remaining to the seizure.

3.1.2.6 Dynamical similarity index

Dynamical similarity index (DSI) is a quantized feature introduced by (Le Van Quyen et al. , 1999) which measures the dynamical similarity of moving test window with respect to a long reference window usually selected very far from any seizure, and possessing the common characteristics of the interictal activity, including isolated spikes. The DSI is quantified by estimating cross-correlation integral between desired EEG segment and the reference window. DSI yields values between 0 and 1, and can be regarded as the degree of stationarity, one representing a completely stationary EEG signal, that is having uniform dynamical properties. Any increase in the dynamical content of a signal, will further shift this measure below 1 (Le Van Quyen et al. , 1999).

Quyen's group (Le Van Quyen et al. , 1999, Le Van Quyen et al. , 2000) studied the capability of DSI on iEEG recordings and found a reduction trend starting before the seizure onset. Later in two other separate studies using more comprehensive data, they evaluated DSI measure on two groups of patients with mesial TLE and neocortical TLE respectively (Le Van Quyen et al. , 2001, Navarro et al. , 2002). The first study was carried out on 26 scalp recording from 23 patients with mesial TLE, whereas the second study was performed on 11 patients with neocortical TLE. By choosing a 300s reference window, a transitional state dynamically differing from the interictal and ictal states was identified. On average the 25 out of 26 seizures (from mesial TLE), and 34 out of 41 seizures (from neocortical TLE) were predictable with the anticipation time of 7~7.5 minutes. Very soon however, several studies started questioning the early optimistic prediction capability reports using DSI measure and argued that its performance was much far from sufficient to be used in clinical applications (De Clercq et al. , 2003, Winterhalder et al. , 2003, Maiwald et al. , 2004).

An improved version of DSI was proposed in (Li et al. , 2006b) by replacing the Heaviside function within the correlation integral by Gaussian function to eliminate sharp boundaries, and found that the new measure was insensitive to the choice of the Gaussian function's radius and segmentation length. Evaluation on EEG recordings of 12 rats, indicated that the improved DSI could achieve better predictions compared to the original DSI proposed by (Le Van Quyen et al. , 1999). In the subsequent year, Ouyang et al. (Ouyang et al. , 2007) introduced wavelet-based nonlinear similarity index (WNSI) for real time seizure prediction, which combined wavelet techniques and nonlinear dynamics. The test results both on rats and humans indicated its ability for tracking hidden dynamical changes in brain, specifically using beta (10–30 Hz) frequency band.

3.1.2.7 Average angular frequency

In 2002, Iasemidis (Iasemidis et al. , 2002) defined a new criterion called average angular frequency which is comparable to Lyapunov index. Compared to Lyapunov index which is a measure of local stability of the system, the average angular frequency represents the changing rate of local states of a dynamic system, in average. The maximum value of this feature appears during of a seizure and decreases after the seizure even below its preictal

value. Furthermore as their objective was to locate the seizure focus, they had employed a criterion for choosing electrodes having the largest variations of this feature. The method however, even in best conditions, results in more false predictions in contrast to Lyapunov index (Iasemidis et al. , 2002, Iasemidis et al. , 2003a). In a later effort by Iasemidis et al. (Iasemidis et al. , 2005) they demonstrated that angular frequency measures obtained from specific intracranial electrodes placed over the foci converge progressively during preictal period.

3.1.2.8 Loss of recurrence

Loss of recurrence quantifies the degree of non-stationarity based on the analysis of distributions of temporal distances of neighboring state space vectors (Rieke et al. , 2002). This measure does not require a partitioning of the time series. Additionally, the deviation of mean recurrence times from frequency distributions obtained for the stationary conditions, allows for estimating of the statistical significance of this method. Mormann et al. (Mormann et al. , 2005) demonstrated the ability of this measure to predict epileptic seizures.

3.1.3 Linear bivariate measures

3.1.3.1 Maximum linear cross-correlation

Maximum linear cross-correlation measure indicates whether two systems are linearly synchronized, that is their characteristic variables evolve identically over the time (Mormann et al. , 2003a). In order to quantify the similarity of two signals x and y, one can use the maximum of the linear cross-correlation function, as a measure for lag synchronization (Rosenblum et al. , 1997). The maximum linear cross-correlation is confined to the interval [0, 1] with high values indicating that the two signals have a similar profile in time (though possibly shifted by a time lag t), while dissimilar signals will result in values close to zero. Mormann et al. (Mormann et al. , 2003a) studied this measure on iEEG recordings of 10 TLE patients, and reported preictal decrease for 12 out of 14 seizures, achieving very high specificity on non-seizure intervals. A preictal decrease of this measure estimated from

simultaneous EEG recordings from different brain sites has also been observed in their later study (Mormann et al. , 2005).

3.1.3.2 Multivariate autoregressive model

In multivariate autoregressive model, each point is described as a linear combination of the previous values from all selected channels. The goodness of fit (GOF) of the model shows how best that model is fitted into the channels. Jouny et al. (Jouny et al. , 2005) considered that a better GOF of multivariate AR model describes a higher degree of synchrony between channels. Using this measure, no significant preictal changes were reported.

3.1.4 Nonlinear bivariate measures

3.1.4.1 Mean phase coherence

Mean phase coherence (MPC) is the most used measure for capturing the level of phase synchronization, in seizure prediction studies. The detailed mathematics of MPC was explained in chapter 2. Early studies had reported loss of synchronization prior to seizure onsets (Mormann et al. , 2000, Chavez et al. , 2003, Mormann et al. , 2003a, Mormann et al. , 2003b). Mormann et al. (Mormann et al. , 2003a) reported preictal decreases in the MPC measure in 12 out of 14 seizures in iEEG recordings of 10 TLE patients, and a similar decrease later in 26 out of 32 seizures from the iEEG recordings of 18 patients with partial epilepsy (Mormann et al. , 2003b). Significant preictal drops in MPC measure extracted from bandpass filtered EEG signals in 10-25 Hz frequency were also reported for two patients suffering from neocortical TLE within 30 min of onsets (Chavez et al. , 2003).

Interestingly however, a later study by Quyen et al. (Le Van Quyen et al. , 2005) involved both increases and decreases of this measure several hours before the seizure onsets, often localized to the neighborhood of dominant epileptogenic zone. Moreover, a quite recent study (Zheng et al. , 2014b) estimated MPC measure from intrinsic mode functions (IMFs) obtained by bivariate empirical mode decomposition, and reported both decreases and increases of this measure prior to seizure onset. Evaluated on 10 patients selected from the

overall 21 available patients of the FSPEEG dataset, their method exhibited superior results in comparison with original MPC method and the random predictor.

Despite promising results reported and backed by several groups, the predictive performance of phase synchronization measures could not however be replicated by some others (Jerger et al. , 2005, Schelter et al. , 2006, Winterhalder et al. , 2006, Schelter et al. , 2007, Kuhlmann et al. , 2010). Jerger et al. (Jerger et al. , 2005) constructed a linear discriminator by aggregating two synchronization measures of MPC and cross-correlation in a single vector, and applied it to over of 6-days iEEG recordings of a patient. Results indicated that these measures of synchronization did not reveal a reliable seizure prediction capability, and failed to predict 7 out of 9 seizures. Schelter et al. (Schelter et al. , 2006) employed MPC and could only predict seizures in 2 out of 4 patients with performances better than random predictor. Similar results (SS=60%, FPR=0.15/h) were also reported from the same group (Winterhalder et al. , 2006), by analyzing of MPC and lag synchronization measures on 21 patients from FSPEEG dataset. Furthermore, Kuhlmann et al. (Kuhlmann et al. , 2010) studied MPC measure on long-term continuous iEEG recordings of 6 patients with focal epilepsy, and concluded that even by using the optimized set of channel pairs for extracting MPC measures, the resulting patient-specific seizure prediction system could be random in general.

3.1.4.2 Dynamical entrainment

Dynamical entrainment quantifies the convergence and divergence of short-term largest Lyapunov exponents in certain selected channels, and is estimated by statistical comparison among STLmax measures extracted from selected EEG channels (Iasemidis et al. , 2001). A growing trend of this measure was reported between the foci and non-foci areas prior to seizure onset, indicating that brain evolves from chaotic to less chaotic states, which is a known property of the epileptic seizures (Iasemidis et al. , 2001).

Iasemidis et al. (Iasemidis et al. , 2003b) developed an adaptive algorithm for real-time seizure prediction using convergence and divergence of short-term maximum Lyapunov exponents (dynamical entrainment) across some adaptively selected channels. Testing on

long-term continuous iEEG recordings of 5 patients with TLE, they reported on average a SS of 82%, a FDR of 0.16 h^{-1}, and the anticipation time of 71.7 min. Another study by same group (Chaovalitwongse et al. , 2005), also reported the predictive performance of dynamical entrainment measure through a similar method on continuous recordings of 10 patients with TLE, as SS of 76.12% and FPR of 0.17 h^{-1} on average. However, several studies have questioned a sufficient prediction performance for this measure (Lai et al. , 2003, 2004, Mormann et al. , 2007).

3.1.5 Combination of features

Combinational methods were employed to achieve improved predictions, by bringing together the advantages of various linear/nonlinear and univariate/bivariate features and techniques. Combinational methods are simply realized using machine learning algorithms, which are capable of handling high dimensional feature spaces. By doing so, the decision about brain's state is actually made by incorporating several viewpoints, making final predictions more robust to failures in traditional non-combinational techniques. In recent years such methods have attracted huge interest from scientists (Feldwisch-Drentrup et al. , 2010, Rasekhi et al. , 2013, Teixeira et al. , 2014b).

Alessandro et al. (D'Alessandro et al. , 2003) combined linear and nonlinear measures, and defined a hybrid system for seizure prediction, based on linear features such as curve length, accumulated energy, variance and nonlinear features such as estimated entropy and largest Lyapunov coefficient. By evaluating this predictor on 4 patients suffering from TLE, they reported 90% sensitivity and over 62% accuracy, and a prediction time of 3.45 minutes on average.

Feldwisch-Drentrup et al. (Feldwisch-Drentrup et al. , 2010) combined the measures of MPC and DSI using logical AND and OR operators. They statistically evaluated the predictive performance of each feature separately and also their combination by logical operators on long-term continuous iEEG recordings of 8 patients. A 30 minutes time interval was selected as the combination window to apply the logical operators. Using the AND combination, an alarm is raised when both measures pass the threshold, whereas by using the

OR combination an alarm is generated even if one of the measures crosses the threshold inside a predefined combination window. According to their study, although both individual methods (MPC, DSI) separately, had statistically significant performances in only few patients, however improvements were achieved for all patients using the AND combination. Furthermore, combination by OR could provide prediction performance somewhere between individual methods and the AND combination. Technically, they could improve the mean sensitivity from about 25% for the individual methods to 43.2% for the AND operator and to 35.2% for the OR combination, for a maximum false prediction rate of 0.15/h.

Soleimani et al. (Soleimani-B et al. , 2012) proposed a simple adaptive online method which could adaptively learn a combination of features. Technically this method was an evolving neuro-fuzzy classifier model starting with a simple structure with patient-independent parameters, and gradually being tuned by recursive methods to achieve a personal seizure predictor. The variance, curve length, average energy, nonlinear energy, sixth power, kurtosis, and skewness were extracted from raw iEEG signals. Moreover a five level Daubechies-4 (db4) discrete wavelet decomposition was applied on raw iEEG data, and the following features were then calculated from the wavelet coefficients of each decomposition level: the average power, mean of the absolute values, standard deviation, and relative absolute mean of sub-bands. By testing their online method on intracranial recordings of 21 epileptic patients from the FSPEEG dataset, they could demonstrate that seizure prediction was improved compared to the offline non-adaptive techniques.

In (Rasekhi et al. , 2013), a set of 22 linear univariate features were extracted from scalp/invasive recordings of 10 patients (1388 hours, 86 seizures), and fed them to the SVM classifier with Gaussian kernel. Features of mean, variance, skewness, and kurtosis, five standard spectral power features, Hjorth mobility and complexity parameters, accumulated energy, autoregressive modelling error, decorrelation time, Spectral edge frequency and spectral edge power, and energy of wavelet coefficients of five level db4 decomposition were extracted using 5-sec non-overlapped windows. Afterwards, different feature preprocessing approaches as well as different preictal periods were investigated to find out proper ones. They concluded that outlier removal and smoothing of features could improve prediction

results. On average, they reported a sensitivity of 73.9% (34 out of 46 seizures in 737.9 h of test data) with a false prediction rate of 0.15 h^{-1}.

Teixeira et al. (Teixeira et al. , 2014b) carried out the most extensive comparative study using the same 22 univariate linear features as in (Rasekhi et al. , 2013), on 278 patients and observed that the parameters such as epileptic focus localization, data sampling frequency, testing duration, number of seizures in testing, type of machine learning, and preictal time significantly affect the prediction performance. For a considerable number of patients it was possible to find a patient-specific predictor with an acceptable performance. Their findings could be helpful in the feasibility study of patient-specific prospective alarming system using machine learning techniques and utilizing a combination of univariate features.

3.1.6 Self-prediction of epileptic seizures

Contrary to most advances achieved in seizure prediction using EEG processing methods, limited number of studies has investigated clinical epileptic precursors (Scaramelli et al. , 2009). A number of recent studies have interestingly reported that some patients were able to self-predict their seizures. Seizure self-prediction is some kind of awareness of prodromal symptoms (PS) (Haut et al. , 2013). Most studies have used diary questionnaires asking patients to write down any changes they would experience in their subjective perception or behavior.

The prodromal symptoms of impending seizures can be categorized as behavioral or cognitive changes in patients. The most frequently reported prodromal symptoms include mood change, blurred vision, hypersensitivity to light/noise, dizziness, feeling emotional, concentration difficulty, hunger/food cravings, tired/weary, thirst, difficulty with thoughts, difficulty reading/writing/speaking, clumsiness, feeling of loss, headaches, polyuria, diarrhea, pallor, and coldness (Petitmengin et al. , 2006, Scaramelli et al. , 2009, Haut et al. , 2012). Depressive mood changes are more frequently noticed compared to joyful changes of mood. Prodromal symptoms were identifiable several hours before impending seizures, and usually would last until the seizure occurred.

In a study reported by Scaramelli et al. (Scaramelli et al. , 2009), on 100 randomly selected patients, PS were found in 39% of patients, and mostly included behavioral, cognitive and mood changes. Although PS is noticeable both in focal and generalized epilepsies, it mostly precede complex partial and generalized tonic-clonic seizures. However, due to the delicate nature of PS, they have not been practically used in seizure prediction, but they represent new hopes for seizure prediction, and may find a role in preventive and therapeutic instruments.

Furthermore, precipitants of seizures are important factors both in treatment of patients, as well as during seizure diagnosis procedure. Nakken et al. (Nakken et al. , 2005) investigated an epilepsy population of 1677 individuals, to determine which seizure precipitants were most often reported by patients. According to this study, 53% of the patients reported at least one factor, whereas 30% of the questioned would mention two or more of such precipitants factors. The three most reported factors were emotional stress, sleep shortage (disturbance), and tiredness. Those with generalized seizures were apparently more susceptible to sleep problems and flickering light, than patients suffering from partial epilepsy. Depression, anxiety, menstruation, and alcohol were also reported among the most commonly seizure precipitants (Schulze-Bonhage et al. , 2011). Precipitants are thought to provide patients with kind of awareness about the risk levels of impending seizures.

3.2 Past efforts in seizure detection

Currently, there is a growing need for dependable automated seizure detection algorithms with high sensitivity and specificity, and short detection latency, to be used in closed-loop neurostimulation systems for suppressing of just-occurring seizures (Shoeb et al. , 2009, Colic et al. , 2011, Kharbouch et al. , 2011), or to alarm doctors and relatives about the hazardous situation of the patient. Moreover, the automated detection methods can be used by researchers and neurologists to label long-term continuous scalp and intracranial EEG recordings for further studies such as pre-surgical evaluation of epilepsy and localization of the seizure onset zone (Lesser, 2009, Nanobashvili et al. , 2011). Apart from having high detection performances, detection algorithms should also satisfy extra

requirements set by implantable devices, such as low power budget and the miniaturized size. Therefore, detection algorithms should be of low complexity and fast enough for online processing of huge amounts of data. The number and type of the considered features, number of the channels monitored, sampling rate, and decision-making algorithm determine the power consumption of detection algorithm. In general, nonlinear features consume more power than linear ones because they require more computations.

There are many existing seizure detection algorithms. They usually seek to optimize one of two competing goals; (1) early seizure detection: the real-time detection of epileptic seizures without or with a negligible delay from electrographic onset initiation, and (2) seizure event detection: the accurate labeling of the occurrence of seizures with high sensitivity and specificity. The first approach is best suitable for closed-loop therapeutic as well as for patient care systems, where only onset detection delay times of few seconds can be tolerated. The second approach is much appropriate for offline labeling of recorded EEGs for future studies, thus are allowed to undergo longer detection delay times. Either of these two methods may process EEG data using one of the four processing schemes of time domain, frequency domain, both time and frequency domains, and finally time-frequency domain. Although most of the methods employ EEG signals (Adeli et al. , 2010), there are also few studies using other less common approaches such as electrocardiogram signal (Zijlmans et al. , 2002, Greene et al. , 2007, Malarvili et al. , 2009, Osorio, 2014).

3.2.1 Early seizure detection

Although the prime goal of automatic seizure detection has been to facilitate EEG-based long term monitoring, diagnosis and treatment of patients, it may also eventually become the essential part of closed-loop therapeutic solutions currently being developed for containing epileptic seizures (Shoeb et al. , 2009, Shoeb et al. , 2011b). The main issue for developing an applicable algorithm for closed-loop therapeutic systems is the detection latency from start of the electrographic seizure onset, so that the system should have enough time to influence on the impending clinical seizure.

Various studies are found for the early detection of seizure onsets (Schindler et al. , 2001, Shoeb et al. , 2004, Grewal et al. , 2005, Saab et al. , 2005, Meier et al. , 2008, Schad et al. , 2008, Shoeb, 2009, Shoeb et al. , 2009, Zhang et al. , 2010, Kharbouch et al. , 2011, Hunyadi et al. , 2012, Rabbi et al. , 2012, Schindler et al. , 2012, Ayoubian et al. , 2013, Zheng et al. , 2014a). Saab et al. (Saab et al. , 2005) proposed an automatic onset detection using wavelet decomposition and Bayesian formulation, which could estimate the probability of the occurring seizures. Grewal et al. (Grewal et al. , 2005) considered spectral power features of iEEG recordings, and on average obtained a sensitivity of 89.7%, a false detection rate (FDR) of 0.22/h, and a mean detection latency (MDLE) of 17.3 s, on test data including 100 seizures in 389 h recordings of 19 patients.

Meier et al. (Meier et al. , 2008) developed a machine learning approach to detecting seizures by categorizing morphological ictal rhythms into six categories based on the frequency of the dominant rhythm and then training a multi-class support vector machine (SVM) to detect the different types of seizure onsets. Shoeb et al. (Shoeb et al. , 2009) studied the feasibility of a patient-specific onset detection using surface EEG and electrocardiogram (ECG) signals for closed-loop triggering of VNS system, and concluded that closed-loop VNS system may suppress early detected seizures in some patients. They investigated the energies of frequency bands selected from 0-24 Hz, extracted from each of recorded channels. The spectral and spatial relations between channels were captured simultaneously and fed to the SVM classifier.

Kharbouch et al. (Kharbouch et al. , 2011) proposed a patient-specific onset detection using spectral powers of 17 frequency bands extracted from whole recording channels, and classified by linear SVM. Testing on 67 seizures in more than 875 h of iEEG recordings of 10 patients, they reported on average a sensitivity of 97%, a FDR of 0.025/h, and a MDLE of 6.9s. Hunyadi et al. (Hunyadi et al. , 2012) introduced a patient-specific algorithm using a set of time domain (zero crossings, skewness, kurtosis, root mean square amplitude) and frequency domain (total power, peak frequency, mean and normalized power in delta, theta, alpha, and beta frequency bands) features, and classified by SVM. On average, they demonstrated a sensitivity of 74.2%, a FDR of 0.34/h, and a MDLE of 10.2 s, on 131 seizures in 892 h of surface EEG from 22 pediatric patients.

Ayoubian et al. (Ayoubian et al. , 2013) investigated the feasibility of high frequency activities (80–500 Hz) in seizure detection using wavelet decomposition and adaptive thresholding. Applying the trained algorithm on 18 seizures in 36h iEEG test data from 15 patients, they could achieve on average a sensitivity of 72%, a FDR of 0.7/h and a MDLE of 10.9s. Zheng et al. (Zheng et al. , 2014a) proposed a multichannel patient-specific onset detection method using variances of intrinsic mode functions (IMFs) as features, and classifying them through SVM. Evaluating on 51 seizures in 463 h of iEEG recordings of 17 patients from FSPEEG database, they reported, on average, a sensitivity of 92%, a FDR of 0.17/h, and a MDLE of 12 s.

3.2.2 Seizure event detection

Long-term continuous multichannel recordings produce huge amounts of data, sometimes up to several hundred of megabytes just for a single recording site. Real-time monitoring of these bulky recordings by EEG experts can therefore be sometimes impossible, whereas offline analysis can become very costly, tedious and tiresome. The first efforts for automatic detection of epileptic seizures go back to early 1970s (Gotman et al. , 1976), and afterwards several works were published for detection of seizure events (Gotman, 1982, Liu et al. , 1992, Adeli et al. , 2003, Hassanpour et al. , 2004, Wilson, 2006, Adeli et al. , 2007, Ghosh-Dastidar et al. , 2007, Acharya et al. , 2011, Liu et al. , 2012, Martis et al. , 2012, Acharya et al. , 2013, Martis et al. , 2013, Sharma et al. , 2014, Yuan et al. , 2014).

Gotman (Gotman, 1982) studied EEG signals for the presence of rhythmic activity with a dominant frequency between 3 and 20 Hz to detect seizure onsets. Liu et al. (Liu et al. , 1992) investigated the degree of periodicity in the autocorrelation function of 30-sec epochs of EEG signals, and then used this parameter to classify those epochs as seizure or non-seizure. Hassanpour et al. (Hassanpour et al. , 2004) studied a time-frequency distribution approach, performing singular value decomposition of all epochs. The resulting SVs are then used to train artificial neural networks and to detect seizures. Wilson et al. (Wilson, 2006) extracted the so-called atoms using the matching pursuit algorithm from EEG channels, and used hand-coded and neural network rules to determine whether the features extracted from those atoms indicated a seizure taking place on that channel or not.

Adeli et al. (Adeli et al. , 2007) applied the four level Daubechies-4 wavelet decomposition on EEG signals to obtain four sub-bands of delta (0–4 Hz), theta (4–8 Hz), alpha (8–15 Hz), beta (15–30 Hz), and gamma (30–60 Hz), and then estimated nonlinear measures of correlation dimension and largest Lyapunov exponent (LLE) from each sub-band. By examining these measures for categorizing of EEG segments in three groups of healthy, ictal, and interictal, they concluded that correlation dimension measure extracted from beta and gamma bands as well as LLE estimated from alpha band could better distinguish the three groups from each other. Ghosh-Dastidar et al. (Ghosh-Dastidar et al. , 2007) employed a similar methodology and incorporated four different supervised and unsupervised machine learning algorithms to automatically classify the three groups.

Martis et al. (Martis et al. , 2012) investigated empirical mode decomposition, and then extracted spectral peaks, spectral entropy and spectral energy features from intrinsic mode functions, and classified them by decision tree classifiers. In their later study (Martis et al. , 2013), the features of energy, fractal dimension and sample entropy were extracted from intrinsic time-scale decomposition of EEG signal, and then classified using decision tree method. In a comparative study, Acharya et al. (Acharya et al. , 2013) employed continuous wavelet transform, higher order spectra and textures to classify EEG signals using four types of classifiers into normal, interictal and ictal states, which indicated SVM as the best classifier among all.

3.3 Summary

In this chapter we reviewed a vast range of measures and methods for epileptic seizure prediction and detection. In the early attempts for seizure prediction, the results usually indicated good capability of the introduced features in discriminating preictal/interictal classes. Most prediction algorithms have been evaluated mainly using short-term fragmented recordings, and not validated by satisfactorily long-term continuous recordings, lasting over weeks. However, later with the availability of long-term continuous EEG recordings, new approaches were proposed for evaluating the prediction capability of the earlier introduced

criteria. In most cases, new studies were challenging the brilliant and dazzling findings of the previous works.

Furthermore, algorithms proposed for seizure prediction and detection mostly suffer from low sensitivities, high false prediction/detection rates, and relatively long detection delays (in the early detection approaches), which makes them clinically unacceptable to be used in closed-loop neurostimulation systems and clinical applications. Also, since the patterns of preictal and ictal activities usually vary from patient to patient, most of methods were only developed as patient-specific solutions. Moreover, complexity of the current algorithms can be further reduced by utilizing a fewer number of channels, lower-cost features, as well as cost-effective classification schemes.

For seizure prediction, the advantages of bivariate and multivariate measures over univariate ones have been pointed out in several studies (Lehnertz et al. , 2005, Mormann et al. , 2005, Mormann et al. , 2007). In 2005, various groups published the results from a series of their studies generated for the first seizure prediction workshop held on 2002 in Bonn, and the results of these studies demonstrated the advantages of bivariate and multivariate criteria in contrast to week functionality of univariate criteria (Lehnertz et al. , 2005). A comprehensive study (Mormann et al. , 2005) was also carried out to compare most of the linear and nonlinear methods involving univariate and bivariate features, concluding that univariate measures such as effective correlation dimension, Lyapunov exponents, and accumulated energy of the signal could not produce better results than a random predictor. In contrast, they reported some evidences showing that the measures quantifying the relations between recording electrodes and representing the interaction between different regions of brain exhibit a promising capability, beyond the chance level demonstrated by statistical validation. For synchronization criteria such as phase synchronization and lag synchronization, a distinctively better functionality could be obtained, also supporting the importance of bivariate features.

Moreover, the most recent studies have mainly focused on using combination of features to achieve better prediction results. Since all criteria bear some extent of unreliability

in correctly predicting seizures, thus if a combination of the features is used, the overall percentage of system unreliability will apparently be decreased.

Chapter 4 Novel seizure prediction approaches

This chapter presents our main contribution to seizure prediction, which is using ratio of spectral power features across different channels. This method compares spectral powers within different sub-bands of different electrodes, and exploits relations between them to be used as features. An approach was also introduced for selection of the best features from the high dimensional relative bivariate features space. Selected features can reflect the relationships between different frequency bands in the different regions of the brain. For instance, if spectral power of gamma band of a focal channel divided by spectral power of theta band of an opposite channel achieves the highest rank, one may conclude that this measure can better track the transient changes. Therefore, the selection of the most discriminative features plays an important role in this study, and a feature selection method was developed. The seizure prediction is faced as a binary classification problem between preictal and non-preictal states. Non-preictal state covers the three states of ictal, postictal, and interictal. The identification of preictal state is made using the computational intelligence SVM classifier and its output regularization by firing power (FP) method. Results from both scalp and intracranial recordings were compared in order to examine whether the iEEG prevails over sEEG predictions or not. The advantages of the proposed approaches have been evidenced by the comparison of the results.

In the first study reported in this chapter, we investigate four different preictal periods, and train classifiers to find the one providing the best results. However the proper length of preictal period is unclear and varies from seizure to seizure. In the second part of this chapter, we present a novel criterion to overcome the problem of selecting the most discriminative preictal period to be used in seizure predictors. The proposed criterion is based on a modification of the feature selection method introduced in the first section of this chapter.

4.1 Seizure prediction using ratio of spectral powers

4.1.1 Dataset description

Long-term continuous multichannel EEG recordings of twenty-four patients (19 males and 5 females, aged 15–57 years, median 35.5 years) with refractory partial epilepsy from the European Epilepsy Database (Klatt et al. , 2012) were used. From among the high number of available patients in the database, we selected randomly from those patients with partial epilepsy and having at least three recorded epileptic seizures. Recordings were obtained at the epilepsy units of the University Hospitals of Coimbra, Portugal, the Pitié-Salpêtrière Hospital of Paris, France, and the University Clinic of Freiburg, Germany. Sixteen patients were monitored through scalp electrodes whereas the other eight were monitored through intracranial electrodes. The 10-20 electrode montage was used for scalp recordings.

The onset times were marked by epileptologists by visual inspection of sEEG/iEEG recordings and using the video recordings of the patient during his/her stay in the hospital. Information of both electrographic and clinical onsets is available in the database, and we considered electrographic onsets for this study, as they usually start earlier than clinical onsets. Just in two epileptic seizures of one patient (subject 15) the electrographic onsets could not be identified unequivocally, and thus the clinical onset times were used instead. The European Epilepsy Database includes other details about the seizures, also annotated by epileptologists. Patient characteristics are summarized in Table 4.1.

For each patient, six channels were selected, three close to the foci and the other three far from the foci. The three focal electrodes were selected using prior knowledge on seizure propagation information. The initialization and propagation of the seizures on the electrodes were annotated in the database by epileptologists. Three non-focal channels were also chosen on the opposite side of focal electrodes. The continuous long-term raw iEEG/sEEG data were first segmented into non-overlapping 5 seconds windows and then were filtered using an infinite impulse response (IIR) forward-backward Butterworth 50 Hz notch filter to eliminate sinusoidal distortion of the ac power supply without introducing phase shift. No additional artifact suppression methods were employed.

Table 4.1 – Information of the 24 studied patients

ID	Gender	Patient age (y)	Onset age (y)	Recording type	Recording time (h)	No. of seizures	Seizure type	Localization of seizures	Sampling rate	Hospital
1	M	57	6	Scalp	110.2	8	CP(7), UC(1)	Right T	512	Coimbra
2	F	38	23	Scalp	103.8	7	CP(5), UC(2)	Left T	512	Coimbra
3	M	42	32	Scalp	104.6	6	CP(3), SP(3)	Left T	512	Coimbra
4	M	33	12	Scalp	101	7	CP(6), UC(1)	Left T	512	Coimbra
5	M	20	no info	Scalp	89.8	13	CP(12), UC(1)	Left T	512	Coimbra
6	M	34	12	Scalp	92.8	5	CP(5)	Right T	1024	Coimbra
7	M	15	3	Scalp	113.5	7	CP(6), UC(1)	Right T	512	Coimbra
8	M	57	17	Scalp	109	6	CP(2), UC(4)	Bilateral T	512	Coimbra
9	F	27	13	Scalp	106.6	7	CP(4), UC(3)	Right T	1024	Coimbra
10	M	16	12	Scalp	91.9	7	SG(1), UC(6)	Left T	512	Coimbra
11	M	35	1	Scalp	141.5	4	CP(3), UC(1)	Right T	512	Paris
12	M	41	19	Scalp	140.6	6	CP(4), SP(1), UC(1)	Right T	400	Paris
13	M	45	14	Scalp	246	6	CP(2), SP(3), UC(1)	Right P	512	Paris
14	M	28	18	Scalp	164.5	3	CP(1), SP(1), UC(1)	Right P	400	Paris
15	M	51	3	Scalp	120	6	SG(4), SP(2)	Right T	256	Freiburg
16	F	29	18	Scalp	138.4	6	CP(2), SG(3), UC(1)	Left T	250	Freiburg
17	M	55	no info	Invasive	188.8	6	CP(6)	Right F	1024	Coimbra
18	M	27	16	Invasive	234.9	8	SP(2), SG(2), CP(1), UC(3)	Left T	400	Paris
19	F	31	10	Invasive	159.2	7	CP(2), SG(2), SP(1), UC(2)	Left T	400	Paris
20	M	40	12	Invasive	221.2	8	CP(4), SG(1), UC(3)	Left T	400	Paris
21	M	36	1	Invasive	211.7	12	UC(12)	Right F	400	Paris
22	F	32	8	Invasive	151.6	9	CP(2), SP(2), UC(5)	Right F	1024	Freiburg
23	M	21	5	Invasive	170.6	22	CP(19), UC(3)	Right T	1024	Freiburg
24	M	42	16	Invasive	252.4	7	SG(2),SP(2),CP(1),UC(2)	Right T	1024	Freiburg
mean	--	35.5	12.3	--	148.56	7.62	--	--	--	--
sum	--	--	--	--	3565.4	183	CP(97),SP(17),SG(15),UC(54)	--	--	--

- Localization of seizures; T: Temporal lobe, F: Frontal lobe, P: Parietal lobe (between frontal and occipital).
- Seizure type: Type of the clinical seizures; SP: Simple Partial, CP: Complex Partial, SG: Secondarily Generalized, UC: Unclassified.

4.1.2 Methods

The block diagram of the utilized seizure predictor is depicted in Figure 4.1, where prediction relies on the SVM classifier trained to discriminate different states in the incoming EEG signal. The diagram also includes a relative bivariate feature extraction stage using 5-sec windows, a preprocessing unit, as well as a regularization operation for decision-making on alarming. As seen in Figure 4.1, the feature extractor is first applied to the windowed raw EEG signal, and the resulting relative bivariate feature vector is further processed by feature selection methods to reduce the dimension of the feature space. The features are subsequently fed to the SVM classifier to discriminate the resulting sequence into the two predefined brain states (preictal, non-preictal). The outputs of the SVM are submitted to a moving average to regularize the output signal in order to reduce the number of false alarms.

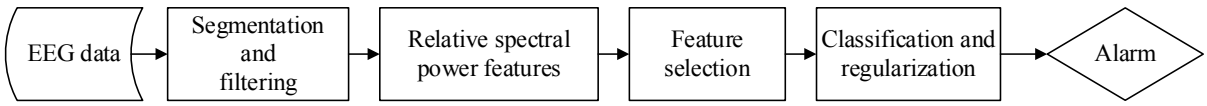

Figure 4.1 – Overall diagram of the proposed method for seizure prediction

4.1.2.1 Relative spectral power feature

Around 65% of the epileptic patients suffer from partial seizures which are related to a specific brain region (Téllez-Zenteno et al. , 2012). The most common epileptogenic region of the brain is the temporal lobe. Comparing the EEG of the focal region with the EEG of the other regions it is more likely to find significant differences, at least during the ictal phase before the propagation of the seizure. Hence, the features that explore this spatial dependence should be considered. Multivariate features developed in this way have extra advantages, such as the rejection of common mode interferences that are not related with ictogenesis. With the previous assumptions, a relative bivariate approach based on spectral power in different sub-bands was developed.

The EEG signal was considered in terms of well-known frequency sub-bands: Delta ‘δ’ (0.5-4 Hz], Theta ‘θ’ (4-8 Hz], Alpha ‘α’ (8-15 Hz], Beta ‘β’ (15-30 Hz], and Gamma ‘γ’ (30 Hz - Nyquist frequency]. Due to the different equipment used in the three centers that contributed to the European Epilepsy Database, the sampling rate was not unique for the 24 studied patients. The minimum sampling rate was 256 Hz, corresponding to a bandwidth of 128 Hz. This puts a constraint on the definition of a unified range for all subjects in higher frequencies.

We considered that almost of the power in a non-synthesized EEG signal is located below 100 Hz, as reported in (Sanei et al. , 2008). Therefore the amount of energy in the frequencies higher than 128 Hz would be negligible in comparison with the frequency range of 30-128 Hz, which is common for all patients. As a reasonable choice, the range of Gamma band was varied among patients, depending on the Nyquist frequency of the recorded signals. Figure 4.2 represents the spectrogram of 10 minutes of hippocampal iEEG signal sampled at 1024 Hz, corresponding to one of the studied patients.

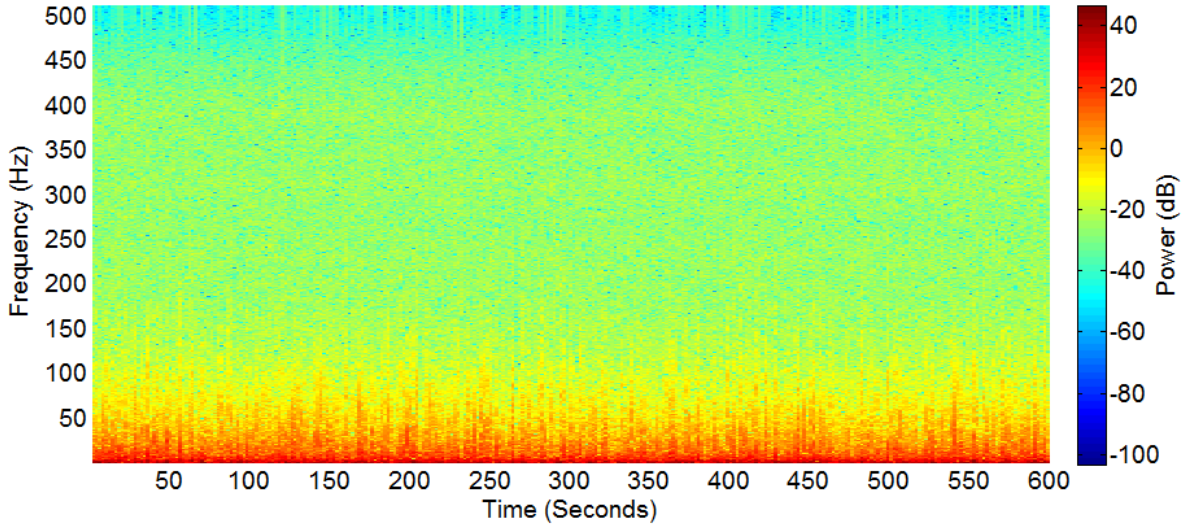

Figure 4.2 – Time-frequency representation of 10 min of raw hippocampal iEEG signal. The sampling rate for this patient was 1024 Hz. Most of the spectral energy is limited to <100 Hz frequencies, showing that the power within the frequencies higher than 128 Hz is negligible in comparison to the frequency range of 30-128 Hz.

Spectral power of raw EEG was obtained using Welch's PSD function applied to the non-overlapping 5-sec windowed EEG signal. The normalized spectral power feature for each sub-band was used, which is computed by dividing the spectral power of the sub-band by the total power. The advantages of normalized spectral power over original ones were mentioned in the chapter 2. The five normalized spectral power features of 6 channels (α_n, β_n, γ_n, θ_n, and δ_n, n=1,…, 6) were computed in 5-sec epochs and produced 30 normalized spectral power features per epoch. Then the new relative spectral power features were described by (4.1),

$$a_k = \frac{np_{i_1 j_1}}{np_{i_2 j_2}} \quad , \begin{cases} i_1, i_2 = 1,\ldots,n \\ j_1, j_2 = 1,\ldots,m \\ if \quad j_1 = j_2 \quad then \quad i_1 \neq i_2 \end{cases} \tag{4.1}$$

where a_k stands for relative normalized spectral power, given by the ratio between the normalized spectral power for the i_1-th band in the j_1-th channel, and the normalized spectral power for the i_2-th band in the j_2-th channel. n is the number of considered frequency sub-bands and m is the number of selected channels for the study. This feature gives the cross-power information not just between two channels but also between two frequency bands. These new features were targeted to find preictal trends that can be used to predict seizures. If m channels and n sub-bands are considered independently, $k = m \times n$ features will be obtained. The combination of the k features set by the proposed relative bivariate approach would lead to a total of C_2^k new features (4.2).

$$C_2^k = \binom{k}{2} = \frac{k!}{2! \times (k-2)!} \tag{4.2}$$

The relative bivariate features were computed for the 30 normalized spectral power features extracted from 6 channels. The pairwise combinations of the 30 features led to a total of $C_2^{30} = 435$ new features.

4.1.2.2 Normalization and smoothing of features

By long-term monitoring of the elements of each extracted feature vector, it is found that they are highly changing around a gradually varying long-term average value. This behavior is mostly resulting from noise and other interfering sources such as eye movement or EMG signals, and other artifacts. In order to reduce this effect, each feature was processed using a 12-epochs (1-min length) moving average window (Figure 4.3). As noticed from (4.3), the time series of feature vector "*a*" is smoothed by averaging each current value with its 11 past values,

$$\bar{a}_k = \frac{1}{l+1}\sum_{j=0}^{k} a_{k-j} \ , \ l = 11 \tag{4.3}$$

where a_k is *k*-th sample of feature vector, and $\bar{a}_k$ is its smoothed feature value. Furthermore each feature vector was normalized into the interval [0 1] by dividing by the maximum range of that feature across the whole data set as in (4.4).

$$\bar{a}_{norm} = \frac{\bar{a} - \min(\bar{a})}{\max(\bar{a}) - \min(\bar{a})} \tag{4.4}$$

Since the number of features is very high, a feature reduction method was developed to select the most promising feature subset, and is presented in the next sub-section.

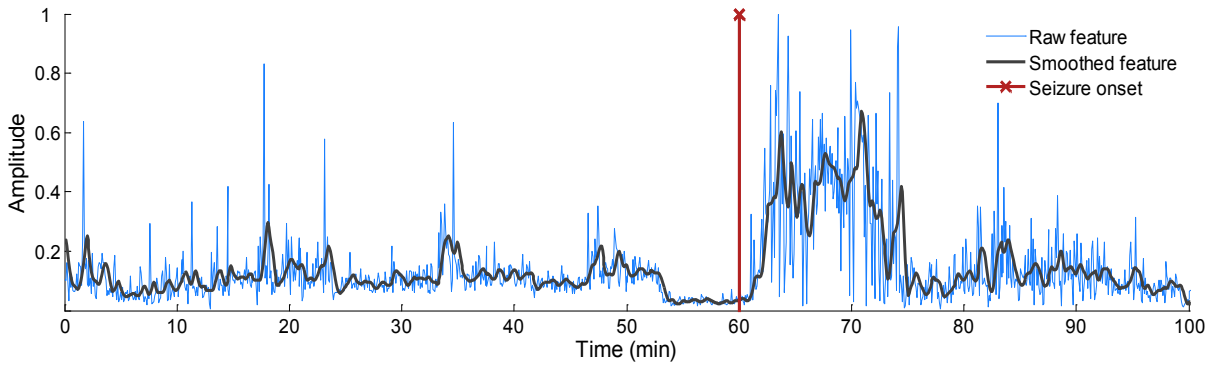

Figure 4.3 – Raw feature and its preprocessed version (α_{ORFRG6} / δ_{AMYGG1} for patient 18). The feature was extracted from 100 minutes of iEEG signals of patient 18. Each smoothed sample was obtained by averaging on current and past 11 raw feature samples. Non-preprocessed features are highly vibrant around the smoothed feature values, indicating that preprocessing has reduced the effects of artifacts.

4.1.2.3 Feature selection based on discrepancy of amplitude distributions

The selection of a subset of relevant features among a high number of candidate features based on a certain criterion is a very challenging problem (Fukunaga, 1990), and plays an important role in building robust learning and decision making models. We developed a features selection method and compared the results with the minimum Redundancy Maximum Relevance (mRMR) (Peng et al. , 2005) feature selection method. Two selection methods were applied on the features labeled with predefined preictal periods, to rank the features.

The proposed supervised feature selection method is based on amplitude distribution histograms (ADHs) of preictal and non-preictal samples. An ADH is the representation of the samples of a given feature corresponding to a specified class, in which the feature axis is discretized into a number of equal smaller bins, each representing the number of features with amplitudes falling within that interval. For a two-class problem, two different ADHs were considered. The basic idea of the method is the selection of the features that have the maximum difference between normalized ADHs (MDAD) of preictal and non-preictal samples. To achieve the normalized ADHs of each class, ADH_{norm}, the original histograms were divided by the number of samples in each class, as in (4.5),

$$ADH_{normj} = \frac{ADH_j}{ns \times w} \tag{4.5}$$

where ADH_j is the original histogram of class j, ns is the number of feature samples of class j, and w is the bin-width. The features were normalized to fall inside the interval [0 1], and the feature axis was discretized into 100 equally spaced bins ($n=100$, $w=0.01$), as required for calculating ADHs. The net area under each normalized ADH is therefore one. The common area between two normalized ADHs of a two-class problem, C_{ADHs} (Figure 4.4), can thus be calculated as (4.6),

$$C_{ADHs} = w \times \sum_{i=1}^{n} \min(ADH_{norm1}, ADH_{norm2}) \tag{4.6}$$

where n is the number of bins, and i indexes the bins where the values of two classes are distributed. The C_{ADHs} has a value in the real interval [0 1]. The difference of normalized ADHs for a two-class problem is defined by (4.7),

$$D_{ADHs} = 1 - C_{ADHs} \tag{4.7}$$

where D_{ADHs} is the difference between normalized ADHs and has a value in the real interval [0 1]. To be able to properly compare different features using MDAD method, all features were normalized to the real interval [0 1]. In summary, higher D_{ADHs} values represent higher separability between samples of different classes, for a given feature. So, features with high D_{ADHs} are more likely to improve seizure prediction performances. Figure 4.4 presents ADH of the first and last selected features using the proposed method for one of the studied patients. Since each sample is labeled, this method is a supervised method, and it was developed for two-class problems such as in seizure prediction (preictal and non-preictal classes).

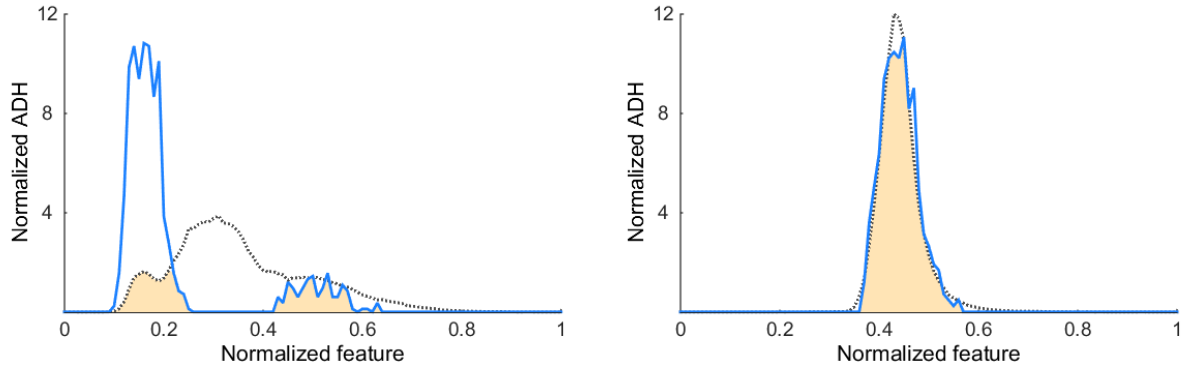

(a) (b)

Figure 4.4 – The normalized ADHs of relative spectral features for patient 19; (a) highest rank: D_{ADHs} =0.70, (b) lowest rank: D_{ADHs} =0.06. The dotted black histogram represents the ADH of non-preictal samples, while the blue histogram represents the ADH of preictal samples. For maximum discrepancy of the features (maximum D_{ADHs}), the common area under two histograms (highlighted area) should be minimized.

4.1.2.4 Patient specific classification and alarm generation

The patient specific SVM classifiers with Gaussian kernel were trained for prediction of seizures within the predefined preictal periods. The two kernel parameters of scale (σ) and cost (C) were optimized through a grid search method. Classification was carried out using LibSVM toolbox (Chang et al. , 2011). SVMs were trained with part of the data (the training set) and were tested with the remaining data (the testing set).

Among the consecutive seizures with less than 40 minutes interval, only the first seizure was considered for training or testing the classifier. By this consideration, we make sure that no residual postictal activity remains from a previous seizure. The total number of considered seizures was 159. For each patient, the first three seizures and their corresponding recordings were considered for training and the last ones for testing. This leads to 72 seizures used for training, and 87 for testing. As the proper length of preictal period is not known and is patient-specific phenomenon, four different preictal periods -10, 20, 30, and 40 minutes- were considered for training and testing the SVM classifier. The remaining samples outside the preictal periods were labeled as non-preictal samples.

Since the number of non-preictal samples was much higher than the preictal ones, and usually classifiers tend to produce higher accuracy over the class with more training samples (Chawla et al. , 2004), the number of non-preictal samples of the training set was reduced by resampling to achieve a balanced number of samples for the two classes. However for the testing phase all of the samples were considered and no resampling was carried out. Afterward, the firing power regularization method, which was introduced in chapter 2, was applied on the SVM classifier outputs. The threshold level for decision making and alarm generation was set to 0.5. Figure 4.5 shows an interval of five hours data illustrating the application of FP method on SVM outputs, for generating alarms.

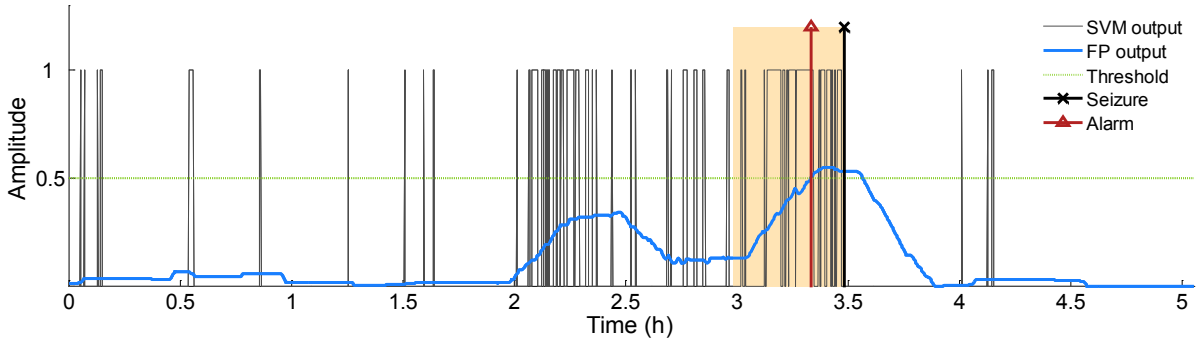

Figure 4.5 – Decision making on the outputs of the SVM classifier for alarm generation using FP method. Highlighted area depicts a 30 min preictal period, and the black, blue and red lines represent the SVM outputs, regularization output and the generated alarm respectively. By upward passing of regularization output across the threshold value (0.5), and fulfilling two constraints of the FP method, an alarm is generated. Alarms outside this preictal window are considered as false alarms. Seizure onset is marked by the longer vertical black line.

4.1.3 Results

Sensitivity (SS) and false prediction rate (FPR) of the raised alarms were used to evaluate the proposed approaches. Unfortunately, both parameters cannot be simultaneously optimally set, as improving one leads to worsening the other, and a tradeoff has to be made in their selection. Therefore the Euclidean distance between the points (in the plane) defined by the pair (sensitivity, normalized FPR) of the raised alarms and the optimal performance point (SS=100, FPR=0) was used to find the best trained SVM model for each patient. The best model would be selected so that this distance is minimized. The normalized FPR values were used instead of the actual FPR in order to limit the effect of narrow range and very low FPR (whose obtained values are easily near 0). The normalized FPR of each alarm series (i) is defined as (4.8),

$$FPR_{norm}(i) = \frac{FPR(i)}{FPR_{\max}} \times 100, \qquad i = 1,\ldots,n \tag{4.8}$$

$$FPR_{\max} = \max\left(FPR(i)\right), \qquad i = 1,\ldots,n \tag{4.9}$$

where the $FPR(i)$ is the false prediction rate of the *i*-th SVM model, and *n* is the number of SVM used. The Euclidean distance is calculated as (4.10),

$$Ed(i) = \sqrt{\left(ss(i) - 100\right)^2 + FPR_{norm}^2(i)}, \quad i = 1,\ldots,n \tag{4.10}$$

where the $ss(i)$ is the sensitivity of raised alarms by the *i*-th model. The SVM model which provides the minimum *Ed* is selected as the best. The seizure prediction performance was evaluated for different sizes of the feature subset: 3, 5, 10, 20 and 40, to find the best performing dimension of feature space. Discriminative features were selected by the proposed method (MDAD) and by the mRMR method.

Table 4.2 reports the best results for each patient in terms of alarm sensitivity and FPR, obtained from the two feature selection methods. The best results were selected so that the SS and FPR be close to the optimal performance condition, i.e., SS=100% and FPR=0 h^{-1}. Using the MDAD method, in average 75.8% of the seizures in the testing set were successfully predicted (66 out of overall 87 seizures within 1537 hours of recording data) with an average FPR of 0.1 h^{-1}. Figure 4.6 illustrates the SS and FPR results of 24 studied patients using MDAD and mRMR feature selection methods to provide visual comparison.

To verify the efficiency of the proposed method, statistical validation was employed, and results were compared with those achieved from the analytical random predictor. As four different preictal periods of 10, 20, 30, 40 min were considered to find the proper one, therefore the value of parameter *d* for random predictor was set to 4. Also the significant level was kept at $\alpha_{RP} = 0.05$. The results are also presented in Table 4.2. For all patients (except one patient, number 20), the observed sensitivities exceed the critical sensitivities of analytical random predictor. On average, the upper critical sensitivity of analytical random predictor was 33.3%, while the sensitivity of the proposed method reached 75.8%.

Table 4.2 – Results for the 24 studied patients

Pat. ID	Test rec.(h)	N. test seiz.	MDAD feature selection						mRMR feature selection					
			SS	FPR	N.S.F.	SOP	SS_{RP}	*p-value*	SS	FPR	N.S.F.	SOP	SS_{RP}	*p-value*
1	62	4	**100**	**0.13**	**3**	**30**	50	0.004	75	0.19	10	40	50	0.024
2	84	4	50	0.01	10	40	25	0.001	**50**	**0**	**5**	**40**	0	0
3	65	3	**66.7**	**0.08**	**3**	**10**	33.3	0.002	66.7	0.11	10	20	33.3	0.015
4	37	4	75	0.24	40	40	50	0.045	**75**	**0.24**	**10**	**30**	50	0.021
5	46	5	**80**	**0.06**	**10**	**30**	20	0.032	60	0.06	10	30	20	0.032
6	17	2	50	0	10	40	0	0	**50**	**0**	**3**	**30**	0	0
7	23	3	**100**	**0.04**	**10**	**40**	33.3	0.008	100	0.13	10	40	66.7	0.002
8	64	3	**66.7**	**0.08**	**3**	**10**	33.3	0.002	66.7	0.11	10	20	33.3	0.015
9	76	4	25	0.01	20	10	0	0.026	**50**	**0.26**	**10**	**10**	25	0.040
10	82	4	**75**	**0.04**	**20**	**30**	25	0.009	75	0.06	10	30	25	0.020
11	65	1	**100**	**0**	**10**	**30**	0	0	100	0	20	40	0	0
12	40	3	**100**	**0.04**	**10**	**40**	33.3	0.008	100	0.17	10	40	66.7	0.005
13	61	3	**100**	**0**	**20**	**40**	0	0	100	0.01	10	40	33.3	0.000
14	43	1	**100**	**0.02**	**3**	**10**	0	0.013	100	0.07	10	40	100	0.001
15	68	3	66.7	0.24	3	10	33.3	0.018	**66.7**	**0.04**	**3**	**40**	33.3	0.008
16	40	3	66.7	0.07	10	40	33.3	0.024	**66.7**	**0.04**	**40**	**40**	33.3	0.008
Mean	54.6	3.125	**73.98**	**0.06**	**11.5**	**28.1**	26	0.012	71.98	0.09	11.3	33.12	34	0.012
Sum	873	50												
17	43	3	**100**	**0.09**	**10**	**40**	33.3	0.038	66.7	0.04	5	40	33.3	0.008
18	110	3	100	0.17	5	40	66.7	0.005	**100**	**0.10**	**3**	**30**	33.3	0.027
19	18	4	**75**	**0.22**	**3**	**40**	50	0.036	50	0.06	40	40	25	0.034
20	80	5	40	0.23	10	40	60	0.007	**40**	**0.19**	**5**	**40**	60	0.004
21	157	9	**77.8**	**0.24**	**5**	**40**	44.4	0.021	22.2	0.09	3	30	22.2	0.023
22	50	5	**80**	**0.16**	**5**	**20**	40	0.005	80	0.18	40	40	40	0.048
23	55	5	**80**	**0.07**	**5**	**20**	20	0.020	60	0.16	3	30	40	0.016
24	151	3	**100**	**0.06**	**10**	**30**	33.3	0.010	66.7	0.03	5	30	33.3	0.003
Mean	83	4.625	**78.36**	**0.15**	**6.6**	**33.7**	43.2	0.018	54.04	0.09	13	35	35.13	0.020
Sum	664	37												
Mean	64	3.625	**75.8**	**0.10**	**9.9**	**30**	33.3	0.014	64.4	0.09	11.9	33.7	34.48	0.015
Sum	1537	87												

- SS: Sensitivity of the raised alarms in percentage
- FPR: False prediction rate per hour
- N.S.F.: Number of selected features
- SOP: The seizure occurrence period (preictal period) in minute
- SS_{RP}: The sensitivity of the random predictor
- *p-value*: The p-value of the random predictor

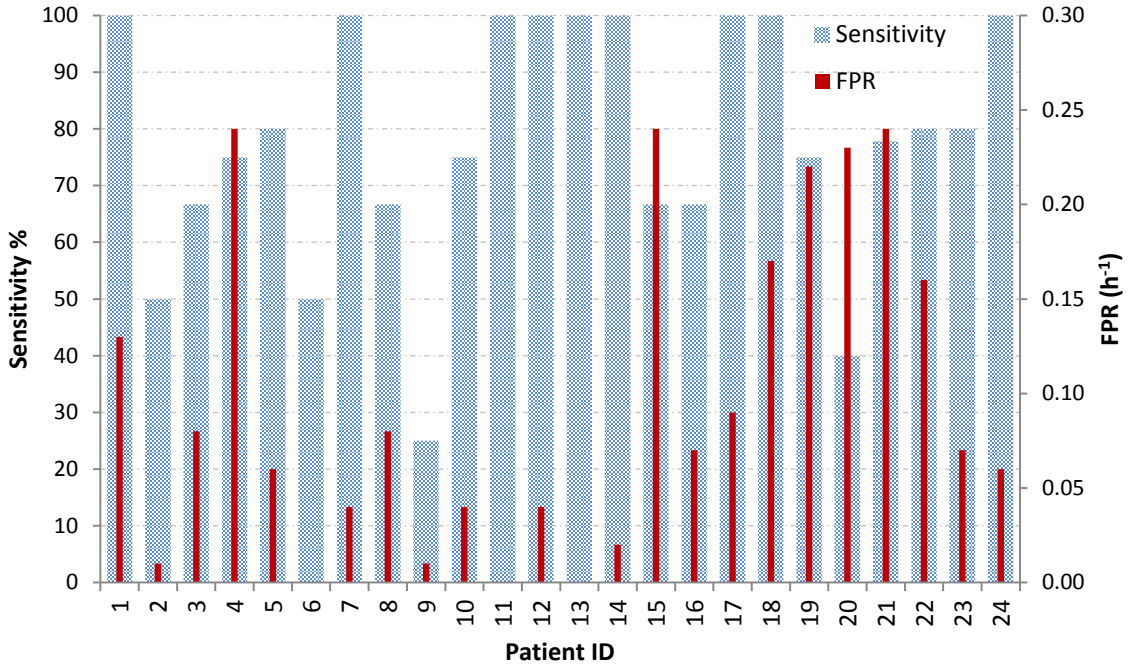

(a) MDAD feature selection

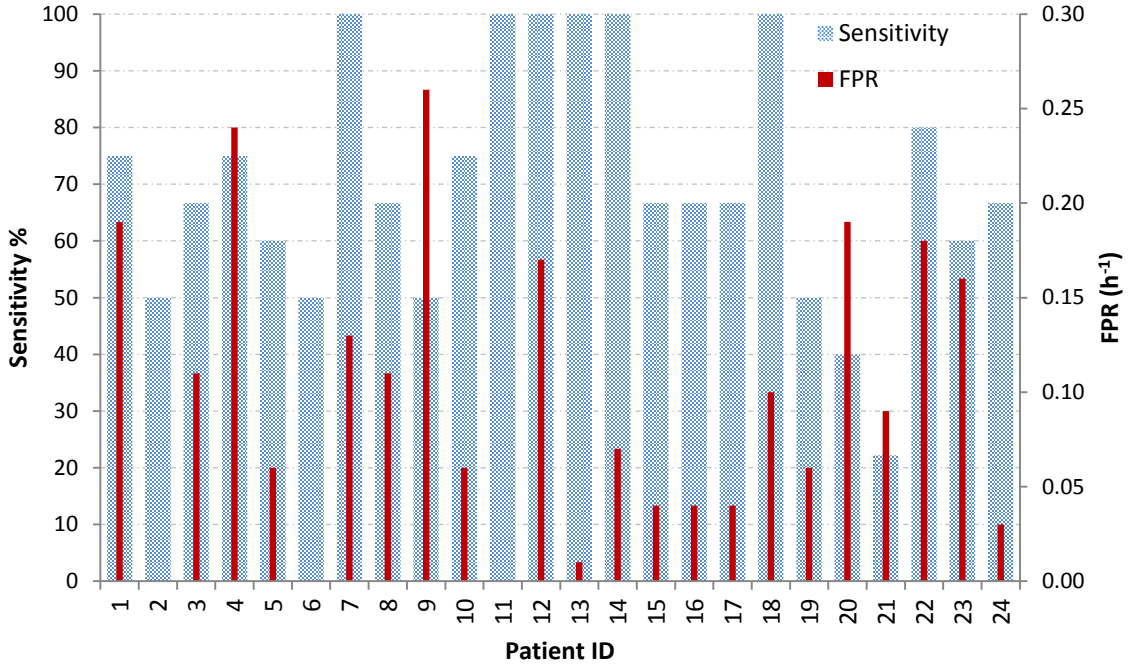

(b) mRMR feature selection

Figure 4.6 – Sensitivity and FPR results achieved by the proposed seizure prediction method for 24 studied patients using both MDAD and mRMR feature selection methods.

The optimal number of features obtained was 9.9 in average, which indicates the discriminative potential of the proposed relative features. In this study long-term continuous recordings have been used, contrasting with short-term discontinuous recordings used in most of the previous studies (Mormann et al. , 2003b, Winterhalder et al. , 2006, Chisci et al. , 2010, Park et al. , 2011, Soleimani-B et al. , 2012, Li et al. , 2013, Zheng et al. , 2014b). Results are in good comparison with other seizure prediction studies using long-term continuous recordings (Feldwisch-Drentrup et al. , 2010, Feldwisch-Drentrup et al. , 2011c, Rasekhi et al. , 2013, Teixeira et al. , 2014b, Rasekhi et al. , 2015). Furthermore, as the awake-asleep cycles have been considered both in the training and testing phases, it is expected that this effect is embedded in the predictor. Figure 4.7 illustrates the output of the proposed approach for entire recordings of test set for one of the studied patients.

On average, for the scalp recordings, the best predictors provided sensitivity of 73.98% and FPR of 0.06 per hour. In contrast iEEG based predictions showed sensitivity of 78.36% and FPR of 0.15 h^{-1}. The results therefore surprisingly indicate comparable prediction performances both for sEEG and iEEG data using the proposed features. Furthermore, it can be argued that the superior performance of the sEEG in terms of FPR has been achieved at the cost of using more features (11.5 in average) compared to that of iEEG (6.6 in average).

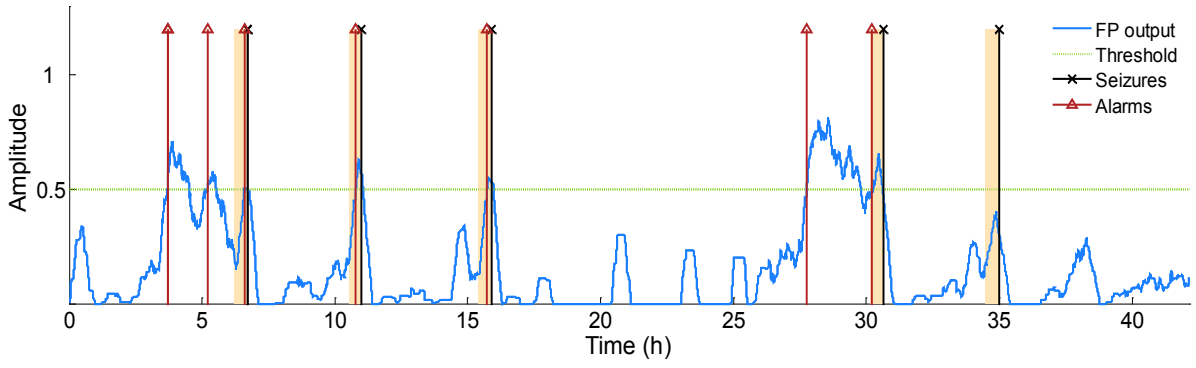

Figure 4.7 – The output of the FP method for 42 h continuous recordings of test data for one of the studied patients. The highlighted areas show 30 min preictal periods, and the vertical red lines are the alarms raised by the firing power method. The five vertical black lines indicate the seizure onsets.

The introduced feature selection method has shown improved performance in comparison to the well-known mRMR feature selection method. The superior performance of the proposed feature selection method was demonstrated in two ways: firstly, referring to Table 4.2, MDAD method is showing higher seizure prediction performance (SS of 75.8%, FPR of 0.1 h^{-1}), using in average a lower number of features (9.9) in comparison to the mRMR method (SS of 64.4%, FPR of 0.09 h^{-1}, for 11.9 features in average). Secondly, if the obtained results from using only three highest ranked features are compared, as presented in Table 4.3, it becomes clear that the MDAD method is also performing better with respect to SS and FPR for the same number of features. The highest ranked features are tabulated in Table 4.4.

Table 4.3 – Results obtained using the three highest ranked features

Patient ID	Total test record. (h)	No. test seizures	MDAD			mRMR		
			SS%	FPR (h^{-1})	SOP (min)	SS%	FPR (h^{-1})	SOP (min)
1	62	4	100	0.13	30	50	0.08	40
2	84	4	25	0.01	40	25	0.11	40
3	65	3	66.67	0.08	10	33.33	0.07	40
4	37	4	75	0.38	30	75	0.26	20
5	46	5	60	0.07	40	40	0.09	40
6	17	2	50	0.23	40	50	0	30
7	23	3	66.66	0.04	40	100	0.4	30
8	64	3	66.66	0.08	10	33.33	0.06	20
9	76	4	25	0.06	10	25	0.06	10
10	82	4	75	0.42	10	50	0.04	30
11	65	1	100	0.05	20	100	0.08	30
12	40	3	66.66	0.2	40	66.66	0.25	10
13	61	3	100	0.05	40	66.66	0.03	30
14	43	1	100	0.02	10	100	0.26	20
15	68	3	66.66	0.25	10	66.66	0.04	40
16	40	3	66.66	0.22	40	33.33	0.15	30
17	43	3	100	0.21	40	66.66	0.09	40
18	110	3	50	0.16	20	100	0.1	30
19	18	4	75	0.23	40	25	0.06	40
20	80	5	60	0.49	20	20	0.17	40
21	157	9	44.44	0.19	30	22.22	0.09	30
22	50	5	100	0.38	30	20	0.04	10
23	55	5	80	0.13	20	60	0.16	30
24	151	3	100	0.11	20	66.66	0.26	30
M./S.	1537	87	68.39	0.17	26.6	47.12	0.12	29.6

4.1.4 Discussion

The proposed relative bivariate features are derived from the normalized spectral power and resulted in an improved performance. Moreover, using the new feature selection method, further improves performance of the predictor. By combining the relative bivariate features with original normalized spectral power features in one feature space, and then ranking the features using the MDAD method, the efficiency of features were compared. Table 4.4 presents the best five features resulting from application of MDAD feature selection method. As seen from this table, for 90% of the cases, relative bivariate features are selected as the best. In Table 4.4 the value under each focal channel represents the ratio of observed seizure initiations on that channel. For example if a patient experiences 8 seizures, four of which initiating in the vicinity of channel F3, the value under F3 will be 0.5.

Two reasons could be pointed out for this superior performance: firstly, doubling effect is achieved in some bivariate features, for which the two building univariate features have opposite up/down trends during preictal state. Therefore preictal transient changes are highlighted. Secondly, univariate features are very dependent upon general status of the brain and patient's daily life, and could not guarantee high preictal discrimination. For example during preictal state the spectral power of Delta band is known to decrease, in conjunction with an increase of the spectral power of Gamma band (Mormann et al. , 2005). However decrease in the power of Delta band occurs in other non-preictal situations as well, possibly not related to epileptogenic activity. This also holds for the increase in the power of Gamma band. Overall the bivariate measure will tend to reject the common mode interferences that are not related with ictogenesis.

Table 4.4 – The five highest ranked features for each of the 24 patients

ID	Focal channels			1st feature	2nd feature	3rd feature	4th feature	5th feature
	Ch1	Ch2	Ch3					
1	F10	P8	T8	$\frac{\beta_{P8}}{\alpha_{P8}}$	$\frac{\gamma_{P8}}{\delta_{F10}}$	$\frac{\gamma_{P7}}{\delta_{F9}}$	$\frac{\delta_{F9}}{\gamma_{P8}}$	γ_{P8}
	1	1	1					
2	F9	T9	T7	$\frac{\beta_{F9}}{\alpha_{F9}}$	$\frac{\beta_{T9}}{\alpha_{T9}}$	$\frac{\beta_{F9}}{\theta_{F9}}$	$\frac{\beta_{F10}}{\alpha_{F10}}$	$\frac{\beta_{T10}}{\alpha_{T10}}$
	1	1	0.86					
3	T7	F7	AF7	$\frac{\beta_{T7}}{\alpha_{T7}}$	γ_{T8}	$\frac{\beta_{F8}}{\theta_{F8}}$	$\frac{\beta_{F8}}{\alpha_{F8}}$	$\frac{\beta_{F7}}{\alpha_{F7}}$
	1	1	1					
4	FT9	T9	F9	$\frac{\delta_{F10}}{\gamma_{FT9}}$	$\frac{\theta_{F10}}{\theta_{T10}}$	$\frac{\delta_{F9}}{\gamma_{FT9}}$	$\frac{\delta_{T10}}{\gamma_{FT9}}$	$\frac{\theta_{F10}}{\beta_{FT8}}$
	1	1	1					
5	AF7	FP1	F3	$\frac{\theta_{P8}}{\delta_{P8}}$	$\frac{\theta_{P8}}{\delta_{AF7}}$	θ_{P8}	θ_{P4}	α_{P8}
	0.93	0.86	0.78					
6	F10	FT10	T10	$\frac{\beta_{FT10}}{\gamma_{F10}}$	$\frac{\gamma_{F10}}{\beta_{F10}}$	$\frac{\beta_{T10}}{\gamma_{FT10}}$	$\frac{\alpha_{FT10}}{\gamma_{F10}}$	$\frac{\gamma_{T10}}{\beta_{T10}}$
	1	1	1					
7	T8	P8	TP8	β_{P8}	$\frac{\alpha_{P8}}{\delta_{P8}}$	α_{P8}	$\frac{\alpha_{T7}}{\delta_{T7}}$	$\frac{\theta_{T7}}{\delta_{T10}}$
	1	0.86	0.86					
8	AF8	F8	FT8	$\frac{\beta_{O1}}{\beta_{FT10}}$	$\frac{\delta_{Pz}}{\delta_{O1}}$	$\frac{\alpha_{Pz}}{\gamma_{O1}}$	$\frac{\delta_{O2}}{\delta_{O1}}$	$\frac{\alpha_{Pz}}{\gamma_{F8}}$
	0.83	0.83	0.83					
9	F4	C4	F8	$\frac{\gamma_{C4}}{\alpha_{C4}}$	θ_{C3}	$\frac{\gamma_{F8}}{\beta_{F8}}$	$\frac{\gamma_{C4}}{\beta_{C4}}$	$\frac{\gamma_{C4}}{\theta_{C3}}$
	0.86	0.71	0.71					
10	AF7	F3	FP1	$\frac{\alpha_{AF8}}{\theta_{AF7}}$	$\frac{\beta_{AF8}}{\alpha_{FP1}}$	$\frac{\beta_{AF8}}{\alpha_{AF7}}$	$\frac{\beta_{F3}}{\gamma_{FP1}}$	$\frac{\beta_{AF8}}{\theta_{F4}}$
	0.86	0.86	0.86					
11	T10	FT10	T4	$\frac{\alpha_{FT9}}{\beta_{T3}}$	$\frac{\beta_{T9}}{\gamma_{FT9}}$	$\frac{\alpha_{T9}}{\beta_{FT9}}$	$\frac{\beta_{T10}}{\gamma_{FT10}}$	$\frac{\beta_{T10}}{\gamma_{FT9}}$
	1	1	No info					
12	T10	TP10	FT10	δ_{TP10}	$\frac{\gamma_{O1}}{\delta_{TP10}}$	$\frac{\gamma_{O1}}{\delta_{F3}}$	$\frac{\gamma_{TP10}}{\delta_{TP10}}$	$\frac{\gamma_{O1}}{\delta_{O1}}$
	0.83	0.83	0.83					
13	FT10	T10	TP10	$\frac{\beta_{T10}}{\alpha_{T10}}$	$\frac{\gamma_{TP10}}{\alpha_{TP10}}$	$\frac{\beta_{FT9}}{\alpha_{FT9}}$	$\frac{\beta_{FT10}}{\alpha_{FT10}}$	$\frac{\beta_{TP10}}{\gamma_{T10}}$
	0.83	0.83	0.83					
14	CZ	FZ	PZ	γ_{TP9}	$\frac{\alpha_{TP9}}{\theta_{FZ}}$	γ_{TP10}	$\frac{\beta_{TP10}}{\delta_{TP10}}$	$\frac{\beta_{TP9}}{\delta_{TP9}}$
	0.66	0.66	0.33					
15	FT10	SP2	T8	$\frac{\alpha_{T5}}{\alpha_{SP2}}$	γ_{T1}	$\frac{\alpha_{SP1}}{\gamma_{SP2}}$	$\frac{\theta_{T5}}{\alpha_{SP2}}$	$\frac{\theta_{T4}}{\delta_{SP2}}$
	0.50	0.50	0.33					
16	SP1	F7	F3	$\frac{\beta_{SP2}}{\gamma_{F4}}$	$\frac{\gamma_{F7}}{\beta_{F7}}$	$\frac{\gamma_{SP2}}{\gamma_{SP1}}$	$\frac{\gamma_{SP2}}{\alpha_{SP1}}$	$\frac{\gamma_{SP2}}{\beta_{SP1}}$
	1	0.83	0.17					
17	ELA05	ELA06	ELA07	$\frac{\alpha_{ELA12}}{\gamma_{ELA06}}$	$\frac{\theta_{ELA12}}{\gamma_{ELA06}}$	$\frac{\alpha_{ELA13}}{\gamma_{ELA06}}$	$\frac{\beta_{ELA13}}{\gamma_{ELA06}}$	$\frac{\beta_{ELA12}}{\gamma_{ELA06}}$
	1	1	1					
18	HIPAG1	AMYGG1	TEMPO4	$\frac{\alpha_{ORFRG6}}{\delta_{AMYGG1}}$	$\frac{\alpha_{ORFRG6}}{\delta_{TEMPO4}}$	$\frac{\theta_{ORFRG6}}{\delta_{TEMPO4}}$	γ_{TEMPO4}	$\frac{\gamma_{TEMPO4}}{\delta_{AMYGG1}}$
	0.625	0.5	0.125					
19	AHIPG3	AHIPG2	AHIPG4	$\frac{\gamma_{AHIPG4}}{\beta_{AHIPG3}}$	$\frac{\delta_{TEMAD4}}{\delta_{AHIPG3}}$	$\frac{\delta_{AHIPG4}}{\delta_{AHIPG3}}$	$\frac{\gamma_{AHIPG4}}{\beta_{AHIPG2}}$	$\frac{\gamma_{AHIPG4}}{\alpha_{AHIPG3}}$
	0.71	0.43	0.43					
20	HIPPP1	HIPPP2	No info	$\frac{\beta_{HIPPA2}}{\beta_{HIPPP2}}$	$\frac{\gamma_{HIPPA2}}{\theta_{HIPPA2}}$	$\frac{\alpha_{T1INS1}}{\theta_{HIPPA2}}$	$\frac{\alpha_{HIPPP1}}{\theta_{HIPPP1}}$	$\frac{\alpha_{TPOL1}}{\beta_{HIPPA2}}$
	1	0.125	No info					
21	F2IM2	F2IM1	F2M3	$\frac{\gamma_{F2A1}}{\delta_{F2IM1}}$	$\frac{\gamma_{F2A1}}{\delta_{F2IM2}}$	$\frac{\gamma_{F2A1}}{\delta_{F2A1}}$	$\frac{\gamma_{F2A1}}{\delta_{F2M3}}$	$\frac{\delta_{F2IA1}}{\gamma_{F2A1}}$
	1	0.83	0.66					
22	LFB1	LHA1	LHB1	$\frac{\gamma_{RBC1}}{\gamma_{LA1}}$	$\frac{\theta_{RBC1}}{\alpha_{LHB1}}$	$\frac{\alpha_{RBB1}}{\alpha_{LA1}}$	$\frac{\alpha_{RBC1}}{\beta_{LHB1}}$	$\frac{\theta_{RBC1}}{\theta_{LHB1}}$
	0.56	0.33	0.44					
23	TBA1	TBA2	HRA5	$\frac{\theta_{TRB9}}{\theta_{HRA5}}$	$\frac{\theta_{TRB9}}{\alpha_{HRA5}}$	$\frac{\alpha_{TRB9}}{\alpha_{HRA5}}$	$\frac{\alpha_{TRB9}}{\theta_{HRA5}}$	$\frac{\alpha_{HRA5}}{\theta_{HRA5}}$
	0.86	0.86	0.36					
24	TLB2	TLB3	TLB4	$\frac{\delta_{TBB1}}{\beta_{HR1}}$	$\frac{\beta_{HR1}}{\delta_{TLB4}}$	$\frac{\beta_{HR1}}{\delta_{TLB3}}$	$\frac{\delta_{HR1}}{\gamma_{TLB3}}$	$\frac{\gamma_{HR1}}{\gamma_{TLB2}}$
	0.71	0.14	0.14					

Comparing the results of sEEG and iEEG recordings, they showed similar performances, where the iEEG data could provide slightly higher SS and FPR than the sEEG signals in average. However, the lower FPR of sEEG data has been reached at the cost of using more features (11.5 in average) compared to that of iEEG (6.6 in average), which will increase the computational cost and power consumption of the implemented method. The need for less number of features (channels) suggests that iEEG data carry more clear but localized epileptogenic information than sEEG. The scalp level sEEG present a more generalized spatial view of the brain activity, whereas the iEEG are restricted to the region where surgery was performed and where electrodes are placed. This spatial view of the sEEG may reinforce the capture of the different dynamics in the different regions of the brain during the preictal phase, leading to a slightly better performance in seizure prediction. But further investigation is needed.

Concerning the artifacts' issue, especially with sEEG recordings, there are several opinions about how to solve it. Because there are no techniques to eliminate them without any elimination of good information, several recent studies (Gadhoumi et al. , 2012, Williamson et al. , 2012) seem to consider the raw signal, including the artifacts, and this was also done in the present study. The question is if this fact influences in a significant way the performance of the predictors. There are two stages in our methodology that reduce the influence of the artifacts to a level that we consider satisfactory: (i) by smoothing the feature vector by a moving average with 12 epochs in (5); (ii) the regularization of the classifier output further reduces the effect of artifacts.

Moreover, the choice of six channels, three from the focal area and the remaining three far away from that area can be a questionable decision. We adopted this approach by the following three reasons: (i) a subset of channels close to the seizure onset zone are more discriminative in most patients (Gadhoumi et al. , 2012); (ii) remote areas contain much weaker seizure traces, but may possess richer information about general brain state, which in turn can aid detecting gradual preictal changes; (ii) the use of a higher number of channels is avoided here, because the long-term aim of the work is the development of a portable device to warn the patients and this recommends the use of a low number of scalp channels or recording implants (comfort of the patient). By considering these trade-offs, six channels

were considered adequate to profit from the spatially embedded information. This number has also been suggested by other authors (Mirowski et al. , 2009, Feldwisch-Drentrup et al. , 2010, Park et al. , 2011, Williamson et al. , 2012).

4.2 On the proper selection of preictal period

This section addresses the proper selection of preictal period using a novel statistical approach. The proposed seizure prediction method in the previous section labelled preictal samples using 10, 20, 30, and 40 min preictal periods, and it was found that the proper preictal periods differ from patient to patient. Therefore we developed a new approach to deal with this issue using an optimal preictal criterion. Additionally, the optimal preictal criterion can be helpful in two ways. First it can provide a means of measuring the efficiency of a feature, and second it can say whether a specific seizure has distinguishing preictal changes or not.

In the context of present neuroscience knowledge, the length of preictal period is unclear and varies from seizure to seizure. For some seizures, the epileptogenic transient changes develop very late close to the onset, whereas for some others appear much earlier several tens of minutes prior to the onset. Recently, several studies were proposed for seizure prediction using the combination of different univariate/bivariate and linear/nonlinear features, which lead to higher performances compared to using a single measure (Mirowski et al. , 2009, Park et al. , 2011, Valderrama et al. , 2012, Williamson et al. , 2012, Rasekhi et al. , 2013, Moghim et al. , 2014, Teixeira et al. , 2014b, Bandarabadi et al. , 2015). For this purpose, we need to use machine learning approaches, which are mostly supervised. Therefore, the accurate labeling of feature samples in preictal and non-preictal classes becomes very important issue for the proper training of a model. In fact, the improper choice of preictal intervals can affect prediction results drastically. Preictal periods larger than the optimal value will increase false predictions, while smaller values can decrease the sensitivity of prediction (Mormann et al. , 2005).

The optimal preictal period (OPP) of each seizure for the training set should be separately computed, and then be considered for the proper labelling of the training samples. However, as there exist no straightforward method for finding the appropriate preictal interval, previous machine-learning-based approaches have considered a fixed preictal period or examined different preictal periods to train/test the classifier in order to find a proper period (Mirowski et al. , 2009, Park et al. , 2011, Valderrama et al. , 2012, Williamson et al. ,

2012, Rasekhi et al. , 2013, Moghim et al. , 2014, Teixeira et al. , 2014b, Bandarabadi et al. , 2015).

Mormann et al. (Mormann et al. , 2005) used statistical analysis of several univariate and bivariate features to prove the existence of such a transient preictal period. They used the amplitude distributions histograms (ADHs) of preictal and interictal samples achieved from four predefined preictal periods of 5, 30, 120, and 240 min, and then calculated the receiver operating characteristic (ROC) curve of these two distributions to find out the predictability of epileptic seizures. Here we propose a new criterion which is statistically superior to ROC analysis, and also examine a wide range of preictal periods to find the OPP value for each seizure. The OPP can maximize the separability of training samples, and the maximum separability will boost the classification results by building a more accurate trained model. The resulting model is thus expected to provide the highest success rate with unseen data (test data), which is a fundamental hypothesis of classification and pattern recognition theories. The method is evaluated on 470 hours of iEEG and sEEG recordings related to 94 epileptic seizures.

4.2.1 Dataset description

In order to evaluate the proposed method, the long-term continuous iEEG and sEEG recordings of 18 patients (12 females and 6 males, aged 11–63 years, mean 28.5 years) with refractory partial epilepsy from the European Epilepsy Database (Klatt et al. , 2012) were considered. Recordings were obtained from eleven patients using intracranial electrodes with a sampling rate of 1024 Hz, and from seven patients through surface electrodes at 2500 Hz. The international 10-20 electrode montage was used for surface recordings. The overall length of recordings is 2692.6 hours and contains 239 epileptic seizures. The electrographic onsets were considered in this study, as they usually precede the clinical onsets. For each patient, two channels located on the foci were selected using prior knowledge on seizure initiation and propagation information, also available in the database. Patients' characteristics are summarized in Table 4.5.

Table 4.5 – Characteristics of 18 studied patients and their EEG recordings

ID	Rec. type	Gender	Age	Onset age (y)	Localization of seizure onsets	Seizure type	Recording duration (h)	N. of seizure	N. studied seizures
1	Inv.	F	29	10	RMT, RLT	CP1, SP7, UC1	183	9	7
2	Inv.	F	32	1	LMT	CP8, UC1	162.6	9	4
3	Inv.	F	11	3	RMT	CP4, SP4, UC6	155	14	2
4	Inv.	F	32	8	RBF, RMT, LMT	CP2, SP2, UC5	151.6	9	4
5	Inv.	F	18	6	L-T, L-F	CP13	127.8	13	10
6	Inv.	M	21	5	RLT, RMT	CP19, UC3	170.6	22	4
7	Inv.	M	17	1	LMT, LLT, L-T	SP25, SG6	142	31	5
8	Inv.	M	18	11	LBT, LLT, RBT	CP4, SP4, SG4, UC1	246.2	13	7
9	Inv.	F	63	30	LMT, R-T	CP15, UC4	118.9	19	5
10	Inv.	M	39	8	L-F, L-C	CP2, SP3, UC25	110.6	30	5
11	Inv.	F	14	13	L-T, LLT	CP6, SG4, UC4	217.1	14	6
12	Scalp	F	46	14	R-T, L-T	CP7, UC1	204.2	8	4
13	Scalp	M	18	17	RPT	SG4, SP3, CP2, UC5	165.1	14	9
14	Scalp	F	28	no info	no info	SP5, SG3	111.2	8	4
15	Scalp	F	31	20	R-T, L-T	SP3, SG2, CP1, UC2	93.6	8	4
16	Scalp	F	18	18	R-T	SP3, SG1, SP1, UC1	100.3	6	5
17	Scalp	F	46	no info	no info	CP3, SP1, UC2	73.1	6	5
18	Scalp	M	32	28	L-T, R-T	SG4, CP1, UC1	159.7	6	4
Mean			28.5	12.1			149.6	13.3	5.2

- Localization of seizure onsets: ABC; A (R: right, L: left), B (-: none, B: basal, L: lateral, M: mesial, P: polar), C (F: frontal, T: temporal, C: central). E.g. RMT (right mesial temporal lobe), L-F (left frontal lobe), RBF (right basal frontal lobe).
- Seizure type: type of clinical seizures; CP: complex partial, SP: simple partial, SG: secondarily generalized, UC: unclassified. Numbers following the abbreviations represent the number of seizures of that type.

For this study, instead of the whole recordings, we have used only 5 hours of the recording before each seizure. For a proper evaluation of the method, we have considered only those seizures that occur following at least 6 hours of seizure-free data. Doing so ensures that every seizure activity completely fades out during the 5 hours preceding the candidate seizures. With this limitation 470 h recordings of 94 epileptic seizures were considered. Afterwards and prior to feature extraction, the selected EEG data was segmented into 8 seconds windows with 50% overlap. We chose overlapped windows to provide more feature samples for each class, so that we could have a better estimation of ADHs, and also to obtain more smoothed ADHs especially for shorter preictal periods.

4.2.2 Optimal preictal criterion

The proposed method encompasses an optimal preictal criterion, which is calculated using ADHs of preictal and interictal samples. To find the proper preictal, we considered a two-class preictal/interictal problem as well as their corresponding ADHs. The optimal preictal criterion is defined as the common area between two normalized ADHs (C_{ADHs}), and the proposed method relies on the idea that the optimum preictal period should increase discriminability among two classes and minimize this criterion (Figure 4.8).

To obtain the normalized ADHs, feature samples of each feature vector was normalized to fall inside the interval [0 1] by (4.4). Each feature vector contains the interictal and preictal feature samples of a seizure. Also the feature axis is discretized into 50 equally spaced bins, as required for calculating ADHs. The net area under each normalized ADH is therefore one, and the common area between two normalized ADHs (C_{ADHs}), which was explained in the previous chapter, can be achieve by (4.6).

Lower C_{ADHs} values represent higher separability between samples of the two classes for a given feature. Therefore, the preictal period having the lowest C_{ADHs} represents an adequate choice, and is more likely to improve the seizure prediction performance. Figure 4.8 presents a sample feature corresponding to one of the studied seizures and the resulted normalized ADHs for preictal values of 10, 30, 50 and 70 minutes. The lowest C_{ADHs} is obtained for the preictal period of 30 minutes among the four preictal periods.

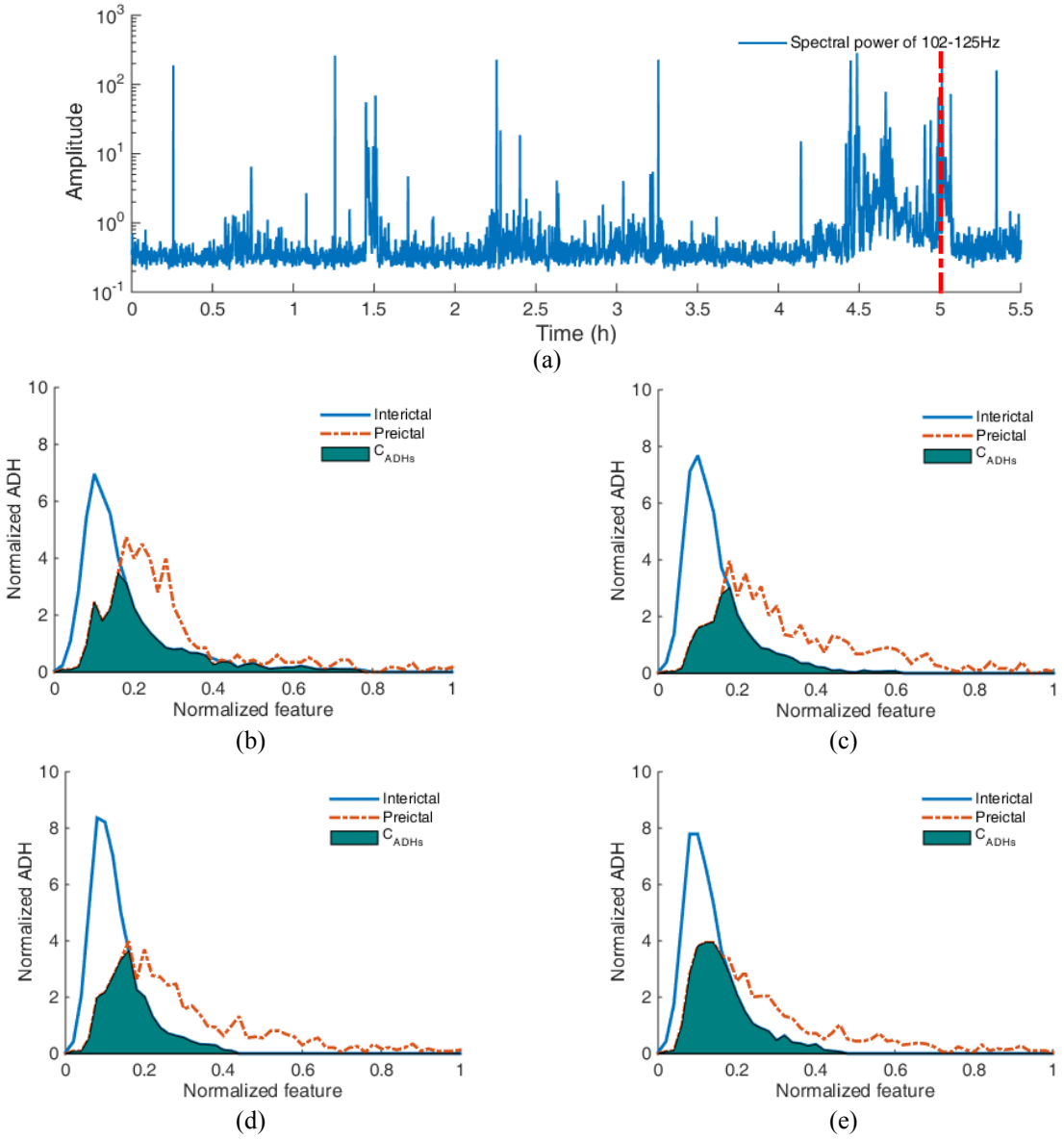

Figure 4.8 – Finding the proper preictal period for a feature/seizure. (a) Spectral power of 102-125 Hz extracted from 5.5 hours of iEEG recordings, including a seizure onset at 5h (seizure 4, patient 1). (b, c, d, e) The normalized ADHs of preictal and interictal samples using four preictal periods of 10, 30, 50, and 70min, respectively. Among these four preictal periods, the 30min preictal period provided less C_{ADHs}.

To find the OPP, C_{ADHs} is calculated for various preictal periods sweeping between 5 and 180 min, with constant increments. Finally, by studying the resulting C_{ADHs} curve, the preictal period providing the lowest C_{ADHs} could be empirically found. Figure 4.9 illustrates the C_{ADHs} curve obtained for the same seizure of Figure 4.8, and the OPP is obtained as 32 min.

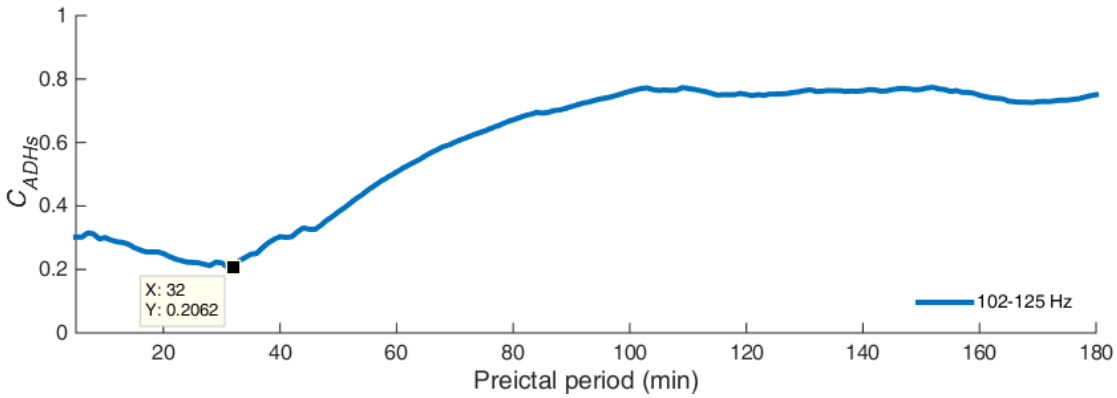

Figure 4.9 – The graph presents the C_{ADHs} of preictal and interictal classes with respect to different preictal periods for the same feature and seizure as in Figure 4.8. The OPP is located at 32min.

4.2.2.1 Studied features

To evaluate the proposed method for finding the OPP, the spectral power features were extracted from the windowed EEG signals. The spectral power features are computationally very cost effective, which make them suitable candidates for implantable and portable warning systems. Furthermore, these features recently have demonstrated promising results for seizure prediction (Jacobs et al. , 2009, Park et al. , 2011, Bandarabadi et al. , 2013, Pearce et al. , 2013, Rasekhi et al. , 2013, Alvarado-Rojas et al. , 2014, Bandarabadi et al. , 2015), specifically in the high gamma frequency bands (Jacobs et al. , 2009, Park et al. , 2011, Bandarabadi et al. , 2013, Pearce et al. , 2013, Alvarado-Rojas et al. , 2014).

Therefore, we investigated high quality iEEG and sEEG recordings (with the sampling rates of 1024 Hz and 2500 Hz), and divided the gamma band into several narrower sub-bands to study the spectral behavior more precisely. Instead of using the well-known frequency bands, the sub-bands were selected as (0.5-4], (4-8], (8-15], (15-30], (30-48], (52-75], (75-98], (102 125], (125-148], (152-198], (202-248], (252-348], (352-512] Hz, for the iEEG signals sampled at 1024 Hz. However, for the sEEG signals sampled at 2500 Hz, the highest sub-band of (352-512] Hz was replaced with four new sub-bands of (352-548], (552-748], (752-948], (952-1248] Hz. Furthermore, the spectral power of the whole bandwidth was also considered.

The spectral powers were obtained using PSD estimated through Welch method (Welch, 1967). The PSD is extracted using a rectangular moving window of length 8s and 50% overlap, providing a feature sample every four seconds. Prior to calculation of the ADHs, the extracted features were preprocessed by outlier removal and normalization. The outlier samples which are usually the result of physiological interferences, e.g. EMG, eye movement, and blinking artifacts, were removed by eliminating the values above percentile 98 of each class. Subsequently, each feature vector (a) was normalized to the interval of [0 1] by (4.4).

4.2.3 Results

OPP was calculated for each of the 94 individual seizures separately, including 59 from iEEG and 35 from sEEG recordings. The extracted features from the 5 hours of EEG data preceding each seizure were investigated. By choosing various preictal periods starting from 5 min and ending at 180 min, with 1 min increments, and calculating their corresponding C_{ADHs}, the OPP was found for each seizure. To evaluate the feature dependency of OPPs, they were initially presumed different among the features obtained for each seizure. By calculating the OPPs for all individual features, we found that OPPs are similar for discriminative features of each seizure.

Table 4.6 and Table 4.7 present the OPP and C_{ADHs} results of different electrode montages for iEEG and sEEG signals respectively, obtained from the three highest ranked features of each seizure. The resulting OPPs varied significantly among the seizures, even for the same patient. The OPPs range from 5 min up to 173 min, with an average value of 44.3 min. Furthermore, for 31 (22 from iEEG, 9 from sEEG) out of the 94 studied seizures, no OPP was found. An example is demonstrated in Figure 4.10, where C_{ADHs} of all spectral power features are traced with respect to different preictal periods for two seizures. The first seizure is depicted in Figure 4.10.a which was found to be predictable. The second seizure is also shown in Figure 4.10.b with no predictability using the studied features.

Table 4.6 – OPPs of 59 seizures recorded using iEEG signals and the three high ranked features for each seizure

		Monopolar							Bipolar						
Pat. ID	Sz. ID	OPP (minute)	1st feature		2nd feature		3rd feature		OPP (minute)	1st feature		2nd feature		3rd feature	
			C_{ADHs}	Frq. Hz	C_{ADHs}	Frq. Hz	C_{ADHs}	Frq. Hz		C_{ADHs}	Frq. Hz	C_{ADHs}	Frq. Hz	C_{ADHs}	Frq. Hz
1	1	-	-	-	-	-	-	-	-	-	-	-	-	-	-
	2	159	0.04	202-248	0.05	152-198	0.06	102-125	160	0.34	0.5-4	0.35	0.5-512	0.49	15-30
	3	-	-	-	-	-	-	-	-	-	-	-	-	-	-
	4	32	0.13	202-248	0.21	102-125	0.22	75-98	46	0.46	0.5-512	0.47	0.5-4	0.51	8-15
	5	17	0.37	352-512	0.41	52-75	0.42	75-98	-	-	-	-	-	-	-
	6	16	0.34	75-98	0.35	52-75	0.37	102-125	15	0.65	202-248	0.72	252-348	0.78	152-198
	7	-	-	-	-	-	-	-	-	-	-	-	-	-	-
2	8	-	-	-	-	-	-	-	-	-	-	-	-	-	-
	9	151	0.1	8-15	0.13	4-8	0.16	0.5-4	151	0.3	202-248	0.31	252-348	0.32	102-125
	10	149	0.08	8-15	0.08	4-8	0.11	15-30	149	0.19	102-125	0.21	75-98	0.22	52-75
	11	-	-	-	-	-	-	-	-	-	-	-	-	-	-
3	12	-	-	-	-	-	-	-	-	-	-	-	-	-	-
	13	54	0.1	152-198	0.11	252-348	0.12	202-248	52	0.3	0.5-512	0.32	0.5-4	0.37	15-30
4	14	-	-	-	-	-	-	-	-	-	-	-	-	-	-
	15	-	-	-	-	-	-	-	-	-	-	-	-	-	-
	16	-	-	-	-	-	-	-	-	-	-	-	-	-	-
	17	72	0.04	252-348	0.05	352-512	0.05	202-248	9	0.22	75-98	0.25	52-75	0.27	102-125
5	18	105	0.47	125-148	0.48	152-198	0.56	202-248	37	0.2	0.5-512	0.24	0.5-4	0.33	4-8
	19	62	0.49	8-15	0.5	15-30	0.54	4-8	62	0.43	15-30	0.56	8-15	0.59	4-8
	20	59	0.46	0.5-4	0.46	0.5-512	0.65	4-8	61	0.47	152-198	0.48	125-148	0.49	75-98
	21	-	-	-	-	-	-	-	-	-	-	-	-	-	-
	22	22	0.08	352-512	0.19	252-348	0.34	202-248	15	0.61	52-75	0.62	0.5-4	0.63	75-98
	23	42	0.19	102-125	0.19	125-148	0.19	202-248	42	0.3	52-75	0.31	75-98	0.32	0.5-512
	24	17	0.6	0.5-512	0.63	0.5-4	0.68	52-75	17	0.58	102-125	0.59	0.5-4	0.59	52-75
	25	24	0.08	102-125	0.08	125-148	0.1	75-98	58	0.06	0.5-4	0.07	0.5-512	0.08	30-48
	26	22	0.55	15-30	0.56	30-48	0.57	125-148	22	0.73	52-75	0.75	75-98	0.76	102-125
	27	15	0.06	202-248	0.08	252-348	0.09	102-125	15	0.04	0.5-4	0.05	0.5-512	0.07	52-75
6	28	173	0.13	102-125	0.15	75-98	0.18	125-148	173	0.18	0.5-4	0.2	0.5-512	0.34	75-98
	29	73	0.41	0.5-4	0.45	4-8	0.52	352-512	73	0.33	152-198	0.35	125-148	0.4	202-248
	30	-	-	-	-	-	-	-	-	-	-	-	-	-	-
	31	-	-	-	-	-	-	-	-	-	-	-	-	-	-
7	32	16	0.56	152-198	0.58	202-248	0.63	252-348	-	-	-	-	-	-	-
	33	10	0.27	75-98	0.28	30-48	0.34	52-75	10	0.29	75-98	0.39	202-248	0.48	252-348
	34	28	0.34	75-98	0.42	152-198	0.47	202-248	28	0.33	75-98	0.57	4-8	0.59	0.5-4
	35	7	0.38	202-248	0.4	125-148	0.43	152-198	7	0.55	0.5-4	0.6	252-348	0.64	352-512
	36	-	-	-	-	-	-	-	-	-	-	-	-	-	-
8	37	-	-	-	-	-	-	-	-	-	-	-	-	-	-
	38	-	-	-	-	-	-	-	-	-	-	-	-	-	-
	39	46	0.36	15-30	0.41	8-15	0.44	0.5-4	48	0.18	152-198	0.19	125-148	0.24	0.5-4
	40	32	0.11	252-348	0.15	202-248	0.16	75-98	27	0.06	0.5-4	0.08	0.5-512	0.23	15-30
	41	36	0.43	102-125	0.43	75-98	0.45	125-148	32	0.12	52-75	0.12	30-48	0.13	75-98
	42	21	0.11	202-248	0.12	125-148	0.15	102-125	-	-	-	-	-	-	-
	43	15	0.32	125-148	0.49	152-198	0.62	102-125	-	-	-	-	-	-	-
9	44	6	0.37	252-348	0.4	202-248	0.43	152-198	6	0.54	52-75	0.58	125-148	0.6	102-125
	45	-	-	-	-	-	-	-	-	-	-	-	-	-	-
	46	-	-	-	-	-	-	-	-	-	-	-	-	-	-
	47	22	0.44	252-348	0.51	202-248	0.56	125-148	-	-	-	-	-	-	-
	48	9	0.34	0.5-4	0.38	15-30	0.52	8-15	9	0.32	8-15	0.33	15-30	0.37	4-8
10	49	65	0.35	202-248	0.36	152-198	0.44	252-348	65	0.35	252-348	0.37	352-512	0.38	202-248
	50	20	0.42	15-30	0.46	0.5-4	0.52	30-48	20	0.43	0.5-4	0.45	15-30	0.51	30-48
	51	148	0.09	152-198	0.1	75-98	0.1	102-125	148	0.08	75-98	0.08	152-198	0.09	102-125
	52	16	0.14	15-30	0.19	30-48	0.22	0.5-4	16	0.16	30-48	0.21	15-30	0.22	52-70
	53	9	0.1	125-148	0.11	102-125	0.14	75-98	14	0.44	352-512	0.46	252-348	0.48	202-248
11	54	-	-	-	-	-	-	-	-	-	-	-	-	-	-
	55	-	-	-	-	-	-	-	-	-	-	-	-	-	-
	56	-	-	-	-	-	-	-	-	-	-	-	-	-	-
	57	-	-	-	-	-	-	-	-	-	-	-	-	-	-
	58	-	-	-	-	-	-	-	-	-	-	-	-	-	-
	59	46	0.28	8-15	0.31	4-8	0.32	30-48	46	0.3	8-15	0.33	4-8	0.34	15-30
Mean		49.1	0.27		0.30		0.35		49.7	0.34		0.37		0.41	

Table 4.7 – OPPs of 35 seizures recorded using sEEG signals and the three high ranked features for each seizure

		Monopolar							Bipolar						
Pat. ID	Sz. ID	OPP (minute)	1st feature		2nd feature		3rd feature		OPP (minute)	1st feature		2nd feature		3rd feature	
			C_{ADHs}	Frq. Hz	C_{ADHs}	Frq. Hz	C_{ADHs}	Frq. Hz		C_{ADHs}	Frq. Hz	C_{ADHs}	Frq. Hz	C_{ADHs}	Frq. Hz
12	60	103	0.14	15-30	0.14	30-48	0.15	125-148	103	0.12	15-30	0.15	30-48	0.17	152-198
	61	62	0.13	15-30	0.14	252-348	0.16	202-248	62	0.1	15-30	0.12	252-348	0.12	202-248
	62	126	0.09	352-548	0.1	252-348	0.12	202-248	126	0.12	352-548	0.13	252-348	0.13	202-248
	63	37	0.35	30-48	0.35	75-98	0.36	52-75	37	0.38	75-98	0.39	102-125	0.39	30-48
13	64	9	0.16	15-30	0.17	30-48	0.17	252-348	9	0.12	15-30	0.12	75-98	0.12	30-48
	65	9	0.03	52-75	0.04	102-125	0.05	125-148	9	0.02	102-125	0.03	52-75	0.03	75-98
	66	10	0.12	15-30	0.13	52-75	0.14	102-125	10	0.12	15-30	0.12	52-75	0.13	102-125
	67	-	-	-	-	-	-	-	-	-	-	-	-	-	-
	68	-	-	-	-	-	-	-	-	-	-	-	-	-	-
	69	-	-	-	-	-	-	-	-	-	-	-	-	-	-
	70	29	0.05	75-98	0.05	102-125	0.06	52-75	29	0.04	75-98	0.04	52-75	0.05	102-125
	71	34	0.08	352-548	0.07	15-30	0.08	75-98	34	0.06	352-548	0.07	102-125	0.07	75-98
	72	-	-	-	-	-	-	-	-	-	-	-	-	-	-
14	73	5	0.13	152-198	0.13	202-248	0.14	125-148	5	0.12	152-198	0.12	125-148	0.13	202-248
	74	92	0.07	102-125	0.08	125-148	0.08	75-98	92	0.06	30-48	0.11	52-75	0.16	75-98
	75	-	-	-	-	-	-	-	-	-	-	-	-	-	-
	76	71	0.02	125-148	0.02	252-348	0.02	102-125	71	0.02	125-148	0.03	102-125	0.03	202-248
15	77	-	-	-	-	-	-	-	-	-	-	-	-	-	-
	78	13	0.31	8-15	0.33	4-8	0.35	52-75	13	0.28	8-15	0.28	15-30	0.29	30-48
	79	28	0.1	152-198	0.1	102-125	0.1	125-148	28	0.1	152-198	0.1	102-125	0.1	125-148
	80	58	0.21	4-8	0.22	8-15	0.22	352-548	58	0.21	8-15	0.26	4-8	0.27	352-548
16	81	9	0.2	30-48	0.22	52-75	0.24	125-148	9	0.24	52-75	0.25	30-48	0.27	75-98
	82	20	0.21	30-48	0.23	15-30	0.28	75-98	20	0.27	15-30	0.29	75-98	0.3	52-75
	83	8	0.3	202-248	0.34	352-548	0.35	152-198	8	0.28	152-198	0.35	202-248	0.36	252-348
	84	18	0.49	15-30	0.52	202-248	0.53	252-348	18	0.51	202-248	0.52	152-198	0.54	125-148
	85	18	0.1	75-98	0.12	102-125	0.12	152-198	18	0.11	102-125	0.16	75-98	0.18	152-198
17	86	7	0.22	8-15	0.29	0.5-4	0.36	4-8	7	0.24	8-15	0.43	0.5-4	0.51	4-8
	87	78	0.36	30-48	0.48	552-748	0.5	15-30	78	0.38	30-48	0.48	15-30	0.49	352-548
	88	49	0.28	52-75	0.3	75-98	0.34	352-548	49	0.33	75-98	0.36	352-548	0.38	102-125
	89	-	-	-	-	-	-	-	-	-	-	-	-	-	-
	90	8	0.1	15-30	0.11	552-748	0.12	102-125	8	0.12	15-30	0.14	552-748	0.15	202-248
18	91	-	-	-	-	-	-	-	-	-	-	-	-	-	-
	92	42	0.55	0.5-4	0.55	4-8	0.57	8-15	42	0.49	0.5-4	0.5	4-8	0.57	8-15
	93	32	0.31	8-15	0.47	4-8	0.58	15-30	31	0.34	8-15	0.47	4-8	0.51	52-75
	94	-	-	-	-	-	-	-	-	-	-	-	-	-	-
Mean		37.5	0.20		0.22		0.24		37.5	0.20		0.23		0.25	

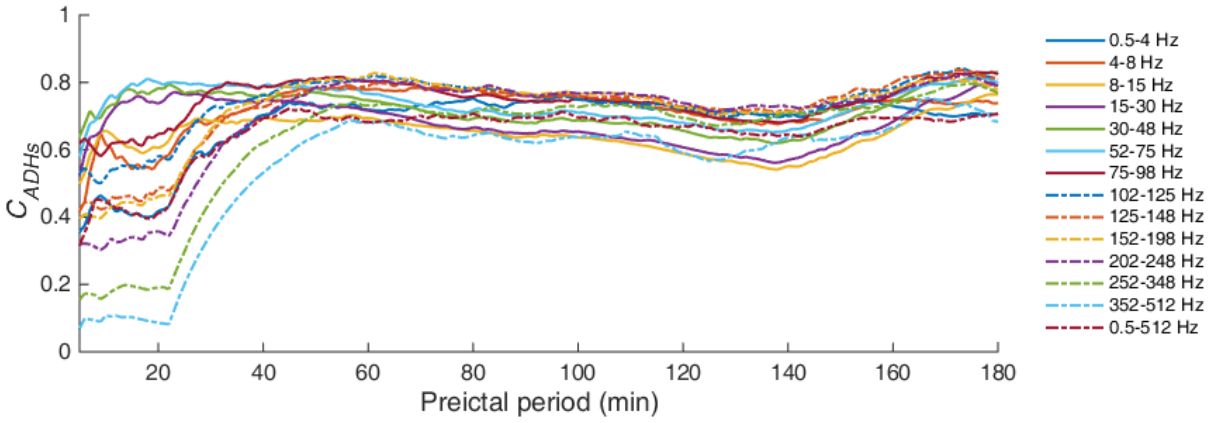

(a)

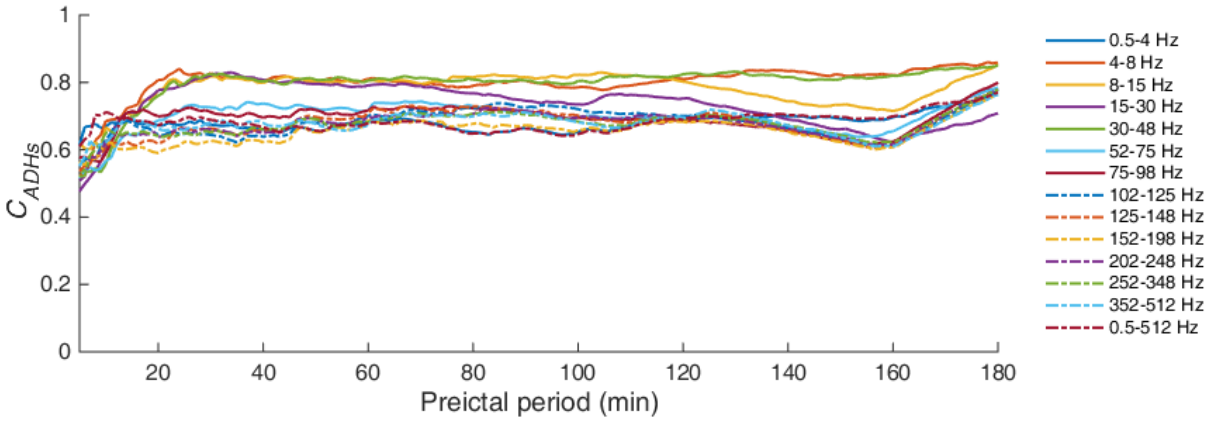

(b)

Figure 4.10 – The C_{ADHs} of interictal and preictal classes with respect to different preictal periods, and for the 14 features of two studied seizures. (a) A seizure with an identifiable OPP using monopolar spectral power features (seizure 22, patient 5): the OPP is located around 22min, with spectral powers of 352-512, 252-348, and 202-248 Hz providing lower C_{ADHs} in OPP. (b) A seizure with no distinguishable preictal period using the monopolar spectral power features (seizure 12, patient 3).

4.2.4 Discussion

The results reveal that the OPPs corresponding to different features and extracted for a same particular seizure are very close. More specifically, for a set of features extracted from a common domain, e.g. spectral power features, the OPPs corresponding to different features were found to be similar. However OPPs vary significantly from one seizure to another, demonstrating the seizure-specific nature of OPPs (Figure 4.11).

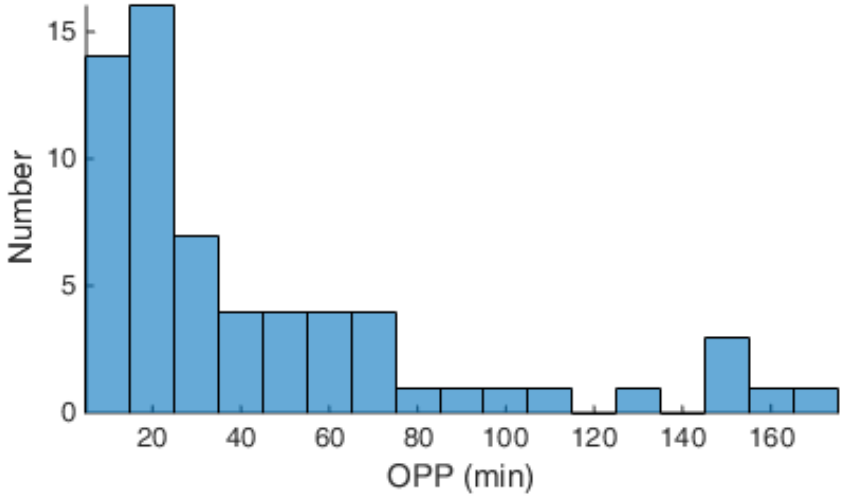

Figure 4.11 – Histogram of OPPs for 63 epileptic seizures with distinguishable preictal period

As a practical outcome of these findings, the OPP values obtained from the training set can be used for building a more consistent model for seizure prediction, through the correct labeling of training feature samples. Figure 4.12 demonstrates distribution of feature samples for three cases of preictal periods for a sample seizure. According to the Figure 4.12, the best separability can be achieved for a preictal period equal to the OPP.

The prediction performance on the unseen data is completely dependent on the trained model. However, for test data (unseen data), the exact length of OPP for each seizure cannot be estimated until the seizure occurs. Therefore, by considering the minimum and maximum of OPP values obtained from the training set, we can define the seizure prediction horizon (SPH), and the seizure occurrence period (SOP) for evaluating the raised alarms on the test set. The SPH can be considered smaller than the minimum of the OPPs, with a safe margin to account for those test seizures whose OPPs are even less than the obtained OPP during the training. Similarly, the SOP can be defined as a value larger than the difference between the maximum of the training OPPs and the assigned SPH, while considering a safe margin to account for the test seizures having OPPs larger than the maximum of the training OPPs (Figure 4.13). In practice, in specifying these safe margin values one should also consider the further delays introduced from the post-processing of the classifier outputs, e.g. by Kalman filter or the moving average (Teixeira et al. , 2012).

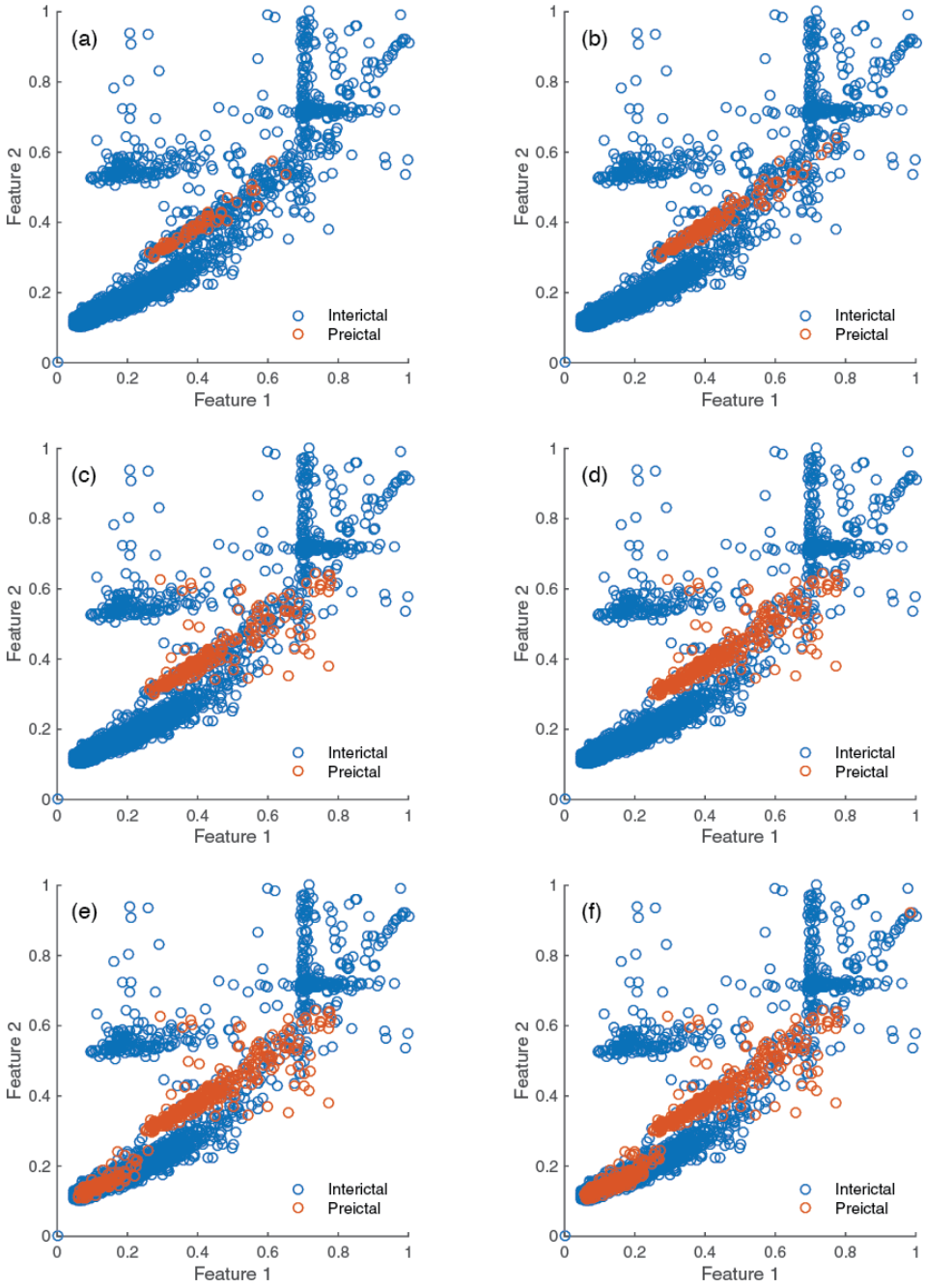

Figure 4.12 – Distribution of training feature samples in a two-dimensional feature space (patient 5, seizure No. 22, spectral powers of 252-348 Hz and 352-512 Hz) using (a) 5 min preictal period, (b) 10 min preictal period, (c) 15 min preictal period, (d) optimal preictal period of 22 min, (e) 30 min preictal period, and (f) 40 min preictal period. The overlap between the preictal and interictal feature samples increases when using preictal periods smaller or larger than the OPP (a, b, c, e, f). As a result, separability of the features is maximal when preictal period is selected equal to the OPP (d). The performance of a trained model would be decreased significantly, if the preictal samples are mislabeled as the interictal samples, or vice versa.

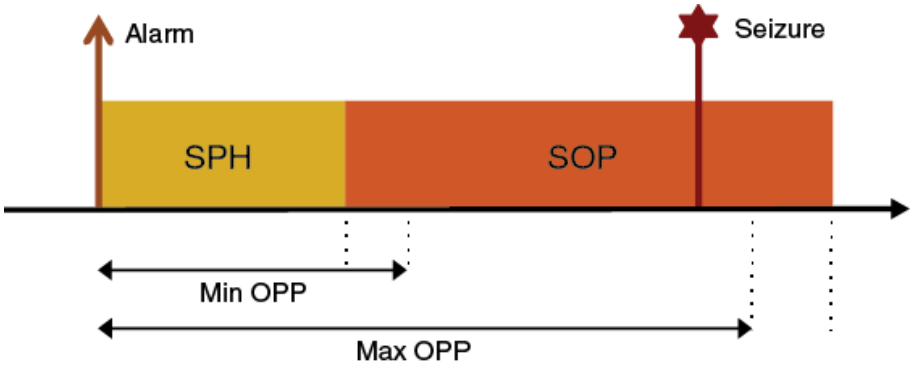

Figure 4.13 – Determining of the seizure prediction horizon (SPH) and the seizure occurrence period (SOP) according to the obtained OPPs from the training set. The SPH can be defined using the minimum OPP, whereas the SOP can be specified using the maximum OPP and this SPH.

4.2.4.1 Prediction capability of spectral powers

The spectral power features of different frequency bands extracted from monopolar and bipolar iEEG/sEEG signals were studied with the aim of choosing the proper preictal periods. However as mentioned earlier, the proposed method can also be used as a criterion to identify the prediction capability of features, and was investigated for the extracted spectral power features. On average, C_{ADHs} values of highest ranked feature in the OPP point were 0.24 and 0.28 for monopolar and bipolar montages respectively, demonstrating very good separability between the samples of preictal and interictal classes.

Table 4.8 presents the five most relevant frequently bands for seizure prediction. These results were obtained by counting how many times each frequency band has appeared among the three highest ranked features of monopolar iEEG, bipolar iEEG, monopolar sEEG, and bipolar sEEG montages. The three highest ranked features for each seizure/montage were presented in Table 4.6 and Table 4.7. For the case of monopolar iEEG, the higher frequency bands in the range of 75-348 Hz provided lower C_{ADHs}. More specifically the frequency bands of 202-248 Hz (16x) and 102-125 Hz (12x) were most repeated among the selected bands. For the case of bipolar iEEG, however, the bands of 0.5-4 Hz (14x) and 75-98 Hz (11x) demonstrated lower C_{ADHs} in most of studied seizures. With respect to sEEG recordings, similar bands were selected for monopolar and bipolar montages, where the bands of 15-30 Hz, 75-98 Hz, and 102-125 Hz were the most repeated among the three best bands.

Table 4.8 – The five most relevant spectral power features for seizure prediction

Channel montage and recording type	1st feature		2nd feature		3rd feature		4th feature		5th feature	
	Freq. Hz	Repetition	Freq. Hz	Repetition	Freq. Hz	Repetition	Freq. Hz	Repetition	Freq. Hz	Repetition
Monopolar iEEG	202-248	16	102-125	12	75-98	11	125-148	11	152-198	10
Bipolar iEEG	0.5-4	14	75-98	11	52-75	9	0.5-512	9	15-30	8
Monopolar sEEG	15-30	10	102-125	8	52-75	7	75-98	7	125-148	7
Bipolar sEEG	15-30	8	75-98	10	102-125	9	52-75	7	30-48	7

- Repetition: the number of times that the spectral power feature appeared in the three highest ranked features.

4.2.4.2 Surface versus intracranial EEG

In order to compare the results of scalp versus invasive recordings, the method was applied on both surface and intracranial recordings. While 74% (26 out of 35) of the seizures recorded using sEEG could provide distinguishing preictal periods, only 63% (37 out of 59) of the seizures captured using intracranial electrodes could provide discriminative preictal periods. Also the spectral power features estimated from sEEG recordings provided slightly lower C_{ADHs}, in overall compared to the iEEG signals (Table 4.9). The average value of C_{ADHs} in the OPP points for the highest ranked feature was 0.2 for sEEG recordings (35 seizures), and 0.27 for iEEG recordings (59 seizures). Although iEEG recordings showed lower separability (higher C_{ADHs}), however they provided higher OPPs, which is preferable for prediction algorithms. Furthermore, comparing the standard deviations of OPPs among scalp and invasive recordings, variation of the OPPs using sEEG is less than iEEG recordings for different seizures (Table 4.9).

Although we have not compared the simultaneous iEEG and sEEG recordings of each seizure, but the results of a large number of seizures indicate that sEEG recordings in general perform better for seizure prediction purpose. This could be the result of recording natures of sEEG and iEEG. Surface EEG is able to capture a more generalized view of the brain, and is more likely to reveal the transient preictal changes within the global state of the brain. In contrast, invasive EEG is strongly localized on a limited region of the brain, probably providing higher CADHs for the seizures developed far from the implanted region.

Table 4.9 – The average of OPP and C_{ADHs} results of the 94 studied seizures

Channel montage and recording type	OPP (minute)				C_{ADHs} (1st feature)		C_{ADHs} (2nd feature)		C_{ADHs} (3rd feature)	
	mean	std	min	max	mean	std	mean	std	mean	std
Monopolar iEEG	49.1	48.3	6	173	0.27	0.17	0.30	0.17	0.35	0.2
Bipolar iEEG	49.7	49.8	6	173	0.34	0.18	0.37	0.20	0.41	0.19
Monopolar sEEG	37.5	33.4	5	126	0.20	0.14	0.22	0.16	0.24	0.17
Bipolar sEEG	37.5	33.4	5	126	0.20	0.14	0.23	0.16	0.25	0.17
Monopolar sEEG/iEEG	44.3	42.9	5	173	0.24	0.16	0.27	0.17	0.3	0.19
Bipolar sEEG/iEEG	44.3	43.4	5	173	0.28	0.18	0.31	0.19	0.34	0.20

4.2.4.3 Monopolar against bipolar analysis

The method was applied on monopolar and bipolar signals of both sEEG and iEEG recordings, to find the proper channel configuration in seizure prediction. It was found that the computed OPPs for monopolar and bipolar montages were equal, the difference being in their prediction capability (C_{ADHs} values) only (Table 4.9). When dealing with sEEG recordings, no significant difference in C_{ADHs} values was observed among monopolar and bipolar recordings. However with respect to iEEG recordings, the spectral power features extracted from monopolar channel provided a better discrepancy between preictal and interictal samples. The average value of C_{ADHs} in the OPP points for the highest ranked feature was 0.27 and 0.34 for monopolar and bipolar iEEG recordings respectively. Furthermore, in five seizures recorded using iEEG, a distinguishing OPP was only found for monopolar montage and none for bipolar. Figure 4.14 shows the C_{ADHs} diagrams for different preictal periods of a seizure using monopolar and bipolar iEEG recordings, and Figure 4.15 depicts the C_{ADHs} diagrams for a seizure from monopolar and bipolar sEEG recordings.

The reason for imperfection of bipolar montage in iEEG could be the loss of information by subtraction of two very close iEEG recordings (in the range of few millimeters). With this subtraction, the electrical brain activities that are induced evenly on two neighboring electrodes could be lost. Such activities may contain critical epileptogenic information. In contrast, bipolar montage in sEEG recordings is obtained by subtracting the signals of two electrodes located in the range of few centimeters, and are not affected with this issue.

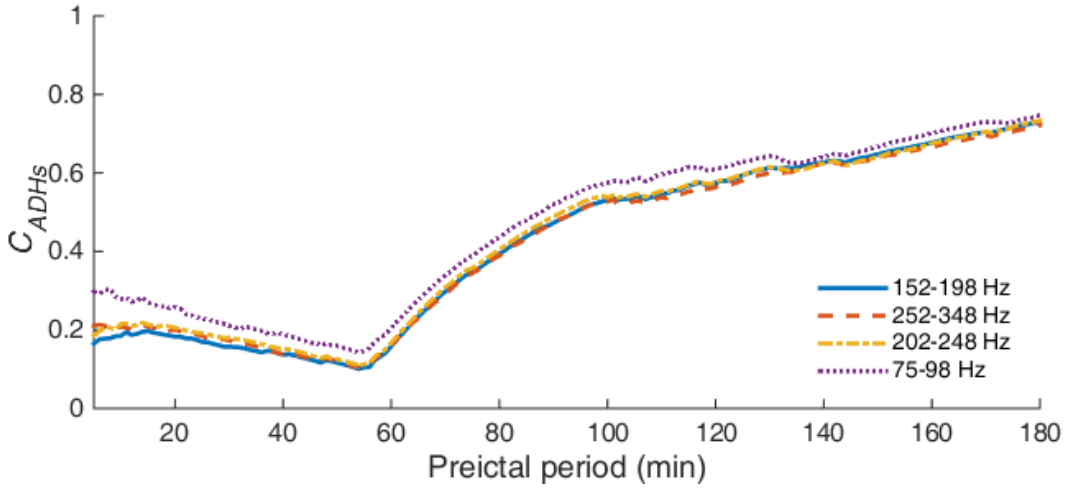

(a) C_{ADHs} achieved from monopolar iEEG

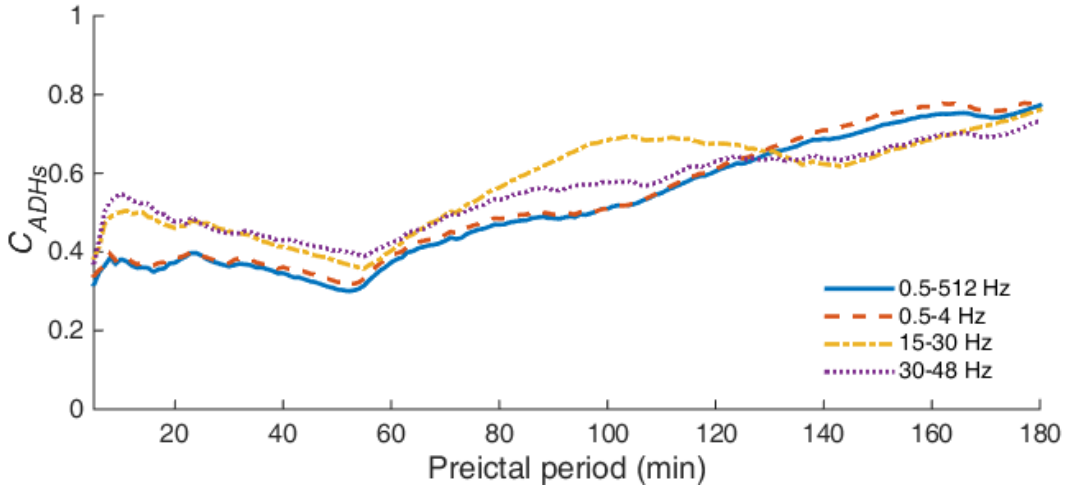

(b) C_{ADHs} achieved from bipolar iEEG

Figure 4.14 – The C_{ADHs} with respect to different preictal periods obtained from (a) monopolar and (b) bipolar iEEG recordings, and for the four highest ranked features of a studied seizure (seizure 13, patient 3). As seen from the graphs, the monopolar montage provided significantly lower C_{ADHs} than bipolar montage using iEEG recordings.

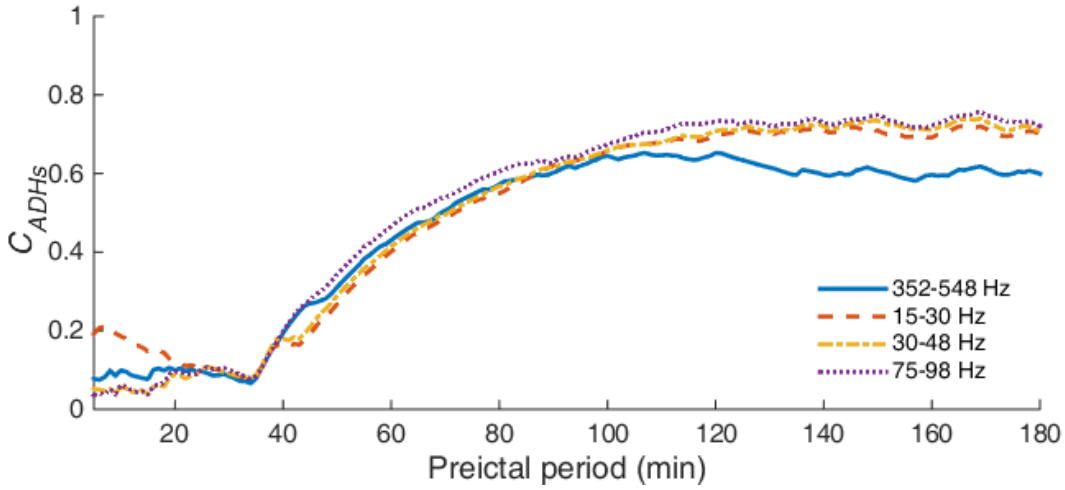

(a) C_{ADHs} achieved from monopolar sEEG

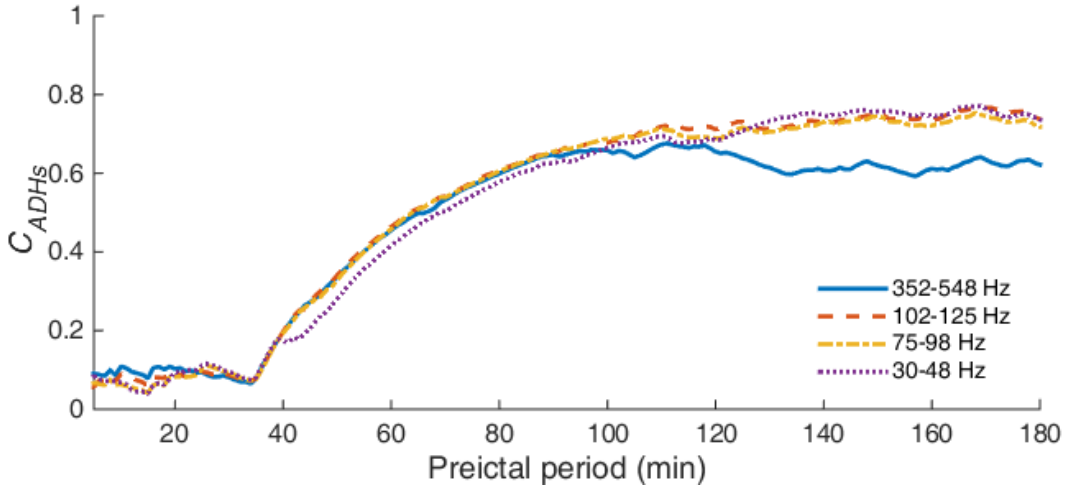

(b) C_{ADHs} achieved from bipolar sEEG

Figure 4.15 – The C_{ADHs} with respect to different preictal periods obtained from (a) monopolar and (b) bipolar sEEG recordings, and for the four highest ranked features of a studied seizure (seizure 71, patient 13). As seen from the curves, there is no significant difference between C_{ADHs} of monopolar and bipolar montages.

4.2.4.4 Computational cost of the method

The method is very fast, since it computes the ADHs of the features using different preictal periods, which impose very low computational costs. The ADHs were obtained using 176 different preictal periods, starting at 5min, ending at 180min, and with one minute increments. On an ordinary desktop computer, it required around 2 seconds for each

feature/seizure to calculate the criterion for 176 distinct preictal periods, and to find the OPP. The overall computation time for the 14/17 spectral power features and for all 94 studied seizures was about 40 min.

4.3 Conclusion

In this chapter we introduced a novel approach for seizure prediction based on a new proposed relative bivariate feature and a specifically developed feature selection method. Features were calculated from the PSD of the six EEG channels, requiring a very low computational power, thus making the method very fast, of relatively low complexity, and suitable for real-time low-power-budget portable devices with recent multicore microprocessors. We believe that the proposed method is a step forward for designing a robust and real-time portable seizure prediction device, suitable to be employed in clinical applications.

Furthermore, the problem of OPP selection, which plays a key role on the efficiency of supervised machine learning algorithms, was approached by a novel yet simple statistical methodology. By examining different preictal periods, and through the investigation of the proposed method, we could find the best discriminative preictal periods for each seizure. We have also found that the OPPs vary significantly from seizure to seizure, even for the seizures of a same patient. This suggests that for building a robust model, the OPP value of each seizure should be obtained separately and considered during the training phase of the model. The proposed statistical approach could also provide a means for quantifying the predictability of a seizure or the prediction capability of a feature. For the particular case study of spectral power features, it was found that the high frequency features were more discriminative. Furthermore, comparing the monopolar and bipolar iEEG/sEEG recordings indicated that monopolar signals perform better in iEEG recordings, whereas no significant difference was observed when using sEEG recordings. This work studied the linear univariate spectral power features, concluding that OPPs of different spectral powers are very close for a specific seizure. However this finding should also be studied for other types of features, such as nonlinear or bivariate ones, and require further researches.

Chapter 5 New seizure detection algorithms

In this chapter a new method for early seizure detection and two novel approaches for seizure detection are proposed. The early seizure detection method is aimed towards the closed-loop neurostimulation systems, whereas seizure event detection methods are introduced for automated labelling of continuous iEEG recordings for future studies. The reasons behind developing new methods are to improve the parameters of sensitivity, false detection rate, and detection latency, the latter parameter being approached by the proposed early seizure detection method.

Early seizure detection refers to the electrographic seizure onset detection without or with a negligible delay, and before the seizure reaches to its clinical phase (Figure 5.1). However in the seizure event detection, an alarm inside the ictal period is considered as a true detection regardless of the detection latency. All proposed methods are applied on the same dataset and channels, in order to achieve comparative conclusions. Also for the proper performance evaluation of the methods, long-term continuous iEEG recordings of 11 patients, with an overall length around two and a half months, are considered.

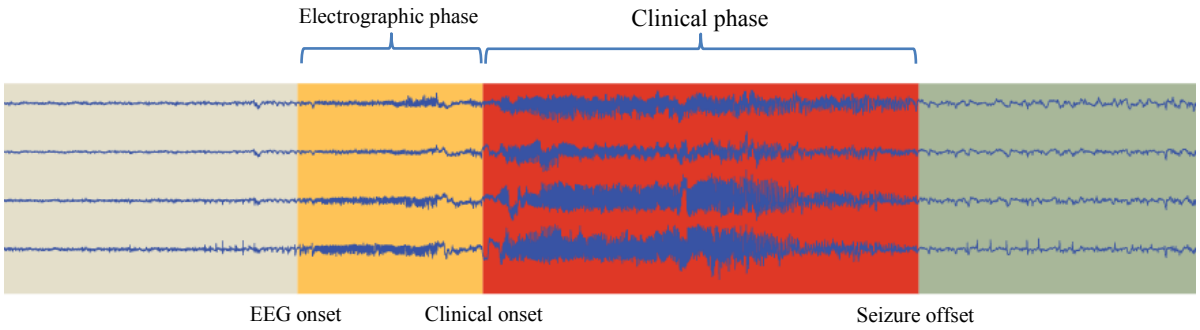

Figure 5.1 – Two states of an epileptic seizure. An early seizure detection method would be suitable for closed-loop neurostimulation systems, if it could detect the seizure during its electrographic phase.

5.1 Dataset description

Long-term continuous multichannel intracranial EEG recordings of 11 patients with refractory partial epilepsy from the European Epilepsy Database (Ihle et al. , 2012, Klatt et al. , 2012) were used to evaluate the efficiency of proposed seizure detection algorithms. Subjects of this study were selected randomly among invasive recordings which were sampled at 1024 Hz. Although there were also numerous patients in the database with lower sampling rates, we confined our selection only to those recorded at higher sampling rates in order to retain a high quality study. The overall length of recordings is 1785 h and contains 183 epileptic seizure events, on average around 2.5 seizures per day. Recordings were obtained at the epilepsy unit of the University Hospital of Freiburg, Germany, with patients being monitored through invasive electrodes during long-term pre-surgical evaluations of the patients. The pre-surgical evaluations were part of the assessments of risks and benefits of those surgeries. Throughout the pre-surgical monitoring of the patients the use of AEDs was very limited (Klatt et al. , 2012).

The invasive electrodes were implanted intracranially as depth, grid, and/or strip electrodes. Seizure onset/offset times were annotated in the database by experienced epileptologists using iEEG recordings and video monitoring of patients. Information of both electrographic and clinical onset/offset times is available in the database, and we considered both in this study for comparison. Electrographic onsets usually start earlier than clinical ones. Information on seizures' origins and their spatial propagation as well as the localization of electrodes is also available in this database. Characteristics of patients and their recordings are summarized in Table 5.1.

Table 5.1 – Characteristics of studied patients and iEEG recordings

Subject ID	Gender	Patient age (year)	Onset age (year)	Type of the selected Electrode array	Euclidean distance	Localization of seizure onsets	Seizure type	Recording length (h)	Number of seizures	Seizure duration (s)		
										Mean	Min	Max
1	F	29	10	Depth (1x12)	4.1	RMT, RLT	CP1, SP7, UC1	183	9	82.3	13	172
2	F	32	1	Depth (1x10)	5.9	LMT	CP8, UC1	162.6	9	121.9	74	157
3	F	11	3	Depth (1x14)	5.8	RMT	CP4, SP4, UC6	155	14	122.7	56	171
4	F	32	8	Depth (1x16)	4.4	RBF, RMT, LMT	CP2, SP2, UC5	151.6	9	122.5	38	210
5	F	18	6	Depth (1x15)	3.2	L-T, L-F	CP13	127.8	13	86.5	68	105
6	M	21	5	Strip (1x4)	9.8	RLT, RMT	CP19, UC3	170.6	22	131.6	19	199
7	M	17	1	Depth (1x10)	5	LMT, LLT, L-T	SP25, SG6	142	31	118.4	33	274
8	M	18	11	Depth (1x10)	5.7	LBT, LLT, RBT	CP4, SP4, SG4, UC1	246.2	13	100.2	36	137
9	F	63	30	Depth (1x14)	6.7	LMT, R-T	CP15, UC4	118.9	19	102.8	8	156
10	M	39	8	Grid (8x8)	10	L-F, L-C	CP2, SP3, UC25	110.6	30	15.4	6	43
11	F	14	13	Strip (1x6)	7.3	L-T, LLT	CP6, SG4, UC4	217.1	14	52.5	7	123
Sum	7F/4M	-	-	D8, S2, G1	-	-	CP74, SP45, SG14, UC50	1785.4	183	-	-	-
Mean	-	26.7	8.7	-	6.2	-	-	162.3	16.6	91.8	32.5	159

- Euclidean distance: Euclidean distance between the three-dimensional MNI coordinates (x, y, z) of two selected electrodes from the array.
- Localization of seizure onsets: ABC; A (R: right, L: left), B (-: none, B: basal, L: lateral, M: mesial), C (F: frontal, T: temporal, C: central). E.g. RMT (right mesial temporal lobe), L-F (left frontal lobe), RBF (right basal frontal lobe).
- Seizure type: type of the clinical seizures; CP: Complex Partial, SP: Simple Partial, SG: Secondarily Generalized, UC: Unclassified. Numbers following the abbreviations represent the number of seizures of that type.
- Seizure duration: mean, minimum, and maximum values of seizure durations, considering electrographic onsets and offsets of the seizures.

For seizure detection studies in this thesis, and for each patient, two immediately adjacent electrodes were selected from a candidate electrode array on the foci (Figure 5.2). For the methods using bipolar signal, the voltage difference between these two monopolar electrodes was considered as a bipolar channel. Afterward the continuous raw iEEG signals were segmented into 2-sec windows with 50% overlap, to provide seizure detections every second. The epochs were selected long enough so as to still carry meaningful brain data, meanwhile ensuring quasistationary iEEG signal. For wideband feature extraction (wideband MPC), each segment was filtered using an infinite impulse response (IIR) forward-backward Butterworth 50 Hz notch filter to eliminate sinusoidal distortion of the ac power supply without introducing phase shift. No additional artifact suppression methods were employed in the studies of this chapter.

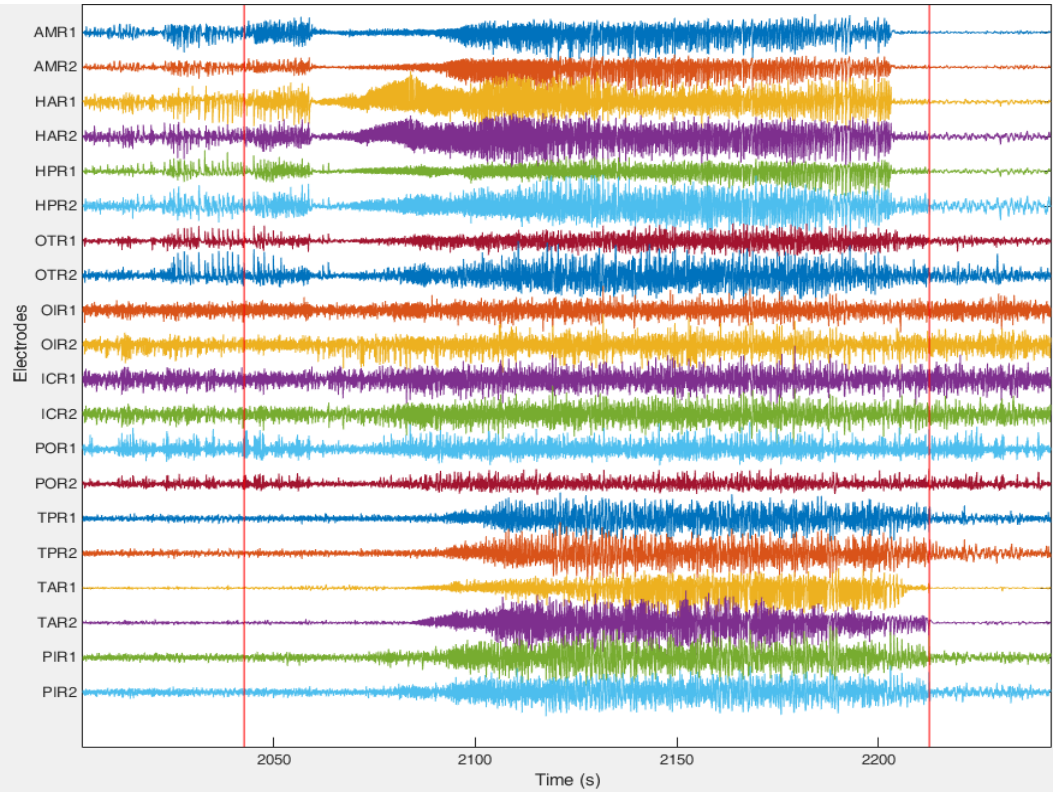

Figure 5.2 – Four minutes multichannel iEEG recordings of a seizure from patient 1. The vertical red lines indicate electrographic onset and offset times. HAR1 and HAR2 electrodes were selected for this patient.

5.2 Methods

In this section we describe a method for early seizure detection and two approaches for seizure event detection in details. The all three methods almost use the same block diagram for seizure event/onset detection, and their difference is just in the extracted features. Figure 5.3 presents the general block diagram of the proposed methods for automated seizure event/onset detection, including a manual channel selection, a segmentation stage, feature extraction, and a threshold box for decision-making.

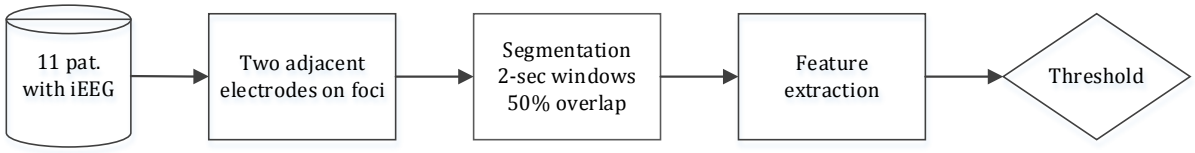

Figure 5.3 – General block diagram of the proposed methods for seizure onset/event detection

5.2.1 Early seizure detection using neuronal potential similarity

During epileptic seizure initiation, development, and termination, neuronal potentials in the vicinity of focus demonstrate different levels of coherency, and usually reach their maximum synchrony prior to seizure termination (Schindler et al. , 2007a, Schindler et al. , 2007b, Jiruska et al. , 2013). As a result of this synchronized firing, electric potentials induced on recording electrodes within close proximity of focus will become quite similar. Quantization, measurement and detection of this electric potential similarity can provide a mechanism for detecting seizures. Neuronal potential similarity is an indication of strong relationship between the two signals recorded from two brain regions. It can be investigated both in terms of amplitude (the intensity of neuronal activities) similarity and phase synchrony of the neural firings occurring in different frequencies.

Several approaches have been proposed for measuring the level of phase synchrony between two time series such as linear cross-correlation and mean phase coherence (Mormann et al. , 2000, Kreuz et al. , 2004, Mirowski et al. , 2009, Feldwisch-Drentrup et al. , 2010, Feldwisch-Drentrup et al. , 2011a, Jiruska et al. , 2013). Here we proposed bipolar spectral power features as a measure of neuronal potential similarity between two signals, which capture both amplitude similarity and phase synchronization in different frequency bands. Suppose two real periodic signals $x_1(t)$ and $x_2(t)$ with zero mean, and composed of N sinusoidal waveforms having different amplitudes and phases,

$$x_1(t) = \sum_{k=1}^{N} a_k \sin(\omega_k t + \varphi_{1k}) \tag{5.1}$$

$$x_2(t) = \sum_{k=1}^{N} b_k \sin(\omega_k t + \varphi_{2k}) \tag{5.2}$$

where a_k and b_k indicate the amplitudes of the Fourier series representation of $x_1(t)$ and $x_2(t)$ time series, and φ_{1k} and φ_{2k} denote their corresponding phase shifts. The difference of two signals, $x_d(t) = x_1(t) - x_2(t)$, also known as bipolar signal, can be written as (5.3),

$$x_d(t)=\sum_{k=1}^{N}(a_k \sin(\omega_k t+\varphi_{1k})-b_k \sin(\omega_k t+\varphi_{2k})) \tag{5.3}$$

The average power of the $x_d(t)$ is obtained as (5.4),

$$P_{x_d}=0.5\times\sum_{k=1}^{N}\left(a_k-b_k\right)^2+2\times\sum_{k=1}^{N}a_k b_k \sin^2(\frac{\varphi_{1k}-\varphi_{2k}}{2}) \tag{5.4}$$

where P_{x_d} is the average power of bipolar signal. Eq. (5.4) indicates that the average power of a bipolar signal is dependent both upon the amplitude and phase differences across all frequencies. The first and second terms of the Eq. (5.4) represent the amplitude and the phase similarities of two stationary time series respectively. Therefore Eq. (5.4) can be considered as a measure of neuronal potential similarity in terms of both amplitude and phase for stationary neural activities.

Although iEEG signals are nonstationary, they can be regarded as quasistationary time series for satisfactorily short periods of time, e.g. 1~2 seconds. As a result of this equation, the power of the difference of two purely sinusoidal signals in particular and two non-sinusoidal EEG signals in general with equal amplitudes and frequencies will become zero, if completely phase synchronized ($\varphi_{1k}=\varphi_{2k}$), and will hold the maximum value when completely out of phase ($\left|\varphi_{1k}-\varphi_{2k}\right|=\pi$). The similarity criterion could also be used as a measure of neuronal potential similarity in the specific frequency bands [i j], hence,

$$NPS_{ij}=0.5\times\sum_{k=i}^{j}\left(a_k-b_k\right)^2+2\times\sum_{k=i}^{j}a_k b_k \sin^2(\frac{\varphi_{1k}-\varphi_{2k}}{2}) \tag{5.5}$$

where NPS_{ij} holding the neuronal potential similarity (NPS) measure of two iEEG signals inside the frequency range of [i j]. In fact, the NPS measures would decrease by amplitude/phase similarity among two adjacent iEEG signals in the frequency range of [i j], and would increase by loss of this similarity. The power of a signal in different frequency bands was calculated using power spectral density (PSD) of bipolar iEEG signal. The PSD indicates the distribution of power of a time series at different frequencies, and was estimated

using Welch's function (Welch, 1967) of MATLAB, which first applies a Hamming window on the segmented bipolar iEEG, and then calculates the PSD. To quantify the neuronal potential similarity between two iEEG signals within desired sub-bands (NPS_{ij}), the spectral power of sub-bands was calculated by an integration over PSD components within those sub-bands, which has been explained in chapter 2.

5.2.1.1 Relative NPS measure

The main idea of the method is to find two frequency sub-bands providing opposite similarity behaviors by seizure initiation, and then using the ratio among NPS measures of these two sub-bands for highlighting of the changes, thus building a more robust measure. To find the most relevant bands, the NPS measure was studied in different frequency bands and for all patients individually. Instead of the well-known frequency bands, twenty eight narrow sub-bands were considered to boost the resolution of the study: (0.5-3], (3-5], (5-8], (8-10], (10-12], (12-14], (14-16], (16-18], (18-22], (22-26], (26-30], (30-35], (35-40], (40-48], (52-60], (60-70], (70-80], (80-90], (90-98], (102-125], (125-148], (152-175], (175-198], (202-248], (252-298], (302-348], (352-398], (402-512] Hz. Since the EEG signals contain predominantly low frequency oscillations, narrower and wider bandwidths were assigned in lower (0.5-40 Hz) and higher (40-512 Hz) frequencies respectively. Furthermore most of the seizure and non-seizure activities fall in the frequency range below 40Hz, which previously has been divided into very narrow bandwidths, e.g. 2~3 Hz, by some power spectral based seizure detection approaches (Shoeb, 2009, Shoeb et al. , 2011a). The NPS indices were extracted using a 2-sec rectangular moving window with 50% overlap, and could provide seizure onset detections every second.

Studying the seizures of 11 patients indicated that the NPS in low frequency band of 0.5-3 Hz (delta band) usually decreases by seizure initiation with respect to interictal period, which is probably resulting from the two adjacent iEEG signals getting increasingly similar, and in turn reflected as decreased bipolar power in Delta band. Contrary to this finding, the NPS measures extracted from some particular patient-specific frequency bands increase by seizure initiation, indicating a decreasing similarity in these frequencies on seizure initiation.

For the sake of generalization, the bandwidth of 12-26 Hz can be considered which covers almost all of these particular frequency bands, to capture most of the decreasing similarity trends. Figure 5.4 shows the bandpass filtered bipolar iEEG signals of a studied seizure from patient 3.

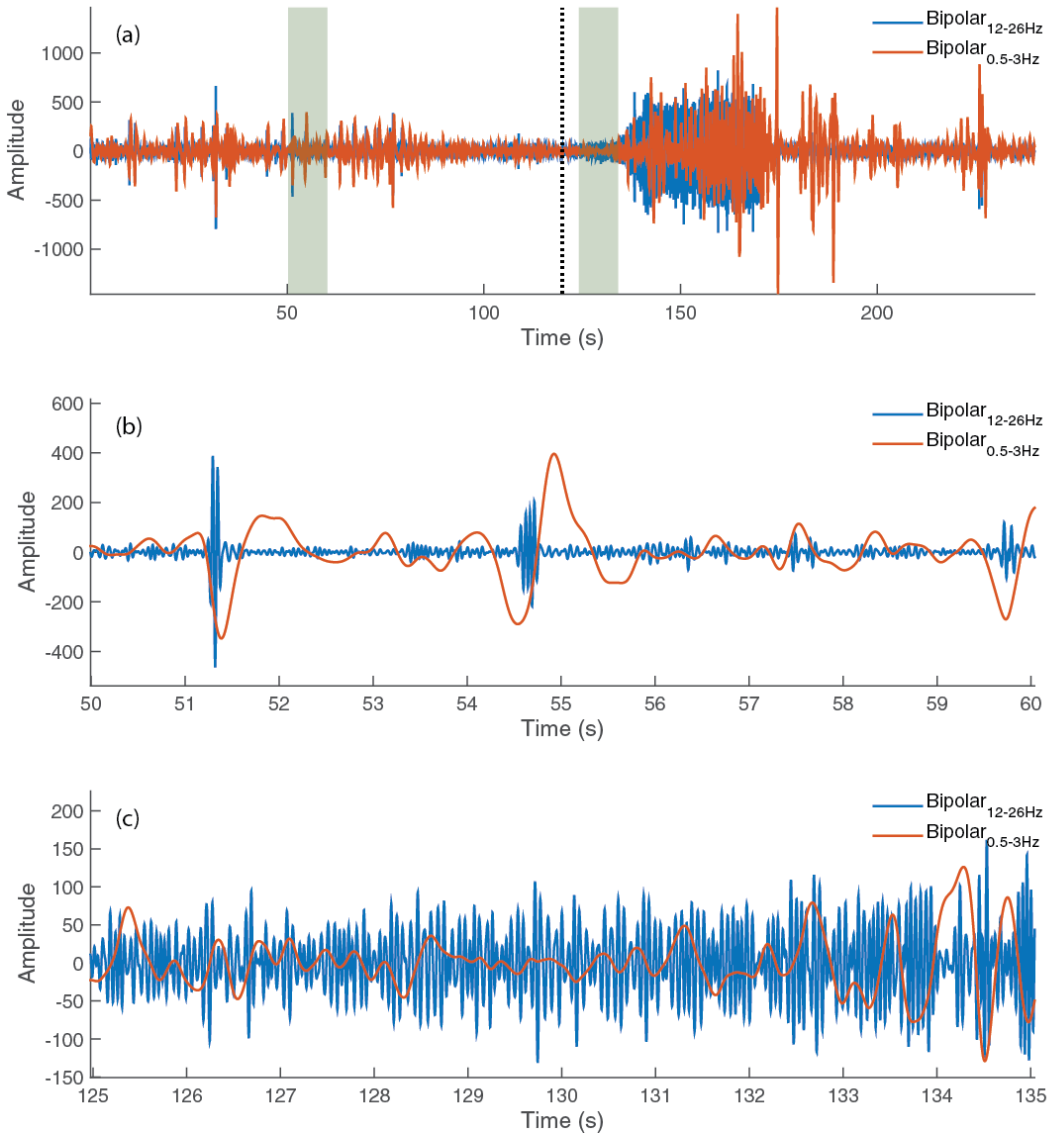

Figure 5.4 – Bandpass filtered bipolar iEEG signals into 0.5-3 Hz and 12-26 Hz (patient 3). (a) four minutes of bandpass filtered signals including a seizure onset at 120s. (b, c) bandpass filtered signals from highlighted non-ictal and ictal periods of figure (a) respectively. As seen from the figures, the average power of 0.5-3 Hz is higher than 12-26 Hz during non-preictal periods, while is less during seizure initiation.

Based on these reverse similarity behaviors in different frequency bands, posing with seizure initiation, the NPS of 12-26 Hz divided by NPS of 0.5-3 Hz is proposed as the generalized candidate measure for the detection of seizure onsets as early as possible (5.6),

$$RNPS = \frac{NPS_{12-26Hz}}{NPS_{0.5-3Hz}} \tag{5.6}$$

where *RNPS* is relative NPS measure. The relative measure acts adaptively, and will not reflect if the NPSs of both frequency bands change in similar direction either decrease or increase. Figure 5.5 shows the NPS measures for a seizure from patient 5, extracted from the closest-to-the-focus bipolar channel (TPL1-TPL2). Seizure onset clearly coincides with an increase in the NPS of 12-26 Hz sub-band, and with a decrease in the NPS of 0.5-3 Hz sub-band. Referring to Figure 5.5, the seizure can be detected within few seconds after the electrographic onset time using the proposed measure (ratio between NPSs of 12-26 Hz and of 0.5-3 Hz). Subsequently, the extracted measure was normalized. In order to obtain a normalization factor for the measure, the average value of the feature extracted from the initial 60 minutes of recordings was evaluated for each patient separately. The feature vector was then normalized by dividing this normalization factor, and fed to the next stages for feature preprocessing (smoothing by a moving average window) and alarm generation using a threshold based classifier.

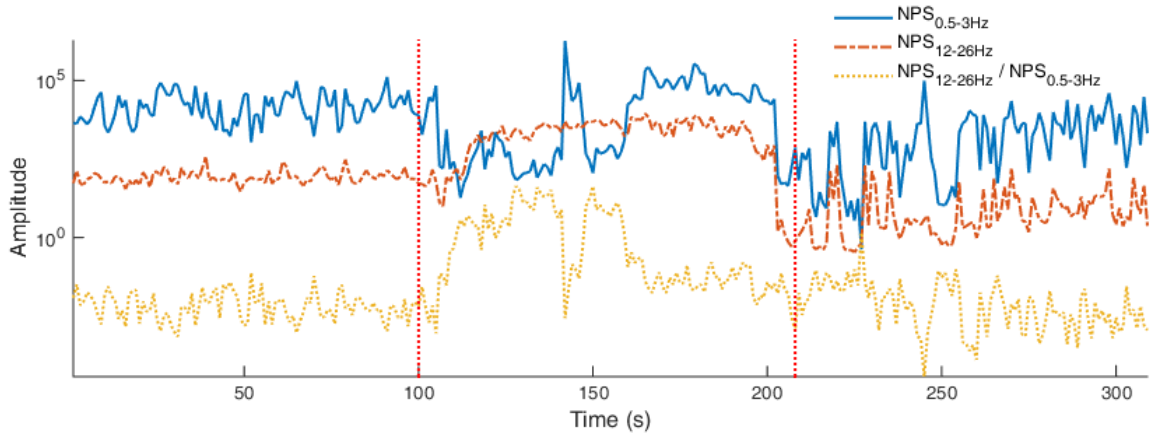

Figure 5.5 – The proposed measure for early seizure detection for one seizure from patient 5. The left and right vertical dotted red lines indicate the electrographic seizure onset and offset times, respectively.

5.2.2 Phase synchronization in frequency sub-bands

Linear cross-correlation and mean phase coherence (MPC) have been widely used as the quantitative measures of the extent of phase synchronization for studying seizure dynamics (Schindler et al. , 2007b, Jiruska et al. , 2013, Zubler et al. , 2014) and also seizure prediction purposes (Mormann et al. , 2000, Mirowski et al. , 2009, Feldwisch-Drentrup et al. , 2010, Feldwisch-Drentrup et al. , 2011a). Schindler et al. (Schindler et al. , 2007a) reported a high level of phase synchronization prior to seizure termination, and a low level of synchronization by seizure initiation. Here MPC measure extracted from frequency sub-bands was used to study seizure dynamics and detect epileptic seizure events.

In order to study the synchrony of two iEEG signals in frequency sub-bands, the raw EEG signals sampled at a rate of 1024 Hz, were first filtered using band-pass filters into thirteen frequency sub-bands of 0.5-4, 4-8, 8-12, 12-18, 18-28, 28-36, 36-48, 52-65, 65-80, 80-98, 102-148, 152-198, and 202-248 Hz. Moreover, the wideband frequency of 0.5-98 Hz was achieved using a high-pass filter (fc = 0.5 Hz) and a low-pass filter (fc = 98 Hz). Band-pass, high-pass, and low-pass filtering were realized using forward-backward Butterworth method, which is preferred due to eliminating the phase distortion side-effect in contrast to the ordinary filtering scheme.

As a preprocessing stage in the wideband feature extraction, a 50 Hz notch filter is also applied to eliminate strong power line interferences. For sub-band feature extraction however, no artifact preprocessing was applied, as they don’t cover power line frequency and its harmonics. The MPC features were subsequently extracted from the band-pass filtered signals and the wideband signals. By examining the MPC behaviors of several epileptic seizures of different patients, we found that the estimated MPC measures usually reach their maximum prior to seizure termination in almost all studied frequency bands. Furthermore, desynchronization was also observable with seizure initiation in several frequency bands, varying from seizure to seizure. Figure 5.6 illustrated the sub-band and wideband MPC measures extracted from a sample seizure from patient 5.

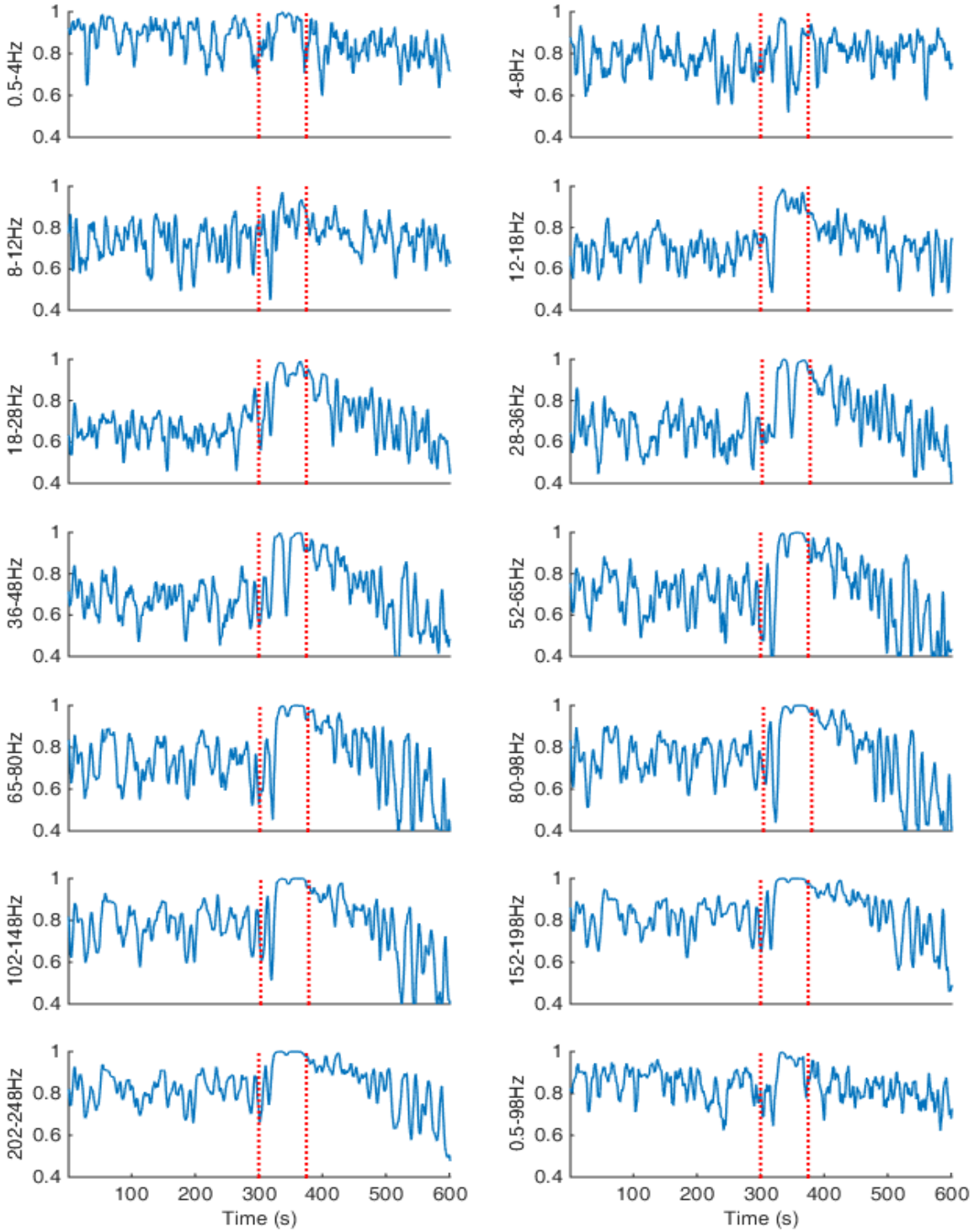

Figure 5.6 – Smoothed MPC measures extracted from bandpass filtered iEEG signals including a studied epileptic seizure (patient 5, seizure 1). The vertical dotted red lines indicate the electrographic onset and offset times. The MPC measure reaches its maximum prior to seizure termination in almost all studied frequency bands. Desynchronization is also observable with seizure initiation.

5.2.3 Singular value decomposition of bipolar EEG

SVD as a common computational tool employed in signal processing and pattern recognition, acts as a mathematical factorization of data matrices obtained from the patients, to highlight the dominant properties of their underlying patterns. The core idea of SVD is to take a collection of data, find the patterns having the highest correlation with that data, and then sort these patterns in a descending order based on their importance. In fact, SVD decomposes data to its correlated parts, with the larger singular values (SVs) corresponding to those parts with more energy (Bandarabadi et al. , 2010). The process decomposes the original matrix T into the product of three sparse matrices (5.7),

$$T_{m,n} = U_{m,m}\Sigma_{m,n}V^{*}_{n,n} \tag{5.7}$$

where Σ is singular value matrix, U and V are left and right singular vector matrices respectively. U and V are orthogonal matrices, and Σ is a rectangular diagonal matrix with its nonnegative real elements sorted in a descending way (5.8), (5.9).

$$\Sigma = \begin{pmatrix} \sigma_1 & & 0 \\ & \ddots & \\ 0 & & \sigma_m \end{pmatrix}, \quad if \quad m = n \tag{5.8}$$

$$\sigma_1 \geq \sigma_2 \geq \cdots \geq \sigma_m \geq 0 \tag{5.9}$$

The singular values (σ_i) indicate the significance of the corresponding left/right singular vectors. The pair of singular vectors related to the highest singular value, contain more information about the dominant patterns than other singular vector pairs (Hassanpour et al. , 2004). The proposed methodology is based on singular values (SVs) extracted from windowed bipolar iEEG signal, and the phenomena of unique bipolar signal manifestations during a seizure event. By highlighting the dominant epileptic activities within a bipolar iEEG data, SVD can be used as a tool for detecting epileptic events.

5.2.3.1 SVD of one-dimensional EEG signal

In order to apply SVD, the raw EEG data should be first expressed in the form of a square matrix. Hankel operator is a square matrix with constant skew diagonals, and was employed here to build such a matrix. Suppose $X = [x_1, x_2, ..., x_n]$ a segment of EEG signal, and *n* being a positive even integer. Then the Hankel matrix of *X* can be written as (5.10).

$$H_X = \begin{pmatrix} x_1 & x_2 & \dots & x_{n/2} \\ x_2 & x_3 & \dots & x_{n/2+1} \\ \vdots & \vdots & \vdots & \vdots \\ x_{n/2} & x_{n/2+1} & \dots & x_{n-1} \end{pmatrix} \tag{5.10}$$

Since the computational cost of SVD is high, the iEEG signal was downsampled from 1024 to 512 Hz to boost the computation time. The iEEG signal was segmented into 2 seconds windows with 50% overlap prior to feature extraction. The Hankel matrix of the bipolar iEEG was first built, after which SVD was calculated to obtain the singular values. Considering a downsampled 2-sec window with 1024 samples, the Hankel matrix would be a square matrix of order 512. The SVD operator will thus produce 512 SVs (σ_i , $i = 1,...,512$) ordered in a descending way.

5.2.3.2 Proposed measure

The main characteristic of an epileptic seizure is the highly coherent activity of the neurons, generating nearly the same electrical voltages by two very close bunches of neurons. This highly coherent state during seizure events, especially at the end of seizures, leads to a significant increase in the level of common mode signal of the adjacent channels, taking more similar waveforms. SVs represent the level and importance of the energies contained within the correlated parts of signal. As a result of excessive coherency during seizure termination, the energy of the resulting bipolar signal and its correlated parts will decrease. Figure 5.7 shows the SVs of a seizure from patient 2.

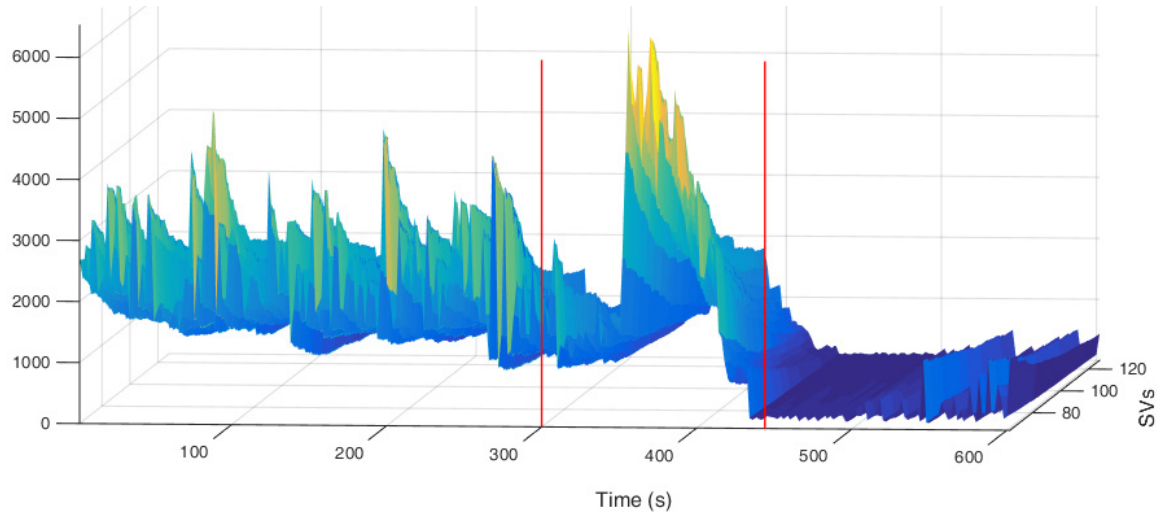

Figure 5.7 – Singular values (65-128) extracted from 10 minutes of bipolar iEEG signal contains one seizure. Vertical red lines indicate electrographic onset and offset times. The SVs first start to increase by seizure development, and then suddenly decrease approaching the seizure termination.

The SVs of the bipolar iEEG signal start to increase by seizure initiation and development and then suddenly decrease approaching the seizure termination. Therefore we could look for both decrease and increase in singular values for detection. Although tracing increases in SVs provides less detection delays, yet it generates higher numbers of false alarms than considering decreases in SVs. As the goal of this method was just seizure detection, and the detection latency is of minor importance, therefore tracing of decreases in SVs was only investigated. For each patient, the average of each SV for the first hour of the recording was calculated as $\sigma_{m,i}$ and each σ_i sequence was normalized by dividing to $\sigma_{m,i}$ as (5.11).

$$\sigma_{n,i} = \sigma_i / \sigma_{m,i} \quad , \quad i = 1, 2, ..., 512 \tag{5.11}$$

Where the $\sigma_{m,i}$ is the average of *i*-th SV sequence extracted from the first hour of recording, and $\sigma_{n,i}$ is the *i*-th normalized SV sequence obtained from the whole recording of the patient. The ranges of all 512 SVs are almost equalized by normalizing SVs obtained from each data segment (Figure 5.8). Subsequently 32 best performing SVs were selected through trial and error, and averaged to build a single unified measure. Specifically the SVs from 9 to 40 were found to perform better in the detection challenge.

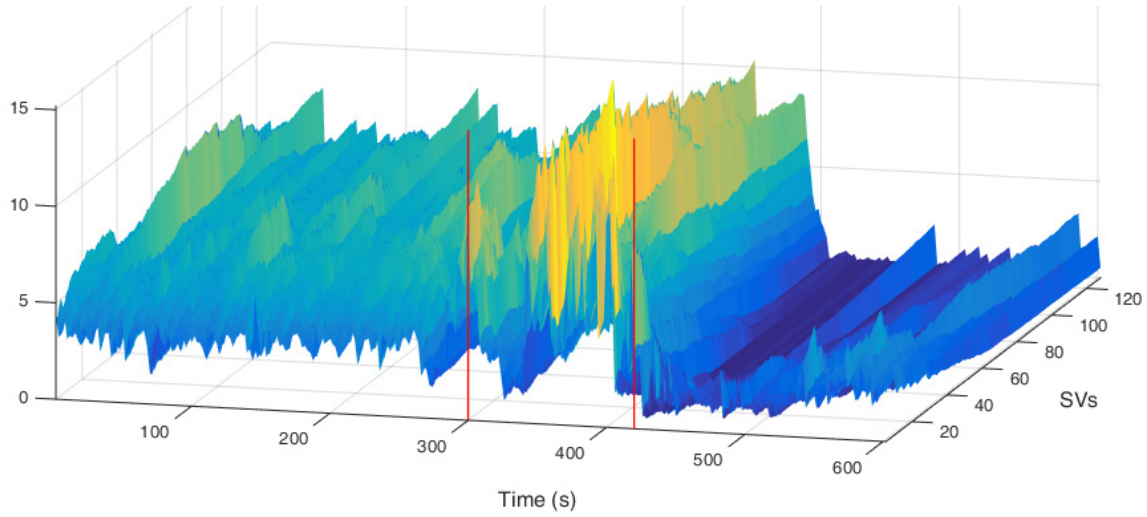

Figure 5.8 – The normalized SVs (1-128) extracted from seizure 7 of patient 2. After normalization by information of first hour of iEEG recording, the range of all SVs is almost equalized.

5.2.4 Preprocessing of features

During long-term recordings, EEG segments may be affected by environmental or physiological interfering sources, which induce high amplitude random spikes in the extracted measure. This may cause the extracted measures to easily pass thresholds, when they should not. Duration of these noisy spikes is usually very short, e.g. less than two seconds. Moreover the synchronous and coherent epileptic neuronal activities last for several seconds, sometimes up to tens of seconds. Therefore smoothing of the feature samples by a proper rectangular moving average window can suppress these undesired short events and would decrease the likelihood of ictal-free segments from being wrongly classified as ictal activities. Smoothing of each measure was carried out by averaging four consecutive feature samples, including the current and three past values (5.12),

$$\bar{a}_k = \frac{1}{l+1}\sum_{j=0}^{m} a_{k-j} \;,\; l = 3 \tag{5.12}$$

where a_k is the k-th sample of feature vector, and $\bar{a}_k$ is its smoothed value. This preprocessing however increases detection latency (for onset detection purpose) by about 2 seconds, while greatly reducing the number of false alarms.

In this chapter we deal with three different measures; similarity measure, sub-band MPC, and bipolar SVD. Since a threshold based classifier is applied on the measures, there would be need to transform the measures so that to they are increased during the seizure onset/event. The proposed relative NPS and the sub-band MPC measures would naturally increase during seizure initiation or event, however the bipolar SVD is decreasing by seizure development. Hence, for the bipolar SVD measure, the inverse of its smoothed version was calculated and fed to the next stage for classification.

5.2.5 Threshold based classifier

As the last stage of the seizure detection algorithms, threshold-based classifiers were investigated to discriminate the extracted measures obtained from each algorithm. As the optimum threshold values vary from patient to patient, therefore threshold values were chosen individually. An alarm is generated when the features exceed this threshold; alarm generation is then blocked for 4 minutes. This limitation guarantees the raising of just a single true alarm per seizure. For NPS and bipolar SVD methods, various threshold values starting from 1.5 and ending at 100 were applied with non-uniform increments, spanning from 0.5 for low values up to 10 for higher values of threshold. For sub-band MPC and wideband MPC measures however threshold values from 0.6 to 0.99 with 0.01 increments were applied.

Afterwards, the three parameters of sensitivity (SS), FDR, and MDLE of the raised alarms were used to evaluate the methods (SS and FDR for seizure event detection methods). Since the three parameters of SS, FDR, and MDLE cannot be simultaneously set optimally, as improving one leads to worsening of others, a tradeoff has to be made in their selection. Therefore the Euclidean distance between the resulting point (SS, normalized FDR, normalized MDLE) and the optimal performance point ($SS = 100$, $FDR = 0$, $MDLE = 0$) of the raised alarms was used to optimize the threshold level for each patient (5.13). The threshold value was chosen so that this distance is minimized.

$$Ed = \sqrt{(SS - 100)^2 + FDR_{norm}^2 + MDLE_{norm}^2} \tag{5.13}$$

To limit the effect of narrow range and small values of FDR - which are very close to zero - on the proper selection of threshold, normalized FDRs obtained by multiplying of FDRs with 100 were considered here. Also the MDLE values (in sec) were normalized by dividing by 2, in order to balance and reduce their effects when seeking optimal threshold. This gives more priority to SS and FDR values, since our primary goal in seizure detection is to detect more onsets, not less seizures with the lowest possible MDLE. The above normalization factors were optimized through extensive trial and error efforts. For the seizure event detection studies however, the MDLE parameter was set to zero in Eq. (5.13).

5.2.6 Improved performance metrics for early seizure detection

The performance of the proposed early seizure detection method was evaluated using five parameters. In addition to SS, FDR, and MDLE as the common performance metrics, we also investigated the mean detection latency from clinical onsets (MDLC). Furthermore a new criterion was proposed for the evaluation of detection latency as mean relative detection latency from electrographic onset (MRDLE). To calculate MRDLE, first the ratio between detection latency of each seizure and the length of that seizure was obtained for all seizures of a patient, followed by an averaging on all of these relative values. In our belief, the MRDLE parameter is the most adequate criterion to measure the detection latency of an onset detection algorithm. For instance, if a seizure of very short length could be detected even on its termination, the detection algorithm still would provide very small detection latency. This condition is easily identified by the MRDLE measure being almost 1, indicating that there is no time for neurostimulator.

5.3 Results

The methods were applied on the continuous long-term iEEG recordings of 11 patients, selected from European database on epilepsy. The iEEG data was also segmented into 2 seconds windows having 50% overlap prior to feature extraction. Performance of the proposed method for early seizure detection was evaluated in terms of sensitivity (SS), FDR, MDLE, MDLC, and MRDLE, whereas the performance of the proposed methods for seizure

event detection was evaluated in terms of SS and FDR only. The results presented in this section were achieved by having a tradeoff between the above mentioned parameters. Although higher detection sensitivities are preferred with seizure detectors, which may easily be achieved by choosing a lower threshold value, yet a low FDR is also essential when it comes to clinical application which contradicts with lower threshold levels.

5.3.1 Results of early seizure detection

The early seizure detection method was evaluated using 2-fold cross-validation. For each patient, the first half of the seizures (or rounded half for the odd number of seizures) and their corresponding interictal recordings were considered as set d1, while the remaining data was assigned as set d2. The method was then trained on set d1 and tested on set d2, followed by training on set d2 and testing on set d1. Using 2-fold cross-validation, the method was evaluated on all seizures in a realistic manner. In each fold, the training set was used to optimize the classifier's threshold value. Various values starting from 1 and ending at 100 with increments of one were applied, and the resulting parameters of sensitivity (SS), FDR, and MDLE of the raised alarms were used to evaluate each threshold. The threshold value was chosen so that the *Ed*, obtained from Eq. (5.13), is minimized.

The optimum threshold obtained from the train set was then applied on the test set to generate alarms. The five parameters of SS, FDR, MDLE, MDLC, and MRDLE were subsequently calculated for the generated alarms of the test set. The arithmetic averages of results obtained from both folds are presented in Table 5.2. On average, the proposed method could achieve a high sensitivity of 86.9% (159 out of 183), a very low FDR of 0.06 per hour (total 107 false alarms in 1785 h), and a MDLE of 13.1 s from electrographic onsets, while in average preceding clinical onsets by 6.3 s. MRDLE parameter, which can act as an improved criterion for evaluation of detection latency, demonstrated a value of 0.17, indicating that the seizures were detected averagely within a time period about one-sixth of their lengths. Furthermore, the results achieved from patient-specific measures are also provided in Table 5.2. On average, the patient-specific results demonstrated a SS of 88.5%, a FDR of 0.046 h^{-1}, a MDLE of 11.9 s, a MDLC of -7.24 s, and a MRDLE of 0.16. Compared to the result of generalized measure, all performance metrics show slight improvements.

Table 5.2 – Results of proposed early seizure detection for 11 studied patients

ID	Generalized measure						Patient-specific measure						
	SS%	FDR (h^{-1})	MDLE (sec)	MDLC (sec)	MRDLE	Thresh (F1, F2)	SS%	FDR (h^{-1})	MDLE (sec)	MDLC (sec)	MRDLE	Thresh (F1, F2)	Up. band (Hz)
1	100	0.027	15.6	-7	0.19	31, 35	100	0.044	13.7	-8.9	0.2	28, 35	16-22
2	100	0.098	24.9	-5.3	0.28	31, 18	100	0.049	25.6	-4.7	0.22	23, 24	16-26
3	85.7	0.058	16	-5.6	0.14	26, 25	85.7	0.052	16.3	-5.2	0.15	31, 33	12-18
4	88.9	0.092	15	-2.5	0.18	27, 23	88.9	0.079	8.7	-8.7	0.09	23, 19	18-26
5	100	0.031	5.8	-3.4	0.07	10, 8	100	0.039	2.5	-6.7	0.03	9, 8	14-18
6	95.4	0.105	16.8	0.6	0.11	14, 24	100	0.018	14	-1.9	0.08	26, 28	18-26
7	93.5	0.119	16	-24.4	0.15	21, 20	93.5	0.119	16	-24.4	0.15	21, 20	12-26
8	61.5	0.016	9.5	0	0.10	44, 46	61.5	0.016	9.5	0	0.10	44, 46	12-26
9	84.2	0.016	14.1	-1.6	0.13	21, 20	84.2	0.017	12.4	-3.2	0.12	27, 21	14-22
10	83.3	0.108	3.8	-2.8	0.24	11, 10	90	0.072	4.2	-2.3	0.27	21, 15	22-26
11	64.3	0.032	13.1	3.7	0.29	74, 84	64.3	0.032	13.1	3.7	0.29	74, 84	12-26
Mean	86.9	0.060	13.1	-6.3	0.17		88.5	0.046	11.9	-7.24	0.16		

- MDLE/MDLC: mean detection latency from electrographic/clinical onsets for each patient in second.
- MRDLE: mean of relative detection latency from electrographic onsets.
- Thresh: optimum thresholds obtained from 2-fold cross-validation; F1and F2 from the training set of the 1st and 2nd fold.
- Up. band (Hz): the patient-specific frequency bands selected for the upper band of proposed measure.

The plot in Figure 5.9 represents the proposed generalized measure for the whole recordings of patient 5, containing 13 seizure onsets within 127.8 h of data. The proposed measure could detect all of the seizure onsets successfully with negligible detection latencies.

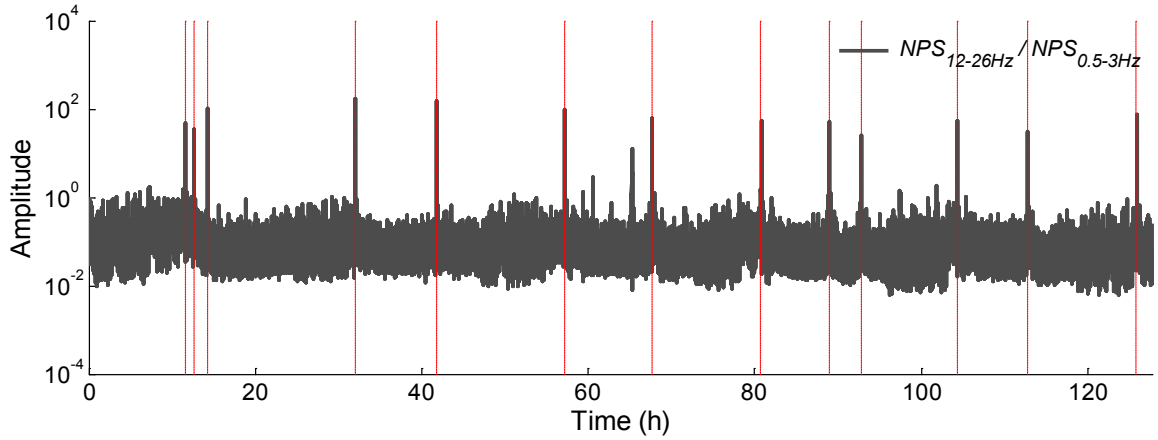

Figure 5.9 – The proposed measure (*RNPS*) for early seizure detection for whole recordings of patient 5. The vertical dotted red lines indicate the seizures.

5.3.2 Results of seizure event detection

The sensitivity is of much higher value in seizure event detections, where the high detection delays can be tolerated. Table 5.3 presents the sensitivity and FDR results for 11 patients obtained from best sub-band MPC measure as well as the wideband iEEG signals. Moreover the results achieved from bipolar SVD are presented in the same table to provide a generalized comparison between different proposed methods for seizure event detection.

Using the sub-band MPC method, the best results provided on average a sensitivity of 84.2% with a FDR of 0.09 h^{-1}, whereas the average results obtained from the wideband signals provided a sensitivity of 62.8% with a FDR of 0.28 h^{-1}. Findings revealed that both parameters of SS and FDR would improve significantly by extracting MPC measure from specific frequency band. Also bipolar singular values provided on average, a sensitivity of 84.2% and a FDR of 0.05 h^{-1} (83 false alarms in 1785h).

Table 5.3 – Results of proposed seizure event detection methods for 11 studied patients

	Sub-band MPC			Wideband MPC			Bipolar SVD		
Pat. ID	SS%	FDR (h^{-1})	Thresh	SS%	FDR (h^{-1})	Thresh	SS%	FDR (h^{-1})	Thresh
1	100	0.12	0.90	66.7	0.58	0.88	100	0.02	2
2	88.9	0.01	0.93	55.6	0.26	0.90	100	0.01	2
3	78.6	0.10	0.89	57.1	0.06	0.86	71.4	0.08	2.5
4	77.8	0.02	0.98	44.4	0.30	0.90	66.7	0.01	2
5	100	0.04	0.96	92.3	0.48	0.96	100	0	1.5
6	100	0.04	0.92	90.9	0.13	0.87	95.4	0.02	5
7	74.2	0.15	0.88	29	0.43	0.83	77.4	0.04	1.5
8	100	0.14	0.84	84.6	0.32	0.75	84.6	0.07	2
9	84.2	0.07	0.96	73.7	0.03	0.91	84.2	0.08	2.5
10	63.3	0.13	0.87	43.3	0.16	0.86	73.3	0.11	3.5
11	92.9	0.12	0.79	92.9	0.23	0.69	92.9	0.07	3.5
Mean	84.2	0.09	0.90	62.8	0.28	0.85	84.2	0.05	2.5

- Thresh: optimal threshold value

5.4 Discussion

In this chapter three automated seizure detection algorithms were developed based on the two iEEG channels. The main idea behind all of these three methods was to capture correlation, similarity or synchrony changes between two adjacent iEEG electrodes located over the seizure onset zone. During seizure initiation, development and termination, the two immediately adjacent iEEG recordings demonstrate different levels of correlation, synchrony or similarity across different frequency sub-bands.

5.4.1 Early seizure detection

This study evaluated the efficiency of bipolar spectral power feature as a measure of neuronal potential similarity for automated early seizure detection. Technically, the NPS measure captures both phase and amplitude similarities of two immediately adjacent iEEG signals located over the seizure onset zone, simultaneously. During seizure initiation, development and termination, the two immediately adjacent iEEG recordings demonstrate different levels of similarity across different frequency sub-bands. To find possible similarity patterns appearing during initiation of the ictal state, the NPS measure was studied in several narrow bands of 11 patients. We found that similarity patterns in the higher frequency bands are patient-specific, and decreasing. In contrast, for the lower frequency band of delta the similarity patterns are increasing, and in general are not patient-specific. Therefore seizure initiation accompanies dissimilarity in middle frequency bands and similarity in the low frequency of delta band.

Although the NPS measures exhibited patient-specific patterns, we proposed a measure with a limited sacrifice on performance. Evaluation of NPS measures indicates that most of the relevant higher frequency bands with increasing NPS trends are covered inside the frequency range of 12-26Hz. Therefore, the ratio between NPS measures extracted from 12-26Hz and 0.5-3Hz frequency bands is the most relevant feature for the generalization purpose of seizure onset detection measure. On average, the results demonstrated very high sensitivity, low FDR, and short detection latency.

5.4.1.1 Comparison with other approaches

Comparing to other published works, the current work represents the most comprehensive study among seizure detection methods in terms of recording length and the number of seizures studied. The average length of recording per patient was about one week, and was the first study of the kind to consider both electrographic and clinical onsets, and also to compare their results. By average, seizures were detected in advance of the clinical phase, which is important for the effective seizure suppression through neurostimulation. Moreover, our method provides the lowest complexity compared to the currently available approaches, by only using two EEG channels, performing PSD analysis on a single bipolar signal, and discriminating through a threshold based classifier.

The results of some important studies on early seizure detection, which also provided numerical results, are tabulated in Table 5.4. Although comparison of the results obtained using different datasets would seem inappropriate, yet our method was evaluated on long-term continuous recordings, and is expected to achieve higher performances (specifically lower FDRs) on short-term fragmented data employed in most of those studies. Results reported by Shoeb (Shoeb, 2009) and Kharbouch et al. (Kharbouch et al. , 2011) demonstrate the best overall performances among these methods, considering a tradeoff between the three parameters of SS, FDR, and MDLE. Shoeb's method achieved a 9% higher sensitivity than ours, while raising around twice more false alarms, using 18 surface channels which is impractical for implantable devices. Kharbouch's method which provides slightly better performances, also suffers from extreme complexity, as it uses 69 electrodes per patient on average that is a clear limitation for the implantable systems. Furthermore, none of these reports are providing information concerning the clinical onset detection time.

Table 5.4 – Reported results for early seizure detection by other researches

Group	Method	Record. Len. (h)	No. of Patient	No. of Seizure	SS%	FDR (h^{-1})	MDLE (sec)
(Saab et al. , 2005)	Wavelet decomposition and Bayesian formulation	652	28	126	76	0.34	10
(Grewal et al. , 2005)	Spectral power features	389	19	100	89.7	0.22	17.3
(Meier et al. , 2008)	Categorizing morphological ictal rhythms	1403	57	91	96	0.45	1.6
(Aarabi et al. , 2009)	Fuzzy rule-based seizure detection system	302.7	21	78	98.7	0.27	11
(Shoeb, 2009)	Spectral power features and SVM classifier	844	23	163	96	0.13	4.6
(Zhang et al. , 2010)	Incremental nonlinear dimensionality reduction	193.8	21	83	98.8	0.49	10.8
(Kharbouch et al. , 2011)	Spectral power features and SVM classifier	875	10	67	97	0.025	6.9
(Hunyadi et al. , 2012)	Time and frequency domain features	892	22	131	74.2	0.34	10.2
(Rabbi et al. , 2012)	Fuzzy rule-based algorithm	112.45	20	56	95.8	0.26	15.8
(Ayoubian et al. , 2013)	High frequency activities (80–500 Hz)	36	15	18	72	0.7	10.9
(Zheng et al. , 2014a)	Variances of intrinsic mode functions	463	17	51	92	0.17	12
This work	Ratio of neuronal potential similarities	1785.4	11	183	86.9	0.06	13.1*

* The mean detection latency for the clinical onsets (MDLC) was obtained as '-6.3 s'.

To evaluate the detection latency of the algorithm three measures of MDLE, MDLC, and MRDLE were provided. This is the first study that considered two last criteria. Regarding to the slightly higher MDLE results obtained from our method compared to some of other studies, it should be noted that the seizure duration has a direct effect on the detection latency. To better highlight this, consider Figure 5.10 which represents the boxplot of durations of the studied seizures for each patient. Comparing Figure 5.10 with the results of patient 10 in Table 5.2 for example, it is observed that while the mean of seizure durations is 15.4 s, all being of short ranges, our method could provide a small MDLE of 3.8 s for this patient. Therefore it is suggested to compare the detection latency results of methods according to the seizure duration. The proposed method could detect the seizures on average within their initial one-sixth lengths and 6.3 s in advance of clinical phase, and therefore still saves a good portion of time for the responsive neurostimulator to suppress the seizure.

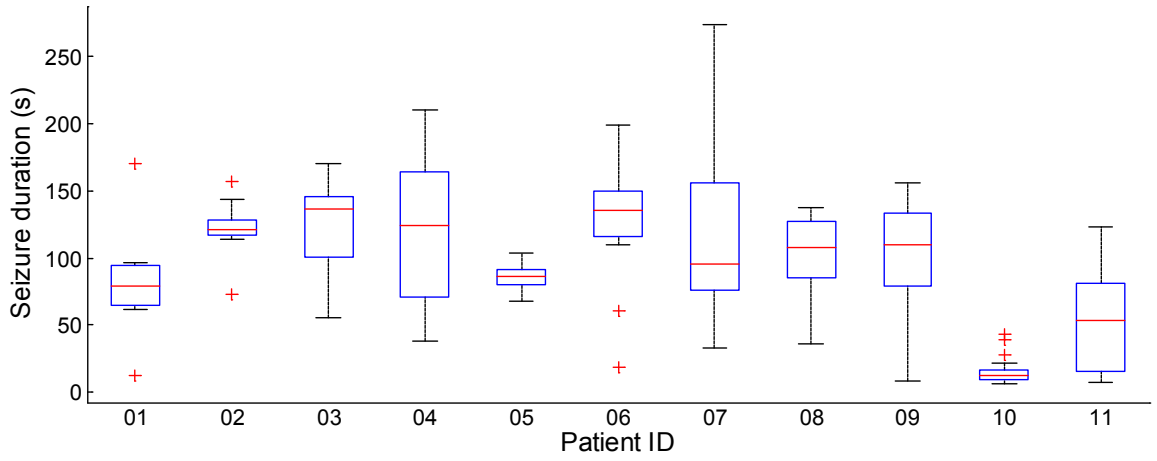

Figure 5.10 – Boxplot representation of seizure durations for 11 studied patients

5.4.1.2 Complexity of the early seizure detection approach

The method is based on a single bipolar signal, as well as a threshold-based classifier. The proposed relative NPS measure was calculated from the PSD of this bipolar iEEG signal, which exposes a very low computational cost, thus making the method very fast, and of low complexity. For instance, as we also mentioned in the second chapter, Parhi et al. (Parhi et al. , 2013) proposed a low-complexity Welch PSD computation mechanism using 65*nm* technology and 1-Volt power supply. The power consumption and hardware area of their method was around 210*nJ* and 176um^2 respectively, for PSD calculation of 8 overlapping segments of length 1024 samples each. In this regard, the proposed method is suitable for implantable low-power-budget closed-loop neurostimulation systems, which are extensively restricted to limited power budgets. A main current limitation is the necessity of surgery for battery replacement in implantable devices, which may be resolved by recent progresses in inductive charging technology (Libbus et al. , 2014). Moreover, a significant space/weight of the implantable products is occupied by their battery, which can be further compacted by using more efficient and lower computational cost algorithms.

5.4.2 Seizure event detection

It has been justified that seizure termination usually accompanies highly coherent and synchronous brain activities (Schindler et al. , 2007a, Zubler et al. , 2014). The basic idea was to highlight the states of highly synchronous and coherence activities of neurons using bipolar SVD and sub-band MPC measures respectively, when seizures are well-developed and reaching their terminations. Extracting MPC measure from band-pass filtered iEEG signals and investigating its trends as the most prominent measure for phase synchrony, we could effectively detect epileptic seizures.

The level of synchrony was augmented in most of the studied seizures and for different frequency bands. Depending on the length of ictal period, this high level of synchrony would last for about few up to tens of seconds. Although MPC measures of different frequency bands are usually increasing, however the measures extracted from wideband iEEG signals and some frequency bands were not robust for seizure detection, and generated relatively higher number of false alarms (Figure 5.11). More specifically, for the patients under study, the MPC measures obtained from particular sub-bands of 12-18 Hz, and 18-28 Hz could provide more detection capability in 10 out of 11 patients. Subject 2 was an exceptional case however, where the MPC measure extracted from 4-8 Hz could detect epileptic seizures with better sensitivity and specificity.

For the bipolar SVD, when the two adjacent iEEG signals become increasingly correlated, difference of those signals (bipolar iEEG) will contain less energy, causing the SVs of bipolar signal to decrease. Therefore the observation of sudden decreases in the SVs would coincide with seizure termination. Moreover, according to the results, the SVs extracted from bipolar iEEG signals were apparently robust to the changes in the state of the iEEG data throughout the patient's daily life, producing just 83 false alarms in 1785 hours of iEEG recordings (Figure 5.12). Furthermore, we observed that patterns of coherency are recurring evenly for all of the seizures for each particular patient. This indicates that the build-up, propagation, and termination of the seizures for a specific patient follow a common neuronal mechanism.

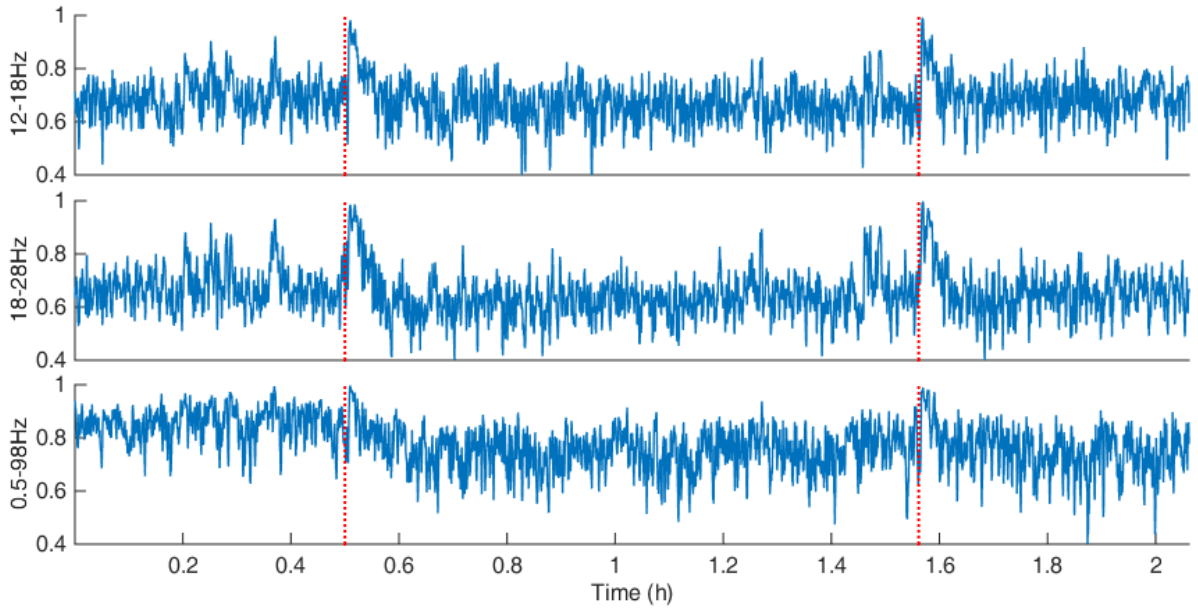

Figure 5.11 – Sub-band and wideband MPC measures extracted from 2 hours of iEEG recordings of patient 5, containing two epileptic seizures. The vertical dotted red lines indicate onset times. The sub-band MPC measures extracted from 12-18 Hz and 18-28 Hz were more robust than wideband MPC measure, and generated lower number of false alarms.

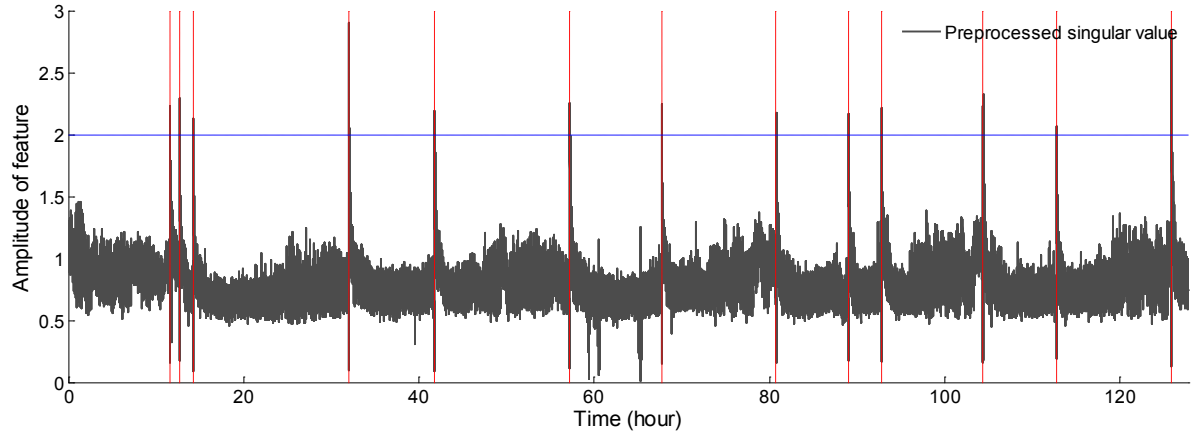

Figure 5.12 – Proposed measure using singular values extracted from bipolar iEEG signals (patient 5). Black line is the measure, and the vertical dotted red lines are seizure onsets. The horizontal dotted blue line is the threshold value.

5.4.3 Channel selection

The two adjacent electrodes placed on the foci were selected using prior knowledge on spatial propagation of seizures, available in the dataset (Figure 5.13). The method was not applied on the whole set of bipolar channels to select the best pair of electrodes, and only benefited from the propagation information. Propagation information and seizure foci were identified by epileptologists using multichannel iEEG recordings and magnetic resonance imaging (MRI) data. Since our method was developed towards using with implantable devices, therefore this prerequisite knowledge should be extracted during the clinical evaluation of implantable system for each candidate patient. This pre-evaluation of patients is an essential part for implantation surgery.

Concerning channel selection, sensitivity and detection latency of the algorithm are both affected. If the selected channel is not placed close enough to the foci, the seizure spread may not reach that channel, inducing a decrease in average sensitivity. On the other hand, if the seizure spreads to the extent enough to reach a remote electrode, it would be detectable with longer detection latency. Overall, both placement and number of selected EEG channels can substantially affect detection sensitivity and delays and therefore had to be taken into consideration.

The selection of one bipolar channel is suggested and satisfactorily works here, as the methods was applied on patients with partial epilepsy, and is quite logical if we are aware of the epileptic onset zone. As a counterexample, eight out of 11 studied subjects developed seizures on either right or left parts of their brain only, whereas the patients 4, 8, and 9 had seizure onset zones on both sides. Therefore the selection of one bipolar channel could not provide acceptable results for subject 8. However, in patients with more than one seizure onset zone, several bipolar channels can be considered to cover different possible onset zones. In turn, decision making can be carried out by incorporating logical channel fusion methods to effectively detect epileptic seizures. Moreover, the current responsive neurostimulation system (RNS) is approved by FDA for the partial epilepsy patients who are diagnosed with no more than two foci (Sun et al. , 2014b).

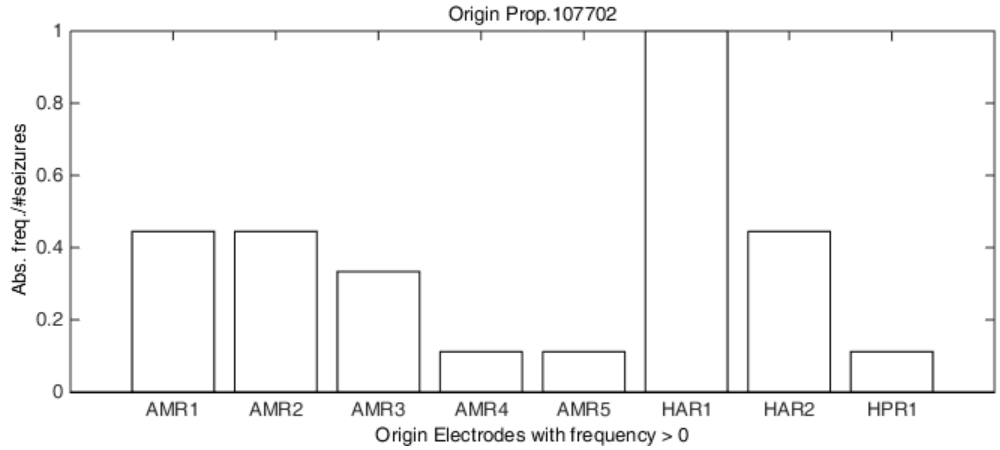

(a)

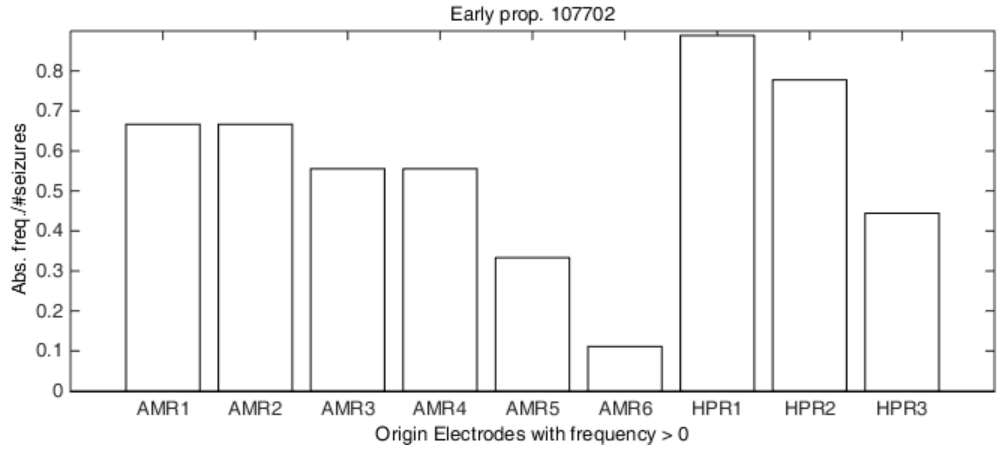

(b)

Figure 5.13 – Seizure propagation information for patient 1, available in dataset. (a) Channels placed over the foci, where the seizures originated, (b) channels involved during early states of seizure propagation. HAR1 and HAR2 electrodes were selected for this patient.

Concerning channel selection, sensitivity and detection latency of the algorithms are affected. If the selected channel is not placed close enough to the foci, the seizure spread may not reach that channel, inducing a decrease in average sensitivity. On the other hand, if the seizure spreads to the extent enough to reach a remote electrode, it would be detectable with longer detection latency. Overall, both placement and number of selected EEG channels can substantially affect detection sensitivity and delays and therefore had to be taken into consideration.

5.4.4 Robustness of algorithms

EEG patterns can change significantly according to the daily living conditions, such as the level of activity, awareness, and sleep stages, that further complicate the detection of seizures. Figure 5.14 represents the histogram of seizure occurrence times with respect to different day/night times. Although seizures are distributed almost evenly across different hours of the day and night (106 night and 77 day seizures), yet the proposed methods could provide a high sensitivity and specificity, showing robustness to the patients' circadian cycles. Daytime and nighttime hours were considered as 9am-9pm and 9pm-9am respectively. Furthermore, there were a few number false alarms raised by the proposed algorithms. By visual inspection of iEEG recordings of these false alarms, it was found that many of them exhibited ictal-like activities, presumably due to the subclinical seizures not been marked in the database as clinical seizures.

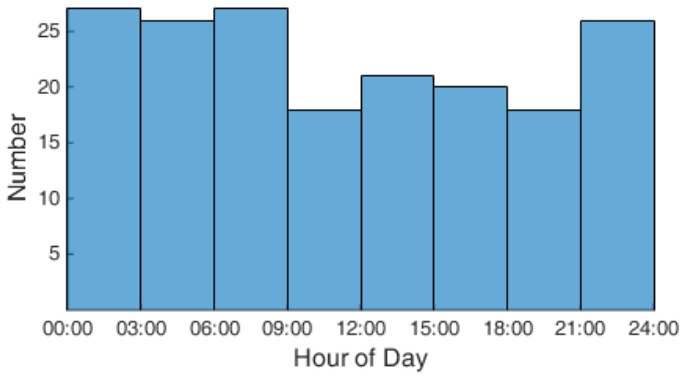

Figure 5.14 – Histogram of seizure occurrence times across circadian cycle, with almost a uniform distribution

Technically, there are several physiological interfering sources such as ECG, blinking, eye movement, electromyogram (EMG) signals, and other environmental artifacts, which can affect the detection performance. However as the invasive recordings were investigated here, the signal to noise ratio (SNR) is very high around 20-100 times better than scalp EEG recordings (Ball et al. , 2009). Furthermore, since most of these interfering noises mount evenly on the immediately adjacent channels, their possible side effects can be largely reduced by considering a bipolar montage (in NPS and SVD methods), in which the common mode of the two neighboring signals is eliminated by subtraction. Moreover the extracted

feature was processed using a 4-epochs (5-sec length) moving average window to further reduce the influence of the artifacts, and as a result of this smoothing the number of false alarms were significantly reduced. For instance, using the relative NPS measure, the number of false alarms was increased from 16 to 23 for the subject 2 without applying smoothing, and reduced detection latency by 1.8 s.

5.5 Conclusion

A novel approach using neuronal potential similarity measures obtained from spectral powers of a bipolar channel was introduced for early seizure detection. The method provided very high performance results and could detect clinical onsets averagely by 6.3 s in advance. Considering the PSD-based nature of the proposed measure, it is much suited to be used in the closed-loop implantable neurostimulation devices. Such a low complexity measure is an essential part of the early seizure detection algorithms, required to continuously monitor electrical activities of the brain and to deliver electrical stimulation in the proper times. As battery replacement in the implantable devices necessitates a surgery, commercialized products needs to introduce devices which can last for several years. A significant space/weight of the implantable products is occupied by its battery, which can be further compacted by using more efficient and lower computational cost algorithms.

Moreover, the SVD and MPC measures were modified to provide higher performance results for seizure event detection. Both of these measures were previously investigated, however in this thesis higher level of sensitivity and lower number of false alarms was obtained by the modified versions of these measures. Although the SVD and MPC measures are of relatively high computational cost, they were proposed only for clinical long-term monitoring, and not to be used in portable devices. Computational cost of these measures is therefore not an important issue in real-time or offline labeling in clinic.

Furthermore, it was essential to justify the efficiency of the proposed methods in practical situations. This issue was approached by the evaluation of proposed methods on long-term iEEG recordings of several months, contrary to most previous studies which have considered short and segmented recordings.

Chapter 6 Conclusions and perspectives

6.1 Conclusions on seizure prediction approaches

In this thesis, two novel approaches were investigated for epileptic seizure prediction. Firstly we introduced a new relative bivariate measure based on spectral power features to detect the preictal state. A specific feature selection method was developed to find the best discriminative features and to reduce the dimension of the resulting feature space. The performance of the method was demonstrated in two ways. The number of selected features was 9.9 in average, showing the efficiency of the introduced bivariate features as well as the feature selection method. By ranking the original normalized spectral power features and relative bivariate features together, relative bivariate features achieved the highest ranks. The proposed method could provide a good performance for seizure prediction. In average 75.8% of the test onsets (out-of-sample) were predicted across 1537 hours of test data with an average FPR of 0.1 h^{-1}.

Compared with other studies, the developed prediction algorithm presented good results considering the long-term continuous recordings (total of 183 ictal events in 3565 h recording). The number of non-preictal training samples was reduced to achieve a balanced number of samples for training of the SVM classifier. However, this might lead to an increase in the number of false alarms. In future investigation, it is suggested to use a cost-sensitive SVM, allowing to use all of the non-preictal samples in the train set, by which it is expected to achieve a lower number of false alarms. However the computational cost of training phase, which is an offline process, will be significantly increased using the cost-sensitive SVM. Furthermore, the EEG bandwidth can be subdivided into narrower sub-bands, which can better highlight the gradual preictal changes, by providing higher spectral resolutions. Finally, here we have followed an empirical method of selecting subsets as 3, 5, 10, 20 or 40 features.

A future study can use sequential feature elimination starting from the complete feature set or start from the best ranked feature and apply sequential feature increments, to find the optimal dimension for the feature space.

Secondly, the problem of optimal preictal period selection, which plays a key role on the efficiency of supervised machine learning algorithms, was approached by a novel yet simple statistical methodology. By examining different preictal periods, and through the investigation of the proposed method, we could find the best discriminative preictal periods for each seizure/feature. We have also found that the optimal preictal periods vary significantly from seizure to seizure, even for the seizures of a same patient. This suggests that for building a robust model, the OPP value of each seizure should be separately obtained and considered during the training phase of the model. After the training stage, the minimum and maximum values of resulting OPPs can be used to define the SPH and SOP parameters for proper evaluation of the model on the test data. Furthermore, the spectral power features of high frequency gamma activities were found to be more discriminative among the features.

One of our conclusions is that the seizure predictor has to be personalized to each patient. In our view the patient will come to a clinical environment where EEG data will be collected, processed, many predictors trained (with optimal preictal periods, different channels, etc.), and the best one will be embedded in the transportable device with high processing power (Teixeira et al. , 2013, Teixeira et al. , 2014a). Then the patient will go to his normal life and the performance of the transportable device will be analyzed after some time; if needed, a new training phase can be performed (not necessarily in clinic). This plan needs that clinics have access to good computational infrastructures and have computer engineers. With the cloud developments it will not be a difficult task. It is the author's opinion that the future medicine will need many personalized computerized studies, not only in seizure prediction.

6.2 Conclusions on seizure detection approaches

An automated early seizure detection algorithm was developed using a novel measure obtained from the ratio of neuronal potential similarities, which in turn were extracted from the PSD of one bipolar channel. The proposed relative NPS method could detect clinical onsets averagely by 6.3 s in advance, and could provide a mean detection latency of 13.1 s from electrographic onsets, with a high sensitivity of 86.9% and a very low FDR of 0.06 h^{-1}. This is an important issue for closed-loop neurostimulation systems which require detection of seizure onsets either immediately or with negligible delays, while achieving high sensitivity and specificity. Additionally, considering the PSD-based nature of the proposed measure it is much suited to be used as an essential detection sub-system in the implantable closed-loop neurostimulation devices, for clinical applications. Such a low complexity measure is an essential part of seizure onset detection algorithms, required to continuously monitor electrical activities of the brain and to deliver electrical stimulation pulses in proper times for efficient seizure suppression. A future investigation may further improve the sensitivity of the algorithm by extracting the proposed NPS measure from several bipolar montages in patients with two or more foci, to cover all epileptic zones, and then applying decision fusion approaches. Furthermore, the relative NPS measure can be examined on the whole set of pairwise combinations of adjacent electrodes, to uncover the spatial propagation information of seizures across brain regions. This is based on the hypothesis that the measure extracted from the focal channels would increase in advance of the measure extracted from other electrodes.

Furthermore, phase synchronization of neural activity in different frequency sub-bands was studied for automated detection of epileptic seizures, as well as for its synchronous behavior during seizures. Mean phase coherence (MPC) was considered as a measure of the phase locking level between two iEEG signals, and was extracted for different sub-bands, using windowed and bandpass filtered signals. The results indicated that the MPC measures extracted from specific frequency bands, especially 12-18 Hz and 18-28 Hz, could

significantly improve both parameters of sensitivity and specificity in comparison to the MPC measure extracted from wideband signals. Additionally, it was observed that the highest level of synchrony in all frequency bands occur mostly prior to seizure termination, whereas the seizure initiation usually coincides with loss of synchronization.

Moreover, the SVD was applied on the bipolar iEEG signal, for studying of the coherency patterns in seizures. Since SVD decomposes data into its correlated parts, therefore when two adjacent electrodes become highly coherent, the correlated components inside their difference signal contain less energy. This phenomenon induced a sudden decrease in the singular values of SVD decomposition, and emerged with the seizure termination. The bipolar SVD approach also provided high level of sensitivity combined with very low number of false alarms.

Furthermore, it was preferable to justify the performance of the proposed detection methods in practical situations. This issue was approached by the evaluation of the proposed methods on long-term continuous iEEG recordings for each patient, averagely around one week recordings per patient and overall several months, contrary to most previous studies which have considered short and segmented recordings prior to seizure onsets only.

References

Aarabi A, Fazel-Rezai R, Aghakhani Y. A fuzzy rule-based system for epileptic seizure detection in intracranial EEG. Clin Neurophysiol. 2009;120:1648-57.

Aarabi A, Grebe R, Wallois F. A multistage knowledge-based system for EEG seizure detection in newborn infants. Clin Neurophysiol. 2007;118:2781-97.

Acharya UR, Sree SV, Suri JS. Automatic detection of epileptic EEG signals using higher order cumulant features. Int J Neural Syst. 2011;21:403-14.

Acharya UR, Yanti R, Zheng JW, Krishnan MM, Tan JH, Martis RJ, Lim CM. Automated diagnosis of epilepsy using CWT, HOS and texture parameters. Int J Neural Syst. 2013;23:1350009.

Adeli H, Ghosh-Dastidar S. Automated EEG-Based Diagnosis of Neurological Disorders: Inventing the Future of Neurology: Taylor & Francis; 2010.

Adeli H, Ghosh-Dastidar S, Dadmehr N. A wavelet-chaos methodology for analysis of EEGs and EEG subbands to detect seizure and epilepsy. IEEE Trans Biomed Eng. 2007;54:205-11.

Adeli H, Zhou Z, Dadmehr N. Analysis of EEG records in an epileptic patient using wavelet transform. J Neurosci Methods. 2003;123:69-87.

Alvarado-Rojas C, Valderrama M, Fouad-Ahmed A, Feldwisch-Drentrup H, Ihle M, Teixeira CA, Sales F, Schulze-Bonhage A, Adam C, Dourado A, Charpier S, Navarro V, Le Van Quyen M. Slow modulations of high-frequency activity (40-140-Hz) discriminate preictal changes in human focal epilepsy. Sci Rep. 2014;4:4545.

Andrzejak RG, Chicharro D, Elger CE, Mormann F. Seizure prediction: Any better than chance? Clin Neurophysiol. 2009;120:1465-78.

Aschenbrenner-Scheibe R, Maiwald T, Winterhalder M, Voss HU, Timmer J, Schulze-Bonhage A. How well can epileptic seizures be predicted? An evaluation of a nonlinear method. Brain. 2003;126:2616-26.

Ayoubian L, Lacoma H, Gotman J. Automatic seizure detection in SEEG using high frequency activities in wavelet domain. Med Eng Phys. 2013;35:319-28.

Ball T, Kern M, Mutschler I, Aertsen A, Schulze-Bonhage A. Signal quality of simultaneously recorded invasive and non-invasive EEG. Neuroimage. 2009;46:708-16.

Bandarabadi M, Dourado A, Teixeira CA, Netoff TI, Parhi KK. Seizure prediction with bipolar spectral power features using Adaboost and SVM classifiers. Engineering in Medicine and Biology Society (EMBC), 2013 35th Annual International Conference of the IEEE2013. p. 6305-8.

Bandarabadi M, Karami-Mollaei M, Afzalian A, Ghasemi J. ECG Denoising Using Singular Value Decomposition. Australian Journal of Basic and Applied Sciences. 2010;4:2109-13.

Bandarabadi M, Teixeira CA, Rasekhi J, Dourado A. Epileptic seizure prediction using relative spectral power features. Clin Neurophysiol. 2015;126:237-48.

Bandarabadi M, Teixeira CA, Sales F, Dourado A. Wepilet, optimal orthogonal wavelets for epileptic seizure prediction with one single surface channel. Engineering in Medicine and Biology Society,EMBC, 2011 Annual International Conference of the IEEE2011. p. 7059-62.

Baranov-Krylov IN, Shuvaev VT. Effects of selective visual attention in the parietal and temporal areas of the human cortex using evoked potential data. Neurosci Behav Physiol. 2005;35:159-64.

Blanco S, Garay A, Coulombie D. Comparison of Frequency Bands Using Spectral Entropy for Epileptic Seizure Prediction. ISRN Neurology. 2013;2013:5.

Box GEP, Jenkins GM, Reinsel GC. Time Series Analysis: Forecasting and Control: Wiley; 2008.

Cabrerizo M, Ayala M, Goryawala M, Jayakar P, Adjouadi M. A new parametric feature descriptor for the classification of epileptic and control EEG records in pediatric population. Int J Neural Syst. 2012;22:1250001.

Carney PR, Myers S, Geyer JD. Seizure prediction: Methods. Epilepsy Behav. 2011;22, Supplement 1:S94-S101.

Cerf R, El Ouasdad EH. Spectral analysis of stereo-electroencephalograms: preictal slowing in partial epilepsies. Biol Cybern. 2000;83:399.

Chang C-C, Lin C-J. LIBSVM: A library for support vector machines. ACM Trans Intell Syst Technol. 2011;2:1-27.

Chaovalitwongse W, Iasemidis LD, Pardalos PM, Carney PR, Shiau DS, Sackellares JC. Performance of a seizure warning algorithm based on the dynamics of intracranial EEG. Epilepsy Res. 2005;64:93-113.

Chavez M, Le Van Quyen M, Navarro V, Baulac M, Martinerie J. Spatio-temporal dynamics prior to neocortical seizures: amplitude versus phase couplings. Biomedical Engineering, IEEE Transactions on. 2003;50:571-83.

Chawla NV, Japkowicz N, Kotcz A. Editorial: special issue on learning from imbalanced data sets. ACM SIGKDD Explor Newsl. 2004;6:1-6.

Chisci L, Mavino A, Perferi G, Sciandrone M, Anile C, Colicchio G, Fuggetta F. Real-Time Epileptic Seizure Prediction Using AR Models and Support Vector Machines. Biomedical Engineering, IEEE Transactions on. 2010;57:1124-32.

Colic S, Zalay OC, Bardakjian BL. Responsive neuromodulators based on artificial neural networks used to control seizure-like events in a computational model of epilepsy. Int J Neural Syst. 2011;21:367-83.

Corsini J, Shoker L, Sanei S, Alarcon G. Epileptic seizure predictability from scalp EEG incorporating constrained blind source separation. Biomedical Engineering, IEEE Transactions on. 2006;53:790-9.

D'Alessandro M, Esteller R, Vachtsevanos G, Hinson A, Echauz J, Litt B. Epileptic seizure prediction using hybrid feature selection over multiple intracranial eeg electrode contacts: a report of four patients. Biomedical Engineering, IEEE Transactions on. 2003;50:1041-.

da Silva FHL, Blanes W, Kalitzin SN, Parra J, Suffczynski P, Velis DN. Dynamical diseases of brain systems: different routes to epileptic seizures. Biomedical Engineering, IEEE Transactions on. 2003;50:540-8.

De Clercq W, Lemmerling P, Van Huffel S, Van Paesschen W. Anticipation of epileptic seizures from standard EEG recordings. The Lancet. 2003;361:970.

DeGiorgio CM, Shewmon A, Murray D, Whitehurst T. Pilot Study of Trigeminal Nerve Stimulation (TNS) for Epilepsy: A Proof-of-Concept Trial. Epilepsia. 2006;47:1213-5.

Direito B, Duarte J, Teixeira C, Schelter B, Le Van Quyen M, Schulze-Bonhage A, Sales F, Dourado A. Feature selection in high dimensional EEG features spaces for epileptic seizure prediction. Proc of the 18th IFAC World Congress. 2011.

Direito B, Teixeira C, Ribeiro B, Castelo-Branco M, Sales F, Dourado A. Modeling epileptic brain states using EEG spectral analysis and topographic mapping. J Neurosci Methods. 2012;210:220-9.

Dressler O, Schneider G, Stockmanns G, Kochs EF. Awareness and the EEG power spectrum: analysis of frequencies. Br J Anaesth. 2004;93:806-9.

Drongelen Wv, Nayak S, Frim DM, Kohrman MH, Towle VL, Lee HC, McGee AB, Chico MS, Hecox KE. Seizure anticipation in pediatric epilepsy: use of kolmogorov entropy. Pediatr Neurol. 2003;29:207-13.

Drury I, Smith B, Li D, Savit R. Seizure prediction using scalp electroencephalogram. Exp Neurol. 2003;184, Supplement 1:9-18.

Ebersole JS. In search of seizure prediction: a critique. Clin Neurophysiol. 2005;116:489-92.

Elger CE, Lehnertz K. Seizure prediction by non-linear time series analysis of brain electrical activity. Eur J Neurosci. 1998;10:786-9.

Engel J. A Proposed Diagnostic Scheme for People with Epileptic Seizures and with Epilepsy: Report of the ILAE Task Force on Classification and Terminology. Epilepsia. 2001;42:796-803.

Esteller R, Echauz J, D'Alessandro M, Worrell G, Cranstoun S, Vachtsevanos G, Litt B. Continuous energy variation during the seizure cycle: towards an on-line accumulated energy. Clin Neurophysiol. 2005;116:517-26.

Feldwisch-Drentrup H, Ihle M, Le Van Quyen M, Teixeira C, Dourado A, Timmer J, Sales F, Navarro V, Schulze-Bonhage A, Schelter B. Anticipating the unobserved: Prediction of subclinical seizures. Epilepsy Behav. 2011a;22, Supplement 1:S119-S26.

Feldwisch-Drentrup H, Schelter B, Jachan M, Nawrath J, Timmer J, Schulze-Bonhage A. Joining the benefits: Combining epileptic seizure prediction methods. Epilepsia. 2010;51:1598-606.

Feldwisch-Drentrup H, Schulze-Bonhage A, Timmer J, Schelter B. Statistical validation of event predictors: A comparative study based on the field of seizure prediction. Physical Review E. 2011b;83:066704.

Feldwisch-Drentrup H, Staniek M, Schulze-Bonhage A, Timmer J, Dickten H, Elger CE, Schelter B, Lehnertz K. Identification of preseizure states in epilepsy: A data-driven approach for multichannel EEG recordings. Front Comput Neurosci. 2011c;5.

Fisher RS. Therapeutic devices for epilepsy. Ann Neurol. 2012;71:157-68.

Fisher RS, Velasco AL. Electrical brain stimulation for epilepsy. Nat Rev Neurol. 2014;10:261-70.

Fukunaga K. Introduction to Statistical Pattern Recognition: Academic Press; 1990.

Gadhoumi K, Lina J-M, Gotman J. Discriminating preictal and interictal states in patients with temporal lobe epilepsy using wavelet analysis of intracerebral EEG. Clin Neurophysiol. 2012;123:1906-16.

Ghosh-Dastidar S, Adeli H, Dadmehr N. Mixed-band wavelet-chaos-neural network methodology for epilepsy and epileptic seizure detection. IEEE Trans Biomed Eng. 2007;54:1545-51.

Gigola S, Ortiz F, D'Attellis CE, Silva W, Kochen S. Prediction of epileptic seizures using accumulated energy in a multiresolution framework. J Neurosci Methods. 2004;138:107-11.

Gotman J. Automatic recognition of epileptic seizures in the EEG. Electroencephalogr Clin Neurophysiol. 1982;54:530-40.

Gotman J, Gloor P. Automatic recognition and quantification of interictal epileptic activity in the human scalp EEG. Electroencephalogr Clin Neurophysiol. 1976;41:513-29.

Gotman J, Koffler DJ. Interictal spiking increases after seizures but does not after decrease in medication. Electroencephalogr Clin Neurophysiol. 1989;72:7-15.

Gotman J, Marciani MG. Electroencephalographic spiking activity, drug levels, and seizure occurrence in epileptic patients. Ann Neurol. 1985;17:597-603.

Grassberger P, Procaccia I. Characterization of Strange Attractors. Phys Rev Lett. 1983;50:346-9.

Greene BR, de Chazal P, Boylan GB, Connolly S, Reilly RB. Electrocardiogram based neonatal seizure detection. IEEE Trans Biomed Eng. 2007;54:673-82.

Grewal S, Gotman J. An automatic warning system for epileptic seizures recorded on intracerebral EEGs. Clin Neurophysiol. 2005;116:2460-72.

Harrison MAF, Frei MG, Osorio I. Accumulated energy revisited. Clin Neurophysiol. 2005a;116:527-31.

Harrison MAF, Osorio I, Frei MG, Asuri S, Lai Y-C. Correlation dimension and integral do not predict epileptic seizures. Chaos: An Interdisciplinary Journal of Nonlinear Science. 2005b;15:-.

Hassanpour H, Mesbah M, Boashash B. Time-frequency feature extraction of newborn EEG seizure using SVD-based techniques. Eurasip J Appl Sig P. 2004;2004:2544-54.

Haut SR, Hall CB, Borkowski T, Tennen H, Lipton RB. Clinical features of the pre-ictal state: Mood changes and premonitory symptoms. Epilepsy Behav. 2012;23:415-21.

Haut SR, Hall CB, Borkowski T, Tennen H, Lipton RB. Modeling seizure self-prediction: An e-diary study. Epilepsia. 2013;54:1960-7.

Hjorth B. EEG analysis based on time domain properties. Electroencephalogr Clin Neurophysiol. 1970;29:306-10.

Howbert JJ, Patterson EE, Stead SM, Brinkmann B, Vasoli V, Crepeau D, Vite CH, Sturges B, Ruedebusch V, Mavoori J, Leyde K, Sheffield WD, Litt B, Worrell GA. Forecasting Seizures in Dogs with Naturally Occurring Epilepsy. PLoS One. 2014;9:e81920.

Hunyadi B, Signoretto M, Van Paesschen W, Suykens JAK, Van Huffel S, De Vos M. Incorporating structural information from the multichannel EEG improves patient-specific seizure detection. Clin Neurophysiol. 2012;123:2352-61.

Iasemidis L, Chris Sackellares J, Zaveri H, Williams W. Phase space topography and the Lyapunov exponent of electrocorticograms in partial seizures. Brain Topogr. 1990;2:187-201.

Iasemidis LD. Epileptic seizure prediction and control. IEEE Trans Biomed Eng. 2003;50:549-58.

Iasemidis LD, Pardalos P, Sackellares JC, Shiau DS. Quadratic Binary Programming and Dynamical System Approach to Determine the Predictability of Epileptic Seizures. J Comb Optim. 2001;5:9-26.

Iasemidis LD, Pardalos PM, Shiau D-S, Chaovalitwongse W, Narayanan K, Kumar S, Carney PR, Chris Sackellares J. Prediction of Human Epileptic Seizures based on Optimization and Phase Changes of Brain Electrical Activity. Optimization Methods and Software. 2003a;18:81-104.

Iasemidis LD, Shiau DS, Chaovalitwongse W, Sackellares JC, Pardalos PM, Principe JC, Carney PR, Prasad A, Veeramani B, Tsakalis K. Adaptive epileptic seizure prediction system. IEEE Trans Biomed Eng. 2003b;50:616-27.

Iasemidis LD, Shiau DS, Pardalos P, Sackellares JC. Phase Entrainment and Predictability of Epileptic Seizures. In: Pardalos P, Principe J, editors. Biocomputing: Springer US; 2002. p. 59-84.

Iasemidis LD, Shiau DS, Pardalos PM, Chaovalitwongse W, Narayanan K, Prasad A, Tsakalis K, Carney PR, Sackellares JC. Long-term prospective on-line real-time seizure prediction. Clin Neurophysiol. 2005;116:532-44.

Ihle M, Feldwisch-Drentrup H, Teixeira CA, Witon A, Schelter B, Timmer J, Schulze-Bonhage A. EPILEPSIAE – A European epilepsy database. Comput Methods Programs Biomed. 2012;106:127-38.

Jacobs J, Zelmann R, Jirsch J, Chander R, Dubeau C-ÉCF, Gotman J. High frequency oscillations (80–500 Hz) in the preictal period in patients with focal seizures. Epilepsia. 2009;50:1780-92.

Jerger KK, Weinstein SL, Sauer T, Schiff SJ. Multivariate linear discrimination of seizures. Clin Neurophysiol. 2005;116:545-51.

Jiruska P, de Curtis M, Jefferys JGR, Schevon CA, Schiff SJ, Schindler K. Synchronization and desynchronization in epilepsy: controversies and hypotheses. The Journal of Physiology. 2013;591:787-97.

Jouny CC, Franaszczuk PJ, Bergey GK. Signal complexity and synchrony of epileptic seizures: is there an identifiable preictal period? Clin Neurophysiol. 2005;116:552-8.

Jouny CC, Franaszczuk PJ, Bergey GK. Improving early seizure detection. Epilepsy Behav. 2011;22, Supplement 1:S44-S8.

Katz A, Marks DA, McCarthy G, Spencer SS. Does interictal spiking change prior to seizures? Electroencephalogr Clin Neurophysiol. 1991;79:153-6.

Kharbouch A, Shoeb A, Guttag J, Cash SS. An algorithm for seizure onset detection using intracranial EEG. Epilepsy Behav. 2011;22, Supplement 1:S29-S35.

Klatt J, Feldwisch-Drentrup H, Ihle M, Navarro V, Neufang M, Teixeira C, Adam C, Valderrama M, Alvarado-Rojas C, Witon A, Le Van Quyen M, Sales F, Dourado A, Timmer J, Schulze-Bonhage A, Schelter B. The EPILEPSIAE database: An extensive electroencephalography database of epilepsy patients. Epilepsia. 2012;53:1669-76.

Kreuz T, Andrzejak RG, Mormann F, Kraskov A, Stögbauer H, Elger CE, Lehnertz K, Grassberger P. Measure profile surrogates: A method to validate the performance of epileptic seizure prediction algorithms. Physical Review E. 2004;69:061915.

Kuhlmann L, Freestone D, Lai A, Burkitt AN, Fuller K, Grayden DB, Seiderer L, Vogrin S, Mareels IMY, Cook MJ. Patient-specific bivariate-synchrony-based seizure prediction for short prediction horizons. Epilepsy Res. 2010;91:214-31.

Lai Y-C, Harrison MAF, Frei MG, Osorio I. Inability of Lyapunov Exponents to Predict Epileptic Seizures. Phys Rev Lett. 2003;91:068102.

Lai Y-C, Harrison MAF, Frei MG, Osorio I. Controlled test for predictive power of Lyapunov exponents: Their inability to predict epileptic seizures. Chaos: An Interdisciplinary Journal of Nonlinear Science. 2004;14:630-42.

Lange HH, Lieb JP, Engel Jr J, Crandall PH. Temporo-spatial patterns of pre-ictal spike activity in human temporal lobe epilepsy. Electroencephalogr Clin Neurophysiol. 1983;56:543-55.

Le Van Quyen M, Adam C, Martinerie J, Baulac M, Clemenceau S, Varela F. Spatio-temporal characterizations of non-linear changes in intracranial activities prior to human temporal lobe seizures. Eur J Neurosci. 2000;12:2124-34.

Le Van Quyen M, Martinerie J, Baulac M, Varela F. Anticipating epileptic seizures in real time by a non-linear analysis of similarity between EEG recordings. Neuroreport. 1999;10:2149-55.

Le Van Quyen M, Martinerie J, Navarro V, Boon P, D'Havé M, Adam C, Renault B, Varela F, Baulac M. Anticipation of epileptic seizures from standard EEG recordings. The Lancet. 2001;357:183-8.

Le Van Quyen M, Soss J, Navarro V, Robertson R, Chavez M, Baulac M, Martinerie J. Preictal state identification by synchronization changes in long-term intracranial EEG recordings. Clin Neurophysiol. 2005;116:559-68.

Lehnertz K, Elger CE. Can Epileptic Seizures be Predicted? Evidence from Nonlinear Time Series Analysis of Brain Electrical Activity. Phys Rev Lett. 1998;80:5019-22.

Lehnertz K, Litt B. The First International Collaborative Workshop on Seizure Prediction: summary and data description. Clin Neurophysiol. 2005;116:493-505.

Lehnertz K, Mormann F, Kreuz T, Andrzejak RG, Rieke C, David P, Elger CE. Seizure prediction by nonlinear EEG analysis. IEEE Eng Med Biol Mag. 2003;22:57-63.

Lerner DE. Monitoring changing dynamics with correlation integrals: Case study of an epileptic seizure. Physica D. 1996;97:563-76.

Lesser RP. Epilepsy: Does continuous EEG monitoring improve seizure control? Nat Rev Neurol. 2009;5:581-2.

Li D, Zhou W, Drury I, Savit R. Non-linear, non-invasive method for seizure anticipation in focal epilepsy. Math Biosci. 2003;186:63-77.

Li D, Zhou W, Drury I, Savit R. Seizure anticipation, states of consciousness and marginal predictability in temporal lobe epilepsy. Epilepsy Res. 2006a;68:9-18.

Li S, Zhou W, Yuan Q, Liu Y. Seizure prediction using spike rate of intracranial EEG. IEEE Trans Neural Syst Rehabil Eng. 2013;21:880-6.

Li X, Ouyang G. Nonlinear similarity analysis for epileptic seizures prediction. Nonlinear Analysis: Theory, Methods & Applications. 2006b;64:1666-78.

Li X, Ouyang G, Richards DA. Predictability analysis of absence seizures with permutation entropy. Epilepsy Res. 2007;77:70-4.

Libbus I, Amurthur B, Kenknight BH. Implantable neurostimulator for providing electrical stimulation of cervical vagus nerves for treatment of chronic cardiac dysfunction with bounded titration. In: Office USPaT, editor. US patent: Cyberonics, Inc.; 2014.

Litt B, Echauz J. Prediction of epileptic seizures. The Lancet Neurology. 2002;1:22-30.

Litt B, Esteller R, Echauz J, D'Alessandro M, Shor R, Henry T, Pennell P, Epstein C, Bakay R, Dichter M, Vachtsevanos G. Epileptic Seizures May Begin Hours in Advance of Clinical Onset: A Report of Five Patients. Neuron. 2001;30:51-64.

Liu A, Hahn JS, Heldt GP, Coen RW. Detection of neonatal seizures through computerized EEG analysis. Electroencephalogr Clin Neurophysiol. 1992;82:30-7.

Liu Y, Zhou W, Yuan Q, Chen S. Automatic seizure detection using wavelet transform and SVM in long-term intracranial EEG. IEEE Trans Neural Syst Rehabil Eng. 2012;20:749-55.

Lopes N, Ribeiro B. Support Vector Machines (SVMs). Machine Learning for Adaptive Many-Core Machines - A Practical Approach: Springer International Publishing; 2015. p. 85-105.

Magiorkinis E, Sidiropoulou K, Diamantis A. Hallmarks in the history of epilepsy: Epilepsy in antiquity. Epilepsy Behav. 2010;17:103-8.

Maiwald T, Winterhalder M, Aschenbrenner-Scheibe R, Voss HU, Schulze-Bonhage A, Timmer J. Comparison of three nonlinear seizure prediction methods by means of the seizure prediction characteristic. Physica D. 2004;194:357-68.

Malarvili MB, Mesbah M. Newborn seizure detection based on heart rate variability. IEEE Trans Biomed Eng. 2009;56:2594-603.

Malmivuo J, Plonsey R. Bioelectromagnetism: Principles and Applications of Bioelectric and Biomagnetic Fields: Oxford University Press; 2002.

Mammone N, Principe JC, Morabito FC, Shiau DS, Sackellares JC. Visualization and modelling of STLmax topographic brain activity maps. J Neurosci Methods. 2010;189:281-94.

Martinerie J, Adam C, Le Van Quyen M, Baulac M, Clemenceau S, Renault B, Varela FJ. Epileptic seizures can be anticipated by non-linear analysis. Nat Med. 1998;4:1173-6.

Martis RJ, Acharya UR, Tan JH, Petznick A, Tong L, Chua CK, Ng EY. Application of intrinsic time-scale decomposition (ITD) to EEG signals for automated seizure prediction. Int J Neural Syst. 2013;23:1350023.

Martis RJ, Acharya UR, Tan JH, Petznick A, Yanti R, Chua CK, Ng EY, Tong L. Application of empirical mode decomposition (emd) for automated detection of epilepsy using EEG signals. Int J Neural Syst. 2012;22:1250027.

McSharry PE, Smith LA, Tarassenko L. Comparison of predictability of epileptic seizures by a linear and a nonlinear method. Biomedical Engineering, IEEE Transactions on. 2003;50:628-33.

Meier R, Dittrich H, Schulze-Bonhage A, Aertsen A. Detecting epileptic seizures in long-term human EEG: a new approach to automatic online and real-time detection and classification of polymorphic seizure patterns. J Clin Neurophysiol. 2008;25:119-31.

Mirowski P, Madhavan D, LeCun Y, Kuzniecky R. Classification of patterns of EEG synchronization for seizure prediction. Clin Neurophysiol. 2009;120:1927-40.

Moghim N, Corne DW. Predicting Epileptic Seizures in Advance. PLoS One. 2014;9:e99334.

Mormann F, Andrzejak RG, Elger CE, Lehnertz K. Seizure prediction: the long and winding road. Brain. 2007;130:314-33.

Mormann F, Andrzejak RG, Kreuz T, Rieke C, David P, Elger CE, Lehnertz K. Automated detection of a preseizure state based on a decrease in synchronization in intracranial electroencephalogram recordings from epilepsy patients. Physical Review E. 2003a;67:021912.

Mormann F, Elger CE, Lehnertz K. Seizure anticipation: from algorithms to clinical practice. Curr Opin Neurol. 2006;19:187-93.

Mormann F, Kreuz T, Andrzejak RG, David P, Lehnertz K, Elger CE. Epileptic seizures are preceded by a decrease in synchronization. Epilepsy Res. 2003b;53:173-85.

Mormann F, Kreuz T, Rieke C, Andrzejak RG, Kraskov A, David P, Elger CE, Lehnertz K. On the predictability of epileptic seizures. Clin Neurophysiol. 2005;116:569-87.

Mormann F, Lehnertz K, David P, Elger CE. Mean phase coherence as a measure for phase synchronization and its application to the EEG of epilepsy patients. Physica D. 2000;144:358-69.

Morrell MJ. Responsive cortical stimulation for the treatment of medically intractable partial epilepsy. Neurology. 2011;77:1295-304.

Nakken KO, Solaas MH, Kjeldsen MJ, Friis ML, Pellock JM, Corey LA. Which seizure-precipitating factors do patients with epilepsy most frequently report? Epilepsy Behav. 2005;6:85-9.

Nanobashvili ZI, Chachua TR, Bilanishvili IG, Khizanishvili NA, Nebieridze NG, Koreli AG. Peculiarities of the Effects of Stimulation of Emotiogenic Central Structures under Conditions of a Kindling Model of Epilepsy. Neurophysiology. 2011;43:292-8.

Navarro V, Martinerie J, Quyen MLV, Clemenceau S, Adam C, Baulac M, Varela F. Seizure anticipation in human neocortical partial epilepsy. Brain. 2002;125:640-55.

Norton MP, Karczub DG. Fundamentals of noise and vibration analysis for engineers: Cambridge University Press; 2003.

Nunez PL, Srinivasan R, Westdorp AF, Wijesinghe RS, Tucker DM, Silberstein RB, Cadusch PJ. EEG coherency. Electroencephalogr Clin Neurophysiol. 1997;103:499-515.

Osorio I. Automated seizure detection using EKG. Int J Neural Syst. 2014;24:1450001.

Ouyang G, Li X, Li Y, Guan X. Application of wavelet-based similarity analysis to epileptic seizures prediction. Comput Biol Med. 2007;37:430-7.

Parhi KK, Ayinala M. Low-Complexity Welch Power Spectral Density Computation. IEEE Trans Circuits Syst I, Reg Papers. 2013;PP:1-11.

Parhi KK, Ayinala M. Low-Complexity Welch Power Spectral Density Computation. Circuits and Systems I: Regular Papers, IEEE Transactions on. 2014;61:172-82.

Park Y, Luo L, Parhi KK, Netoff T. Seizure prediction with spectral power of EEG using cost-sensitive support vector machines. Epilepsia. 2011;52:1761-70.

Pearce A, Wulsin D, Blanco JA, Krieger A, Litt B, Stacey WC. Temporal changes of neocortical high-frequency oscillations in epilepsy. J Neurophysiol. 2013;110:1167-79.

Peng H, Fulmi L, Ding C. Feature selection based on mutual information criteria of max-dependency, max-relevance, and min-redundancy. IEEE Trans Pattern Anal Mach Intell. 2005;27:1226-38.

Petitmengin C, Baulac M, Navarro V. Seizure anticipation: Are neurophenomenological approaches able to detect preictal symptoms? Epilepsy Behav. 2006;9:298-306.

Petrosian A, Prokhorov D, Homan R, Dasheiff R, Wunsch Ii D. Recurrent neural network based prediction of epileptic seizures in intra- and extracranial EEG. Neurocomputing. 2000;30:201-18.

Pugliatti M, Beghi E, Forsgren L, Ekman M, Sobocki P. Estimating the cost of epilepsy in Europe: a review with economic modeling. Epilepsia. 2007;48:2224-33.

Rabbi AF, Fazel-Rezai R. A Fuzzy Logic System for Seizure Onset Detection in Intracranial EEG. Comput Intell Neurosci. 2012;2012:12.

Rasekhi J, Karami-Mollaei M, Bandarabadi M, Teixeira C, Dourado A. Epileptic seizure prediction based on ratio and differential linear univariate features. J Med Signals Sens. 2015;5:1-11.

Rasekhi J, Mollaei MRK, Bandarabadi M, Teixeira CA, Dourado A. Preprocessing effects of 22 linear univariate features on the performance of seizure prediction methods. J Neurosci Methods. 2013;217:9-16.

Rieke C, Sternickel K, Andrzejak RG, Elger CE, David P, Lehnertz K. Measuring Nonstationarity by Analyzing the Loss of Recurrence in Dynamical Systems. Phys Rev Lett. 2002;88:244102.

Rogowski Z, Gath I, Bental E. On the prediction of epileptic seizures. Biol Cybern. 1981;42:9-15.

Rosenblum MG, Pikovsky AS, Kurths J. Phase synchronization in driven and coupled chaotic oscillators. Ieee T Circuits-I. 1997;44:874-81.

Saab ME, Gotman J. A system to detect the onset of epileptic seizures in scalp EEG. Clin Neurophysiol. 2005;116:427-42.

Saeys Y, Inza I, Larrañaga P. A review of feature selection techniques in bioinformatics. Bioinformatics. 2007;23:2507-17.

Salant Y, Gath I, Henriksen O. Prediction of epileptic seizures from two-channel EEG. Med Biol Eng Comput. 1998;36:549-56.

Sanei S, Chambers JA. EEG signal processing: John Wiley & Sons; 2008.

Savit R, Green M. Time series and dependent variables. Physica D: Nonlinear Phenomena. 1991;50:95-116.

Scaramelli A, Braga P, Avellanal A, Bogacz A, Camejo C, Rega I, Messano T, Arciere B. Prodromal symptoms in epileptic patients: Clinical characterization of the pre-ictal phase. Seizure. 2009;18:246-50.

Schad A, Schindler K, Schelter B, Maiwald T, Brandt A, Timmer J, Schulze-Bonhage A. Application of a multivariate seizure detection and prediction method to non-invasive and intracranial long-term EEG recordings. Clin Neurophysiol. 2008;119:197-211.

Schelter B, Winterhalder M, Drentrup HFg, Wohlmuth J, Nawrath J, Brandt A, Schulze-Bonhage A, Timmer J. Seizure prediction: The impact of long prediction horizons. Epilepsy Res. 2007;73:213-7.

Schelter B, Winterhalder M, Maiwald T, Brandt A, Schad A, Schulze-Bonhage A, Timmer J. Testing statistical significance of multivariate time series analysis techniques for epileptic seizure prediction. Chaos: An Interdisciplinary Journal of Nonlinear Science. 2006;16:-.

Schindler K, Elger CE, Lehnertz K. Increasing synchronization may promote seizure termination: Evidence from status epilepticus. Clin Neurophysiol. 2007a;118:1955-68.

Schindler K, Gast H, Goodfellow M, Rummel C. On seeing the trees and the forest: Single-signal and multisignal analysis of periictal intracranial EEG. Epilepsia. 2012;53:1658-68.

Schindler K, Leung H, Elger CE, Lehnertz K. Assessing seizure dynamics by analysing the correlation structure of multichannel intracranial EEG. Brain. 2007b;130:65-77.

Schindler K, Wiest R, Kollar M, Donati F. Using simulated neuronal cell models for detection of epileptic seizures in foramen ovale and scalp EEG. Clin Neurophysiol. 2001;112:1006-17.

Schölkopf B, Smola AJ. Learning with Kernels: Support Vector Machines, Regularization, Optimization, and Beyond: Mit Press; 2002.

Schulze-Bonhage A, Haut S. Premonitory features and seizure self-prediction: Artifact or real? Epilepsy Res. 2011;97:231-5.

Schulze-Bonhage A, Sales F, Wagner K, Teotonio R, Carius A, Schelle A, Ihle M. Views of patients with epilepsy on seizure prediction devices. Epilepsy Behav. 2010;18:388-96.

Sharma P, Khan YU, Farooq O, Tripathi M, Adeli H. A Wavelet-Statistical Features Approach for Nonconvulsive Seizure Detection. Clin EEG Neurosci. 2014;45:274-84.

Shoeb A. Application of machine learning to epileptic seizure onset detection and treatment [Doctoral thesis]. Massachusetts Institute of Technology2009.

Shoeb A, Edwards H, Connolly J, Bourgeois B, Ted Treves S, Guttag J. Patient-specific seizure onset detection. Epilepsy Behav. 2004;5:483-98.

Shoeb A, Kharbouch A, Soegaard J, Schachter S, Guttag J. A machine-learning algorithm for detecting seizure termination in scalp EEG. Epilepsy Behav. 2011a;22, Supplement 1:S36-S43.

Shoeb A, Pang T, Guttag J, Schachter S. Non-invasive computerized system for automatically initiating vagus nerve stimulation following patient-specific detection of seizures or epileptiform discharges. Int J Neural Syst. 2009;19:157-72.

Shoeb A, Pang T, Guttag JV, Schachter SC. Vagus Nerve Stimulation Triggered by Machine Learning Based Seizure Detection. Epilepsy: CRC Press; 2011b. p. 385-95.

Soleimani-B H, Lucas C, N. Araabi B, Schwabe L. Adaptive prediction of epileptic seizures from intracranial recordings. Biomedical Signal Processing and Control. 2012;7:456-64.

Spencer S, Huh L. Outcomes of epilepsy surgery in adults and children. The Lancet Neurology. 2008;7:525-37.

Sprott JC, Sprott JC. Chaos and time-series analysis: Oxford University Press Oxford; 2003.

Srinivasan R, Nunez P, Tucker D, Silberstein R, Cadusch P. Spatial sampling and filtering of EEG with spline Laplacians to estimate cortical potentials. Brain Topogr. 1996;8:355-66.

Stacey W, Le Van Quyen M, Mormann F, Schulze-Bonhage A. What is the present-day EEG evidence for a preictal state? Epilepsy Res. 2011;97:243-51.

Stanski D, Hudson R, Homer T, Saidman L, Meathe E. Pharmacodynamic modeling of thiopental anesthesia. J Pharmacokinet Biopharm. 1984;12:223-40.

Strzelczyk A, Reese JP, Oertel WH, Dodel R, Rosenow F, Hamer HM. Costs of epilepsy and their predictors: Cross-sectional study in Germany and review of literature. Epileptology. 2013;1:55-60.

Sun DA, Sombati S, DeLorenzo RJ. Glutamate Injury-Induced Epileptogenesis in Hippocampal Neurons: An In Vitro Model of Stroke-Induced "Epilepsy". Stroke. 2001;32:2344-50.

Sun F, Morrell M. Closed-loop Neurostimulation: The Clinical Experience. Neurotherapeutics. 2014a:1-11.

Sun FT, Morrell MJ. The RNS System: responsive cortical stimulation for the treatment of refractory partial epilepsy. Expert Rev Med Devices. 2014b;11:563-72.

Tang Y, Chorlian DB, Rangaswamy M, Porjesz B, Bauer L, Kuperman S, O'Connor S, Rohrbaugh J, Schuckit M, Stimus A, Begleiter H. Genetic influences on bipolar EEG power spectra. Int J Psychophysiol. 2007;65:2-9.

Teixeira C, Direito B, Bandarabadi M, Dourado A. Output regularization of SVM seizure predictors: Kalman Filter versus the Firing Power method. Engineering in Medicine and Biology Society (EMBC), 2012 Annual International Conference of the IEEE2012. p. 6530-3.

Teixeira C, Direito B, Bandarabadi M, Grebe HP, Sa F, Sales F, Dourado A. Real-time epileptic seizure prediction at Centro Hospitalar e Universitário de Coimbra. Experiment@ International Conference (expat'13), 2013 2nd2013. p. 196-8.

Teixeira C, Favaro G, Direito B, Bandarabadi M, Feldwisch-Drentrup H, Ihle M, Alvarado C, Le Van Quyen M, Schelter B, Schulze-Bonhage A, Sales F, Navarro V, Dourado A. Brainatic: A System for Real-Time Epileptic Seizure Prediction. Brain-Computer Interface Research: Springer; 2014a. p. 7-18.

Teixeira CA, Direito B, Bandarabadi M, Le Van Quyen M, Valderrama M, Schelter B, Schulze-Bonhage A, Navarro V, Sales F, Dourado A. Epileptic seizure predictors based on computational intelligence techniques: A comparative study with 278 patients. Comput Methods Programs Biomed. 2014b;114:324-36.

Teixeira CA, Direito B, Feldwisch-Drentrup H, Valderrama M, Costa RP, Alvarado-Rojas C, Nikolopoulos S, Le Van Quyen M, Timmer J, Schelter B, Dourado A. EPILAB: A software package for studies on the prediction of epileptic seizures. J Neurosci Methods. 2011;200:257-71.

Téllez-Zenteno JF, Hernández-Ronquillo L. A Review of the Epidemiology of Temporal Lobe Epilepsy. Epilepsy Research and Treatment. 2012;2012:1-5.

Valderrama M, Alvarado C, Nikolopoulos S, Martinerie J, Adam C, Navarro V, Le Van Quyen M. Identifying an increased risk of epileptic seizures using a multi-feature EEG–ECG classification. Biomedical Signal Processing and Control. 2012;7:237-44.

Van Laar JOEH, Peters CHL, Houterman S, Wijn PFF, Kwee A, Oei SG. Normalized spectral power of fetal heart rate variability is associated with fetal scalp blood pH. Early Hum Dev. 2011;87:259-63.

Vapnik V. Statistical learning theory. New York: Wiley; 1998.

Viglione SS, Walsh GO. Proceedings: Epileptic seizure prediction. Electroencephalogr Clin Neurophysiol. 1975;39:435-6.

Voorhies JM, Cohen-Gadol A. Techniques for placement of grid and strip electrodes for intracranial epilepsy surgery monitoring: Pearls and pitfalls. Surg Neurol Int. 2013;4:98.

Welch PD. The use of fast Fourier transform for the estimation of power spectra: A method based on time averaging over short, modified periodograms. IEEE Trans Audio Electroacoust. 1967;15:70-3.

Wendel K, Väisänen O, Malmivuo J, Gencer NG, Vanrumste B, Durka P, Magjarevic R, Supek S, Pascu ML, Fontenelle H, Grave de Peralta Menendez R. EEG/MEG Source Imaging: Methods, Challenges, and Open Issues. Comput Intell Neurosci. 2009;2009:12.

Williamson JR, Bliss DW, Browne DW, Narayanan JT. Seizure prediction using EEG spatiotemporal correlation structure. Epilepsy Behav. 2012;25:230-8.

Wilson SB. Algorithm architectures for patient dependent seizure detection. Clin Neurophysiol. 2006;117:1204-16.

Winterhalder M, Maiwald T, Voss HU, Aschenbrenner-Scheibe R, Timmer J, Schulze-Bonhage A. The seizure prediction characteristic: a general framework to assess and compare seizure prediction methods. Epilepsy Behav. 2003;4:318-25.

Winterhalder M, Schelter B, Maiwald T, Brandt A, Schad A, Schulze-Bonhage A, Timmer J. Spatio-temporal patient-individual assessment of synchronization changes for epileptic seizure prediction. Clin Neurophysiol. 2006;117:2399-413.

Wu C, Sharan AD. Neurostimulation for the Treatment of Epilepsy: A Review of Current Surgical Interventions. Neuromodulation: Technology at the Neural Interface. 2013;16:10-24.

Yoon D, Frick KD, Carr DA, Austin JK. Economic impact of epilepsy in the United States. Epilepsia. 2009;50:2186-91.

Yuan Q, Zhou W, Yuan S, Li X, Wang J, Jia G. Epileptic EEG classification based on kernel sparse representation. Int J Neural Syst. 2014;24:1450015.

Zhang Y, Xu G, Wang J, Liang L. An automatic patient-specific seizure onset detection method in intracranial EEG based on incremental nonlinear dimensionality reduction. Comput Biol Med. 2010;40:889-99.

Zhang Z, Chen Z, Zhou Y, Du S, Zhang Y, Mei T, Tian X. Construction of rules for seizure prediction based on approximate entropy. Clin Neurophysiol. 2014.

Zheng Y-x, Zhu J-m, Qi Y, Zheng X-x, Zhang J-m. An Automatic Patient-Specific Seizure Onset Detection Method Using Intracranial Electroencephalography. Neuromodulation: Technology at the Neural Interface. 2014a:n/a-n/a.

Zheng Y, Wang G, Li K, Bao G, Wang J. Epileptic seizure prediction using phase synchronization based on bivariate empirical mode decomposition. Clin Neurophysiol. 2014b;125:1104-11.

Zijlmans M, Flanagan D, Gotman J. Heart rate changes and ECG abnormalities during epileptic seizures: prevalence and definition of an objective clinical sign. Epilepsia. 2002;43:847-54.

Zubler F, Steimer A, Gast H, Schindler KA. Chapter Eight - Seizure Termination. In: Premysl Jiruska MdC, John GRJ, editors. Int Rev Neurobiol: Academic Press; 2014. p. 187-207.